TESTS FOR THE COMPACT WEB SLENDERNESS OF COLD-FORMED RECTANGULAR HOLLOW SECTIONS

Research Report R744
June 1997

Tim Wilkinson BSc BE MA
Gregory J. Hancock BSc BE PhD

Centre for Advanced Structural Engineering
Department of Civil Engineering
The University of Sydney

SYNOPSIS

This report describes a series of bending tests to examine the influence of web slenderness on the rotation capacity of cold-formed rectangular hollow sections (RHS) for use in plastic design. The results indicate that the plastic web slenderness limits in design standards, which are based on tests of I-sections, are not conservative for RHS. There is considerable interaction between the webs and flange which influences the rotation capacity which is shown by approximate iso-rotation curves. A proposal for a linear interaction formula between the web and flange slendernesses for the Compact limits of RHS is given.

BLANK PAGE

CONTENTS

1 INTRODUCTION 5
1.1 Previous Research 6
1.2 Current Specifications 7

2 TEST PROGRAM 10
2.1 Test Specimens & Section Identification 10
2.2 Tensile Coupon Tests 12
2.3 Stub Column Tests 14
2.4 Geometric Imperfections 14
2.5 Plastic Bending Tests 15
2.5.1 Procedure 15
2.5.2 Other Loading Methods 17
2.5.3 Results 17
2.5.4 Discussion 22

3 CONCLUSIONS 26

4 ACKNOWLEDGEMENTS 27

5 REFERENCES 28

6 NOTATION 30

APPENDIX A OTHER LOADING METHODS 31

APPENDIX B PLASTIC BENDING TESTS 37

APPENDIX C TENSILE COUPON TESTS 49

APPENDIX D STUB COLUMN TESTS 65

APPENDIX E IMPERFECTION PROFILES 77

BLANK PAGE

1. INTRODUCTION

Steel can be idealised as an elastic-plastic material. A steel beam in bending behaves linearly up to its yield moment (M_y). Yielding spreads inwards from the extreme fibres of the cross section and the plastic moment (M_p) is reached when the entire cross section has yielded. At this point, the beam can rotate further maintaining M_p though strain hardening may cause an increase of moment above M_p. The plastic zone in the beam is known as a plastic hinge. The beam may ultimately fail by local instability or material fracture during any of these stages. The rotation capacity (R) of a section is a measure of how much the hinge can rotate.

Sections can be classified as Compact, Non-Compact or Slender (Australian Standard AS 4100 (Standards Australia (1990)), AISC LRFD (AISC (1994))), or Class 1, 2, 3, or 4 (Eurocode 3 (European Committee for Standardisation (1992)), British Standard BS 5950 (British Standards Institute (1990)), Canadian Standard CANS-16.1-94 (Canadian Standards Association (1994))). A Class 4 or Slender section experiences local buckling before M_y is reached. Class 3 sections inelastically buckle between M_y and M_p. A Class 2 section can obtain M_p but cannot sustain this moment for considerable rotations. Class 2 and Class 3 are grouped together as Non-Compact sections. Class 1 or Compact sections can maintain M_p for sufficiently large rotations suitable for plastic design.

The basis of **plastic** design is as follows. In a statically indeterminate frame, when some point reaches its plastic moment, the plastic zone will form a hinge and rotate further, redistributing additional load to other parts of the structure. The process is repeated as other hinges form. When there is a sufficient number of hinges, a plastic collapse mechanism is created for the whole structure or part of the structure. All hinges, particularly those which form early, must be able to rotate sufficiently for this mechanism to form. The maximum load in an **elastically** designed frame is reached when the design moment equals the design moment capacity of one location in the frame. Plastic design more accurately describes the true behaviour of a structure than elastic methods of analysis and can result in higher ultimate loads with associated higher deformations.

Plastic design can be of most benefit in frames which resist loads predominantly in bending. Such structures include low rise portal frames, garages, farm buildings, etc. If deflection due to gravity loads is not a critical limit state, then plastic design can create even more significant economies in construction.

There are two important criteria for the suitability of a member for plastic design:

- Local instability of the unstiffened plate elements is the major factor affecting rotation capacity. The b/t ratios of these elements must be below a limit to avoid inelastic local buckling.
- There must be sufficient material ductility of the steel to avoid fracture. This is a consequence of the high strains caused by the large curvature in a plastic hinge.

1.1 PREVIOUS RESEARCH

The elastic local buckling stress (f_o) for a long plate of width b and thickness t under uniform compression is given by:

$$f_o = \frac{k\pi^2 E}{12(1-\nu^2)(b/t)^2} \quad (1)$$

where k is the plate buckling coefficient and equals 4 for a plate simply supported on all four edges.

From Eq. 1 it can be seen that the width - thickness ratio (b/t) is critical in elastic local buckling problems. The b/t limits are normally given in design standards to classify the effect of local buckling of a section and determine its suitability for plastic design.

There has been considerable research into plastic design of I-sections over fifty years, including slenderness limits and studies on the rotation capacity required to create a plastic collapse mechanism in various frame types. The background documentation to Eurocode 3 (Sedlacek and Feldmann (1995)) provides a good summary of the previous studies into b/t ratios and rotation capacity of I-sections.

There has also been research on the flange slenderness limit for rectangular hollow sections (RHS) (Dwyer and Galambos (1965), Korol and Hudoba (1972), Hasan and Hancock (1988), and Zhao and Hancock (1991)). The flange limit for RHS is different to the limit for I-sections since the flange of an RHS is supported on both longitudinal edges, while the flange of an I-section is unsupported on one edge. Each web of an RHS has similar support conditions to an I-section web although there are two webs in an RHS. This is reflected in the slenderness limits in current design standards, where the web slenderness limits for RHS and I-sections are the same, and are based on tests of I-sections.

When an RHS is subjected to pure major axis bending, the flange is in uniform compression, while the web is in in-plane bending. Bending is less critical for local buckling than compression for elements with the same b/t ratio, since the plate buckling coefficient (k) and hence the local buckling stress is approximately six times higher for in-plane bending compared to uniform compression. Hence for square hollow sections (SHS) and RHS with low aspect (b/d) ratios, flange buckling occurs before the web buckles locally.

More recently, RHS have been produced with higher aspect ratios, such as 3.0 (Tubemakers (1994)). The webs of these sections are considerably more slender than the flange, and the possibility of web local buckling before flange buckling is increased. Zhao and Hancock ((1990) and (1992)) observed inelastic web local buckling in some RHS with an aspect ratio of 2.0. This happened at low rotation values for specimens with flange and web slenderness values below the limits set in current design standards for plastic design. These results provided the impetus for this series of tests in higher aspect ratio RHS.

1.2 CURRENT SPECIFICATIONS

Steel design codes from Europe, America and Australia are considered in this report. They are Eurocode 3 Part 1.1: Design of Steel Structures (henceforth referred to as "Eurocode 3"), American Institute of Steel Construction Metric Load and Resistance Factor Design ("AISC LRFD"), and Australian Standard AS 4100 Steel Structures ("AS 4100"). The web and flange slenderness limits for cold-formed RHS bending about the major principal axis are listed in Table 1 for each standard for the dimensions shown in Figure 1.

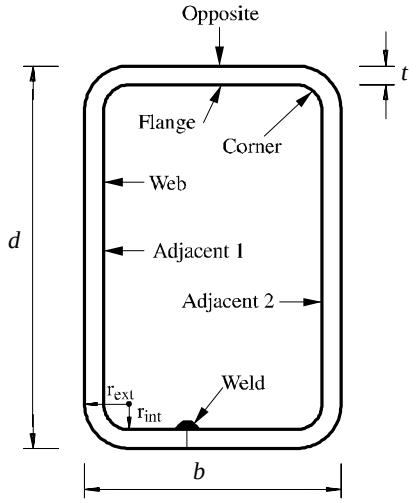

Figure 1: RHS Section Notation

Specification	Web slenderness (λ_w)	Web slenderness limits			
		Class 1 Compact	Class 2	Class 3	Non-Compact
AS 4100	$\frac{d-2t}{t}\sqrt{\frac{f_y}{250}}$	82	-	-	115
Eurocode 3	$\frac{d-3t}{t}\sqrt{\frac{f_y}{235}}$	72	83	124	-
AISC LRFD	$\frac{d-2r_e}{t}\sqrt{\frac{f_y}{E}}$	3.76 (106)*	-	-	5.7 (161)*

Table 1(a): Summary of RHS Web Slenderness Limits

Specification	Flange slenderness (λ_f)	Flange slenderness limits			
		Class 1 Compact	Class 2	Class 3	Non-Compact
AS 4100	$\frac{b-2t}{t}\sqrt{\frac{f_y}{250}}$	30	-	-	40
Eurocode 3	$\frac{b-3t}{t}\sqrt{\frac{f_y}{235}}$	33	38	42	-
AISC LRFD	$\frac{b-2r_e}{t}\sqrt{\frac{f_y}{E}}$	1.12 (31.7)*	-	-	1.4 (39.6)*

Notes: Sections exceeding the Class 3 or Non-Compact limit are Class 4 or Slender respectively.
* Applies to f_y = 250 MPa as a comparison to the AS 4100 limits.

Table 1(b): Summary of RHS Flange Slenderness Limits

It can be seen from Table 1(b) that the flange slenderness limits in these three standards are very similar. However Table 1(a) indicates that the AISC LRFD web slenderness limits are significantly higher than AS 4100 and Eurocode 3.

The rotation capacity (R) is defined as $\kappa/\kappa_p - 1$, where κ/κ_p is the dimensionless

curvature at which the moment falls below M_p on a moment rotation curve. κ_p is the curvature at which the plastic moment is reached assuming an elastic flexural rigidity (EI) and is given by $\kappa_p = M_p/EI$.

Steel design specifications have varying rotation capacity requirements for plastic design. The wide variety of loading patterns and structural frame shapes results in a large range of required plastic rotations. Hence it is appropriate to adopt some arbitrary value of rotation capacity which is satisfactory for most practical situations. Korol (1972) put forward a recommendation of $R = 4$.

Eurocode 3 Class 1 and AISC LRFD Compact limits are based on a rotation capacity of $R = 3$. However AISC LRFD states that greater rotation capacity may be required in seismic regions. A value of $R = 4$ has been adopted in AS 4100 as appropriate for plastic design and is deemed suitable in this report.

AS 4100 only allows plastic design for Compact I-sections and not for RHS. Hence a Compact RHS (in AS 4100) does not strictly have to be able to achieve a rotation of $R = 4$. However in the determination of the flange slenderness limits for RHS in AS 4100, Compact sections were required to have a rotation capacity of $R = 4$ (Hasan and Hancock (1988) and Zhao and Hancock (1991)). This was in anticipation of the possible inclusion of plastic design for RHS in AS 4100 in the future. Henceforth in this report it is assumed that Compact RHS should be able to meet rotation capacity requirements.

Standards have material ductility requirements for the suitability of sections for plastic design. Clause 3.2.2.2 of Eurocode 3 has the following criteria:

- $f_u/f_y \geq 1.2$
- $e_f \geq 15\%$
- $e_u/e_y \geq 20$

where f_y is the yield stress, f_u is the tensile strength, e_y is the yield strain, e_u is the strain at the ultimate tensile strength, and e_f is the percentage strain (elongation) after failure measured across the fracture surface of a tensile coupon.

Clause 4.5.2 of AS 4100 specifies the following for plastic design:

- $f_u/f_y \geq 1.2$
- $e_f \geq 15\%$
- the length of the yield plateau is greater than $6e_y$
- the steel exhibits strain-hardening

and specifically excludes cold-formed steel.

The only material requirement for plastic design in AISC LRFD is that $f_y \leq 450$ MPa (Clause A5.1).

2. TEST PROGRAM

2.1 TEST SPECIMENS AND SECTION IDENTIFICATION

A variety of cold-formed RHS was chosen for the test series. The RHS were manufactured by Tubemakers of Australia Limited (now known as BHP Steel Structural and Pipeline Products). Two strength grades were selected, Grade C350L0 and C450L0 (nominal yield stress f_{yn} of 350 MPa and 450 MPa), manufactured to Australian Standard AS 1163 (Standards Australia (1991)). The L0 suffix indicates the material has Charpy V-notch impact properties for use at temperatures below 0°C. The Grade C450 specimens are known as *DuraGal* sections, produced using a unique cold-forming and in-line galvanising process developed by Tubemakers. In-line galvanising provides extra strength enhancement compared to cold-forming alone. The samples were artificially strain aged by Tubemakers in a furnace at 170°C for 20 minutes. The original strip was TF300 (TUBEFORM 300 - nominal yield stress of 300 MPa) produced by BHP Steel for both the C350 and C450 sections.

The typical chemical composition of these tubes is shown below:

Chemical Composition (Cast or Product), % max						
C	Si	Mn	P	S	Al	CE
0.20	0.05	1.60	0.04	0.03	0.10	0.39

The sections tested are listed in Table 2. This selected range gave experimental data on the effect of the following variables on local buckling and rotation capacity:

- web slenderness,
- flange-web interaction,
- corner radius,
- yield stress.

Each of the various sections is denoted by a section number, Sxx where xx refers to the particular section type. Eight metre lengths of each section type were cut into four two metre lengths. A suffix “A”, “B”, “C”, or “D” distinguishes these four lengths. The prefix “B” for a bending specimen, “T” for tensile coupon, and “SC” for stub column identifies the type of test performed.

After the initial series of bending tests, some extra specimens were obtained to perform additional tests using alternative loading systems (Section 2.5.2 and Appendix A). These are not included in Table 2.

Specimen No.	Section (*nominal dimensions and steel grade*) $d \times b \times t$	Web slenderness $\frac{d-2t}{t}\sqrt{\frac{f_{yn}}{250}}$	Flange slenderness $\frac{b-2t}{t}\sqrt{\frac{f_{yn}}{250}}$	Aspect ratio $\frac{d}{b}$
S01	150 × 50 × 5.0 C450	37.6	10.7	3.0
S02	150 × 50 × 4.0 C450	47.6	14.1	3.0
S03	150 × 50 × 3.0 C450	64.4	19.7	3.0
S04	150 × 50 × 2.5 C450	77.8	24.1	3.0
S05	150 × 50 × 2.3 C450	84.8	26.5	3.0
S06	100 × 50 × 2.0 C450	64.4	30.9[2]	2.0
S07	75 × 50 × 2.0 C450	47.6	30.9[2]	1.5
S08	75 × 25 × 2.0 C450	47.6	14.1	3.0
S09	75 × 25 × 1.6 C450	60.2	18.3	3.0
S10	75 × 25 × 1.6 C350	53.1	16.1	3.0
S11	150 × 50 × 3.0 C350	56.8	17.4	3.0
S12	100 × 50 × 2.0 C350	56.8	27.2	2.0
S13	125 × 75 × 3.0 C350	46.9	27.2	1.7
AS 4100 Compact Limit AS 4100 Non-Compact Limit		82 115	30 40	

Notes: (1) Grade refers to the nominal yield stress, f_{yn}, in MPa.

(2) These sections have Non-Compact flanges, but only exceed the flange Compact limit, $\lambda = 30$, by a very small amount.

Table 2: List of Sections for Plastic Bending Tests

Figure 1 shows the names given to each of the faces of the RHS: “weld”, “opposite”, “adjacent 1”, and “adjacent 2”. For most RHS the longitudinal weld was located on one of the shorter faces (the flange). Since the weld was normally slightly off-centre, the adjacent face of the RHS which was closer to the weld is labelled “adjacent 1". In one case (S01) the weld was located on the longer side (the web). This was an exception to the usual situation and was probably caused by twisting of the coil during the forming process.

2.2 TENSILE COUPON TESTS

Three coupons were taken from the centre of the flats of each tube. One was cut from the face opposite the weld, and one from each of the sides adjacent to the weld. Corner coupons were cut from selected RHS. The coupons were prepared and tested in accordance with AS 1391 (Standards Australia (1991)) in a 250 kN capacity INSTRON Universal Testing Machine.

Since the steel was cold-formed, the yielding was gradual, so that the yield stress used was the 0.2% proof stress. The average of the yield stress from both of the adjacent faces was used in the determination of plastic moment (M_p) and slenderness values. The average of the Young's modulus of elasticity (E) from both of the adjacent faces was used in stiffness calculations. The yield stress of the opposite face was on average 10% higher than that of the adjacent faces. This was a result of the cold-forming process.

The use of the average measured yield stress of the finished tube is derived from AS 4100. AS 4100 refers to AS 1163, and AS 1163 permits the yield stress to be determined from the flats of the finished product. The AISC LRFD makes reference to ASTM A 500 (ASTM (1993)). ASTM A 500 is similar to AS 1163 and allows for the yield stress to be determined from the flats of the finished tube. However Eurocode 3, Figure 5.5.2 states that for cold-formed structural sections, the yield stress should be based on either

(i) a full section tensile test, or
(ii) original strip strength plus enhancement due to cold working.

If option (i) is used, the yield stress may be slightly higher due to the inclusion of the corners. Option (ii) may give a lower yield stress since the effect of in-line galvanising on the yield stress is not included.

All measured yield stresses and ultimate strengths values are static values obtained by stopping the test for approximately one minute near the yield and ultimate loads. These values are often considerably lower than commercial test values which are usually dynamic.

Table 3 summarises the yield stress and Young's modulus of elasticity obtained from the coupon tests. Full details on the testing procedure and results are given in Appendix C, including the yield stress, ultimate strength and material ductility parameters from each face and the corners of the RHS.

Specimen	Cut from section	E[1] (GPa)	f_y[1] (MPa)
TS01D	150 × 50 × 5.0 C450	198	441
TS02D	150 × 50 × 4.0 C450	212	457
TS03D	150 × 50 × 3.0 C450	206	444
TS04D	150 × 50 × 2.5 C450	204	446
TS05D	150 × 50 × 2.3 C450	205	444
TS06D	100 × 50 × 2.0 C450	202	449
TS07D	75 × 50 × 2.0 C450	203	411[2]
TS08D	75 × 25 × 2.0 C450	203	457
TS09D	75 × 25 × 1.6 C450	193	439
TS10D	75 × 25 × 1.6 C350	202	422
TS11D	150 × 50 × 3.0 C350	205	370
TS12D	100 × 50 × 2.0 C350	203	400
TS13D	125 × 75 × 3.0 C350	211	397
TS16D	150 × 50 × 2.5 C450	207	440
TS17D	100 × 50 × 2.0 C450	203	423
TS19D	100 × 100 × 3.0 C450	207	445
TS20D	150 × 50 × 3.0 C350	200	382
TS21D	125 × 75 × 2.5 C350	201	374

Notes: (1) The average of E and f_y for the two adjacent sides is used for the whole section.
(2) For TS07D f_y is from face Adjacent 2 only.
(3) Nominal strengths: Grade C450 specimens f_{yn} = 450 MPa and f_{un} = 500 MPa.
Grade C350 specimens f_{yn} = 350 MPa and f_{un} = 430 MPa.

.

Table 3: Summary of Tensile Test Results

2.3 STUB COLUMN TESTS

Under bending, the stress in the webs of an RHS varies from compression at one edge to tension at the other. A small series of stub column tests was undertaken to examine the slenderness of RHS webs under uniform compression.

Full details of the test procedure and results are given in Appendix D. The main conclusion from the stub column tests is that the yield slenderness limits (which delineate Slender and Non-Compact sections) for RHS webs under uniform compression are satisfactory.

2.4 GEOMETRIC IMPERFECTIONS

RHS are not perfect rectangular specimens. The cold-forming process, welding, handling and other factors can introduce geometric imperfections. Local imperfections can have a significant effect on the moment and rotation capacity (Key and Hancock (1993)). Hence the local imperfections of the RHS were measured as part of the test program. These values will be important in future finite element modelling of the bending tests. Full details on the procedure used and the imperfection profiles obtained can be found in Appendix E.

Most RHS exhibited a “bow-out” (as shown in Figure 2) or “bow-in” that was reasonably constant along the length of the RHS. No significant wave-like imperfections along the length were detected.

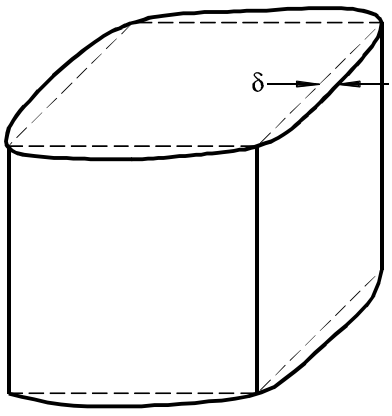

Figure 2: Typical “Bow-Out” Imperfection of an RHS

2.5 PLASTIC BENDING TESTS

2.5.1 Procedure

The bending tests were performed in a 2000 kN capacity DARTEC testing machine, using a servo-controlled hydraulic ram. A diagram of the test set-up is shown in Figure 3. The four point bending arrangement provided a central region of uniform bending moment and zero shear force. Specimens were supported on half rounds resting on greased Teflon pads which simulated a set of simple supports. The members were loaded symmetrically at two points via a centrally loaded spreader beam. Most RHS were arranged so that the longitudinal weld was on the bottom (tension) flange. Samples BS07C, BS08C, BS09C, and BS10C had the weld on the top (compression) flange. For specimens BS01B and BS01C the weld was located along the web of the specimen.

The initial loading method (called the "parallel plate" method) adopted is one that has been used at the University of Sydney for many years (Hasan and Hancock (1988), Zhao and Hancock (1991)) and involved welding plates to the web of the beam as shown in Figure 3. A greased teflon pad was placed between the bottom of the spreader beam and the half round. This allowed for the load points to move due to the axial shortening of the beam caused by curvature without inducing axial strain. The half round also ensured that the applied loads were vertical. The half round bore upon a thick load transfer plate, which in turn transmitted the force to the loading plates. The loading plates and the load transfer plate were connected by bolts and an angle section, but this connection did not transfer load and was for safety only.

Longitudinal strain gauges were placed midspan on each flange and linear displacement transducers were positioned midspan and directly below the loading plates. This enabled the curvature to be calculated from both the strain gauge and displacement measurements (Hasan & Hancock (1988)). For some of the later tests, curvature was determined from the displacements only. Load, deflection and strain measurements were recorded by a SPECTRA data acquisition system.

The lengths of the specimens were chosen to avoid lateral buckling (Zhao, Hancock and Trahair (1995)), and shear failure in the end spans. For RHS with depth $d \geq 100$ mm, the length between the loading points (L_1) was 800 mm, and the distance between the supports (L_2) was 1700 mm. For sections with $d \leq 75$ mm, L_1 was 500 mm, and L_2 was 1300 mm.

Two samples of each specimen size were originally tested using the parallel plate method. In order to examine the effect of loading conditions, extra selected specimens were tested using two other methods.

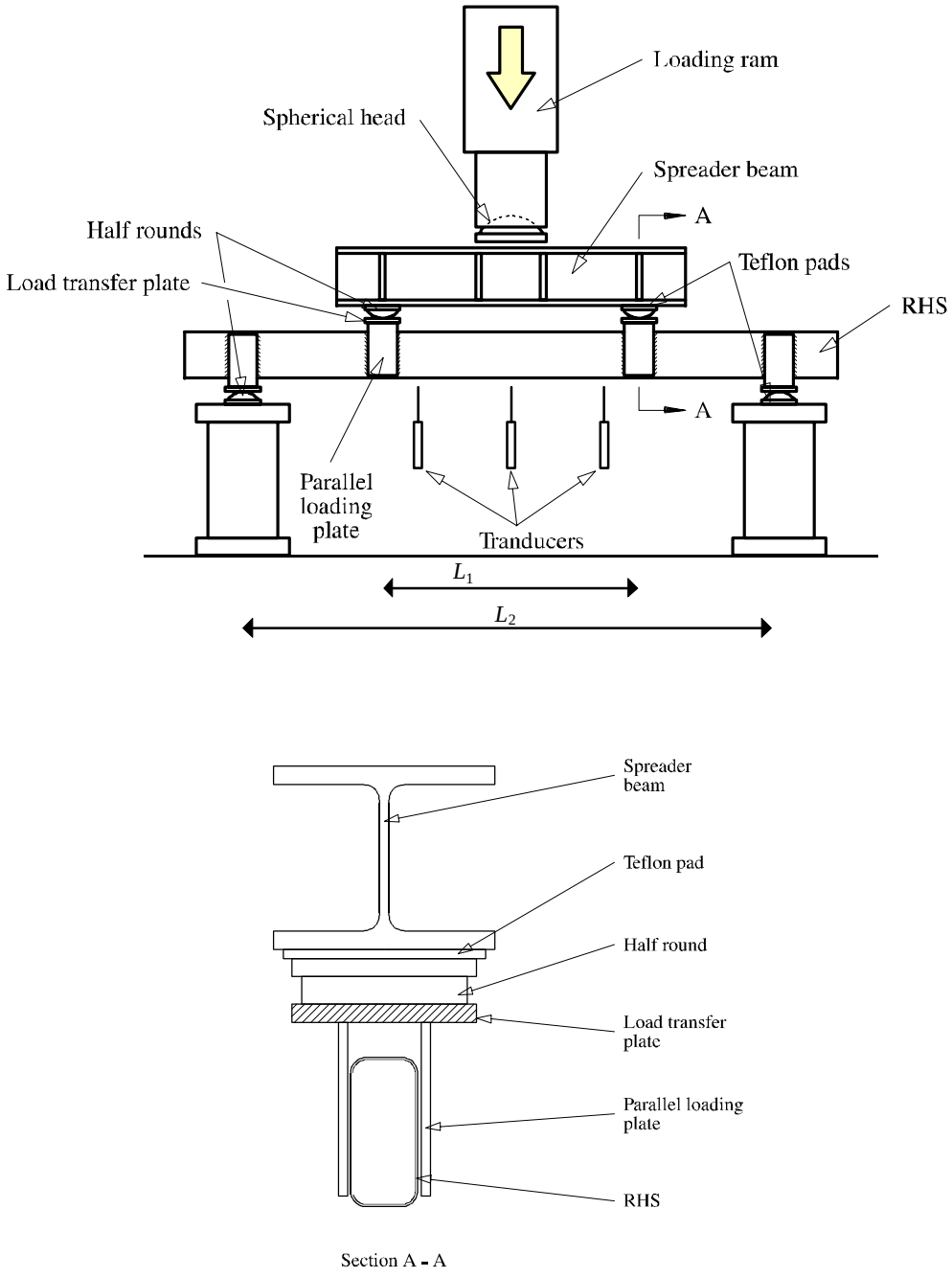

Figure 3: The Parallel Plate Loading Method for Plastic Bending Tests

2.5.2 Other Loading Methods

Two additional loading techniques, known as the "perpendicular plate" and "pin loading" methods were used. The perpendicular plate method involved loading plates welded perpendicular to the web. In the pin loading system, a pin hole was drilled through bearing plates welded to the web. These bearing plates were smaller than the perpendicular plates and did not involve welding near the flanges. Full details are given in Appendix A. A selection of the RHS were retested using these different loading arrangements.

The main conclusion of the latter tests is that the alternative methods had no considerable effect on the rotation capacity of the RHS as evidenced by the results in Appendix A.

2.5.3 Results

The results of the plastic bending tests are presented in Table 4. This table lists the ratio M_{max}/M_p and R. M_{max} is the maximum static moment reached during the test and M_p is the plastic moment of the section based on the measured dimensions and the average measured yield stress of the two adjacent faces as given in Table 3. The static moment is obtained when the test machine is halted for approximately one minute in the vicinity of the ultimate load.

All specimens except the two 150 × 50 × 5.0 C450 specimens (BS01B and BS01C) and the 100 × 100 × 3.0 C450 (BS19A) sample experienced web local buckling which produced a rapid shedding of load with increased deflection. Each web buckled and compatibility of rotation at the corner caused deformation of the flange. A photograph of a typical buckle is shown in Figure 4. In all cases, the buckle formed adjacent to one of the loading plates. BS01B and BS01C exhibited large deflections and an inelastic lateral (flexural-torsional) buckle formed at high curvatures (κ/κ_p) greater than 6. There was no sudden unloading associated with the lateral buckle. BS19A was a square hollow section and, as expected, failed by flange buckling. Specimen BS08C was not loaded to failure. No specimen failed due to insufficient material ductility.

Four typical non-dimensional moment-curvature curves are shown in Figure 5. The four curves clearly demonstrate the difference in behaviour between the classes of section. The moment-curvature relations and all the measured dimensions for each specimen are in given Appendix B.

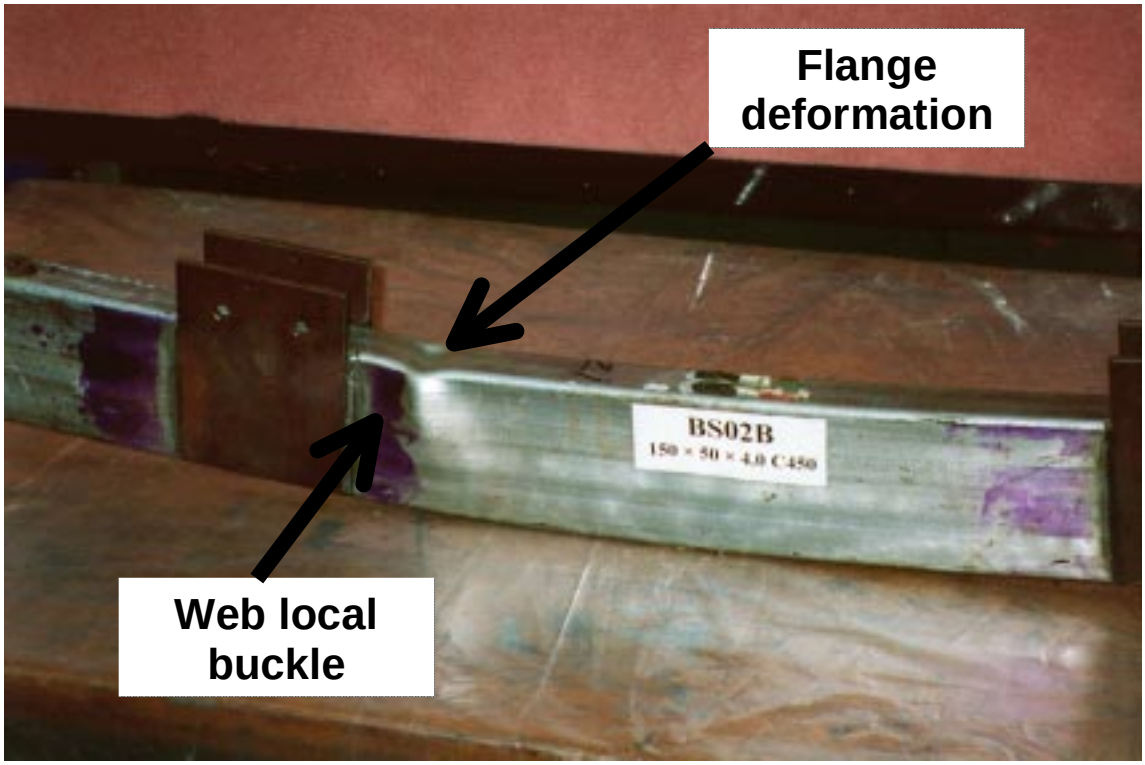

Figure 4: Typical web buckle

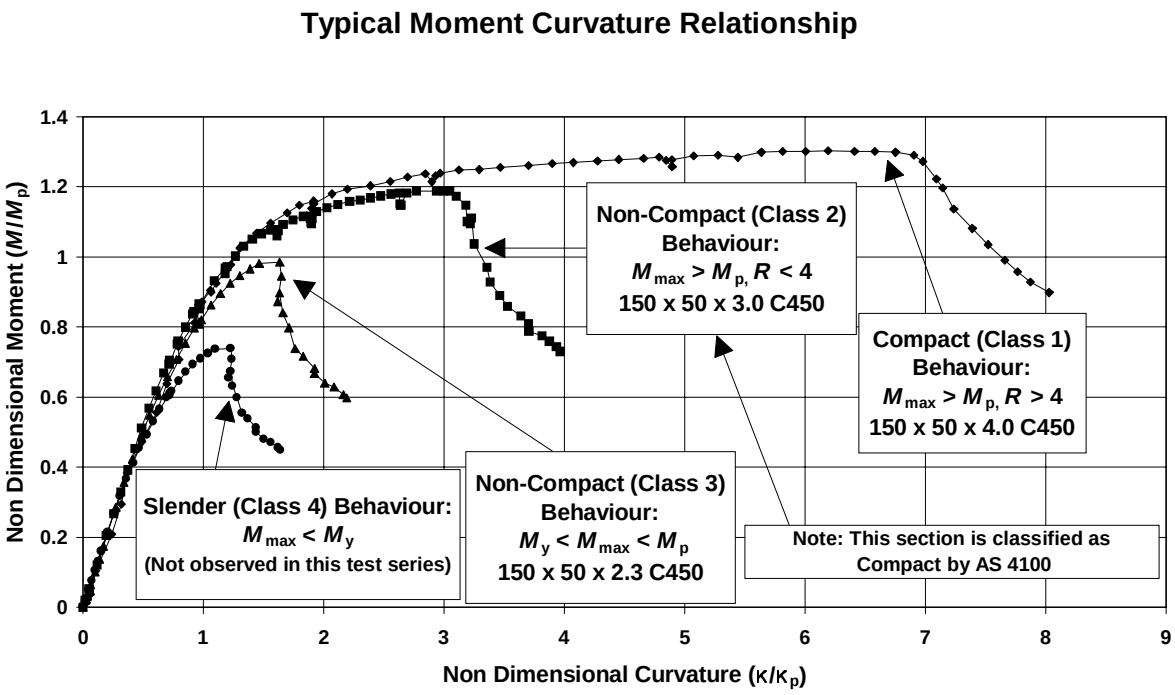

Figure 5: Typical Moment - Curvature Relationships

Specimen	Cut from section	Slenderness[1] (AS 4100)		$\frac{M_{max}}{M_p}$	Rotation capacity R
		Web λ_w	Flange λ_f		
BS01B	150 × 50 × 5.0 C450	38.1	10.9	1.23	>13
BS01C		38.3	11.0	1.17	>8
BS02B	150 × 50 × 4.0 C450	49.1	14.6	1.27	6.6
BS02C		49.9	14.9	1.19	7.7
BS03B	150 × 50 × 3.0 C450	64.9	19.9	1.15	2.7
BS03C		65.4	19.9	1.16	2.3
BS03A		65.3	20.0	1.13	2.9
BS04B	150 × 50 × 2.5 C450	74.6	23.1	1.02	1.4
BS04C		75.4	23.5	1.00	1.2
BS05A	150 × 50 × 2.3 C450	86.4	27.3	0.98	0.0
BS05B		85.2	26.9	1.01	0.6
BS05C		86.0	27.2	0.98	0.0
BS06B	100 × 50 × 2.0 C450	62.5	30.2[2]	1.07	0.8
BS06C		62.3	30.0[2]	1.01	0.8
BS07B	75 × 50 × 2.0 C450	47.4	30.6[2]	1.04	1.7
BS07C		47.1	30.5[2]	1.02	1.9
BS08B	75 × 25 × 2.0 C450	48.7	14.6	1.11	5.7
BS08C		49.4	14.7	1.13	-[3]
BS09B	75 × 25 × 1.6 C450	62.1	19.0	1.08	2.2
BS09C		61.8	19.0	1.13	2.5
BS10B	75 × 25 × 1.6 C350	60.5	18.5	1.03	1.9
BS10C		60.1	18.5	1.00	2.6
BS11B	150 × 50 × 3.0 C350	58.6	17.9	1.21	4.1
BS11C		59.5	18.2	1.15	3.6
BS12B	100 × 50 × 2.0 C350	59.5	28.5	1.00	1.2
BS12C		59.5	28.6	1.00	1.3
BS13B	125 × 75 × 3.0 C350	51.5	30.1[2]	1.03	1.5
BS13C		51.3	30.0[2]	1.03	1.6
BS19A	100 × 100 × 3.0 C450	43.9	43.8	1.00	0.8

Notes: (1) Slenderness based on measured (not nominal) dimensions and yield stress.
(2) These sections have Non-Compact flanges to AS 4100, but only exceed the flange Compact limit, $\lambda = 30$, by a small amount.
(3) Specimen BS08C not tested to failure.

Table 4: Summary of Bending Test Results

The web slenderness is calculated slightly differently in AS 4100, Eurocode 3, and AISC LRFD as demonstrated in Table 1(a). Figures 6, 7 and 8 display the rotation capacity versus web slenderness which can be compared with the web slenderness limit for each standard. In Figure 6, the results circled have Non-Compact flanges, for which the flange slenderness slightly exceeds the AS 4100 flange Compact limit.

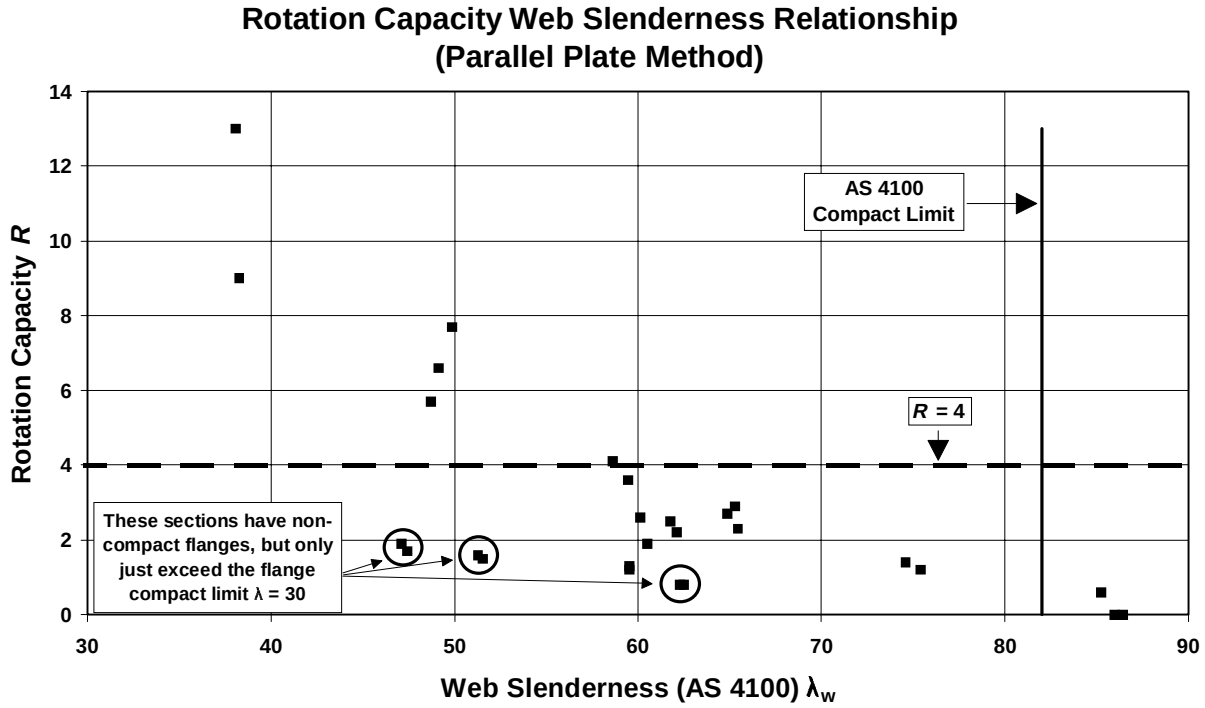

Figure 6: Web Slenderness - Rotation Capacity Curve (AS 4100)

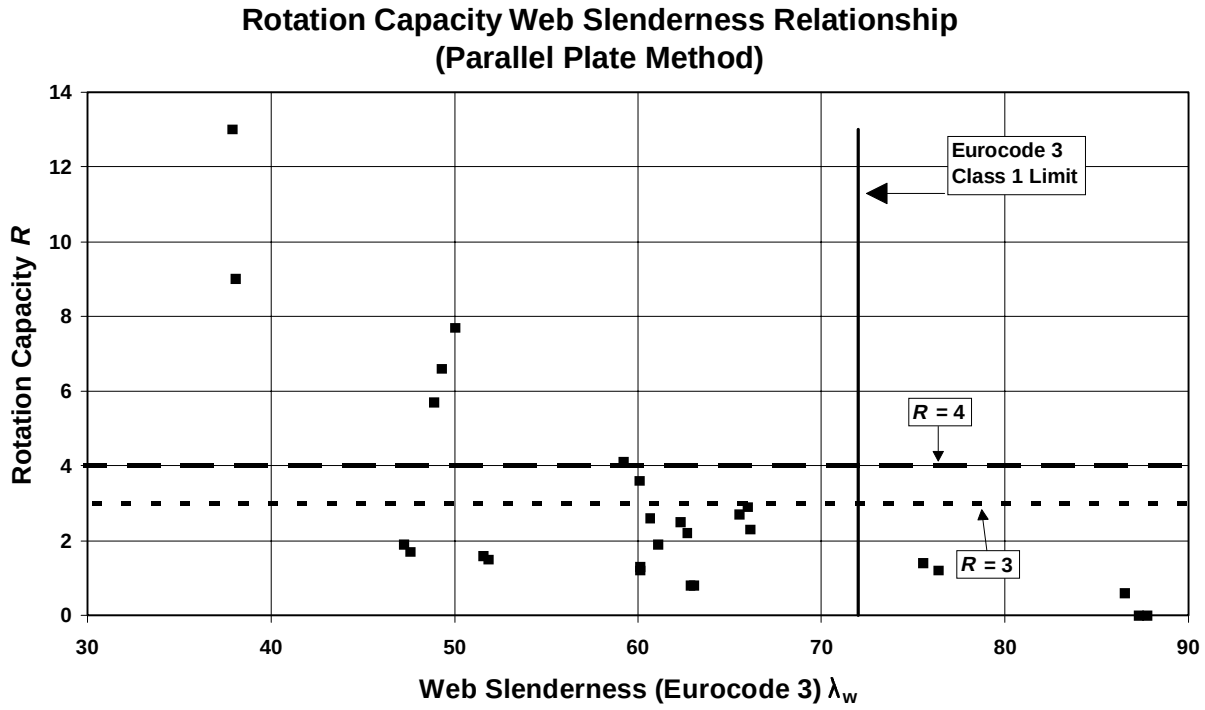

Figure 7: Web Slenderness - Rotation Capacity Curve (Eurocode 3)

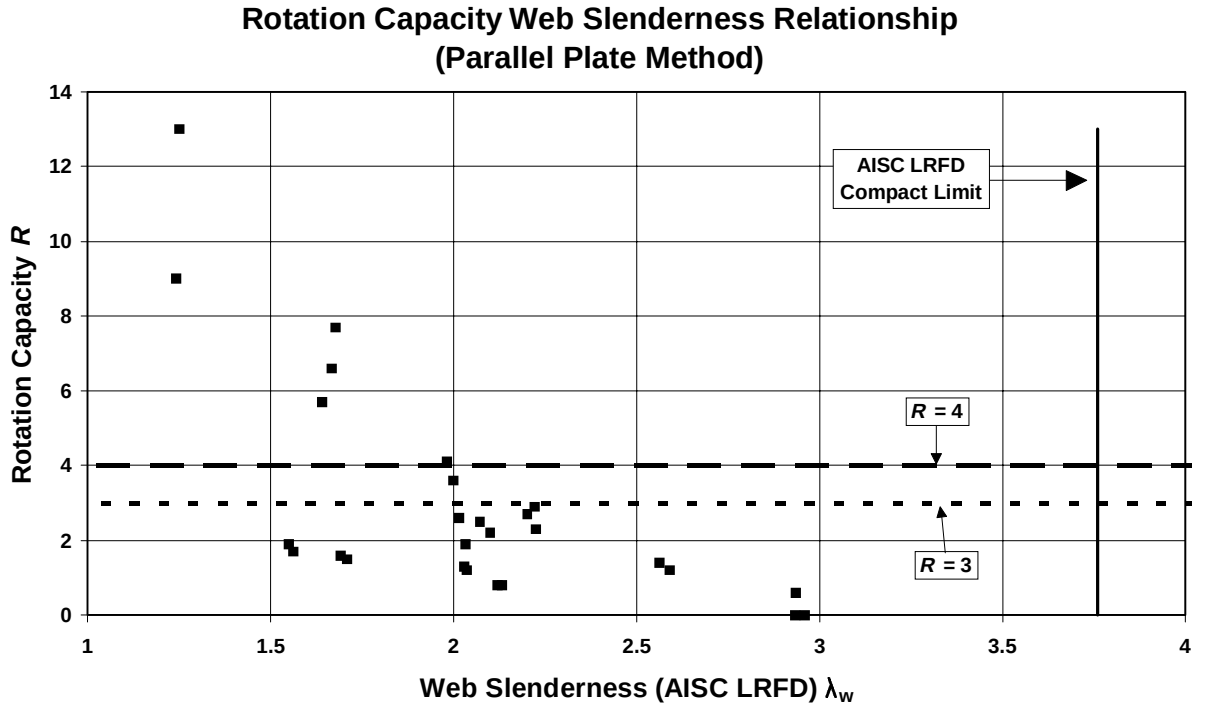

Figure 8: Web Slenderness - Rotation Capacity Curve (AISC LRFD)

2.5.4 Discussion

The results in Figures 6, 7 and 8 clearly indicate that the current web slenderness limits for Compact or Class 1 sections are non-conservative since there is a large number of sections which are currently classified as Compact or Class 1 which demonstrate insufficient rotation capacity for plastic design. The Compact limit for the AISC LRFD specification is the most unconservative as indicated in Figure 8. It may be possible that sections defined as Compact by that standard may not even be able to reach the yield moment M_y let alone maintain the plastic moment for significant rotations. Many of the sections classified by AS 4100 and Eurocode 3 as Compact or Class 1 fail to reach the required rotations as shown in Figures 6 and 7.

As shown in Table 4 and Figure 6, several of the sections have Non-Compact flanges according to the AS 4100 flange limit. However, they have Compact or Class 1 flanges with respect to the AISC LRFD and Eurocode 3 limits. These sections (100 × 50 × 2.0 C450, 75 × 50 × 2.0 C450, and 125 × 75 × 3.0 C450) just exceed the Compact flange limit ($\lambda = 30$ defined in AS 4100) and it is reasonable to expect that they would behave almost identically to sections with Compact flanges.

Figure 9 compares the different steel grades. It appears that there is no significant correlation between the rotation capacity and steel grade since the Grade C350 sections perform similarly to the Grade C450 specimens.

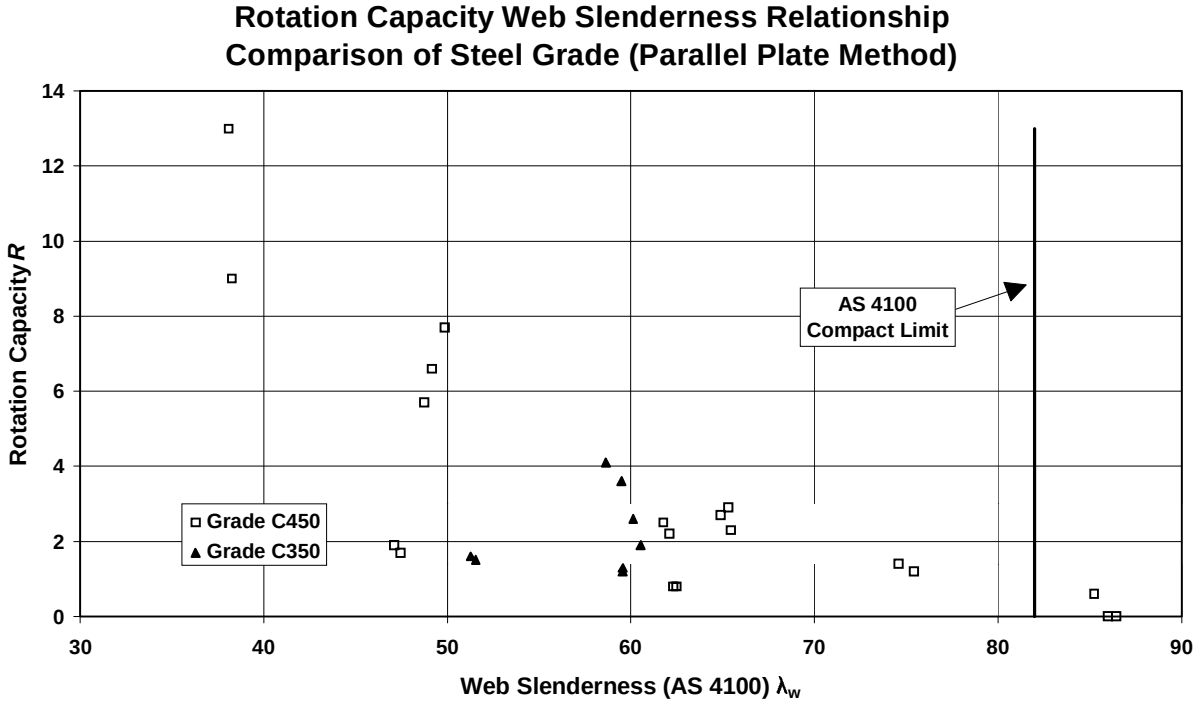

Figure 9: Web Slenderness - Rotation Capacity Curve: Effect of Steel Grade

Figure 10 compares the different aspect ratios of the RHS with respect to web slenderness and rotation capacity. The lower aspect ratio sections tend to show a lower rotation capacity for a given web slenderness, since they have a corresponding increase in flange slenderness. Figure 10 indicates the effect of interaction between the flange and web on the rotation capacity.

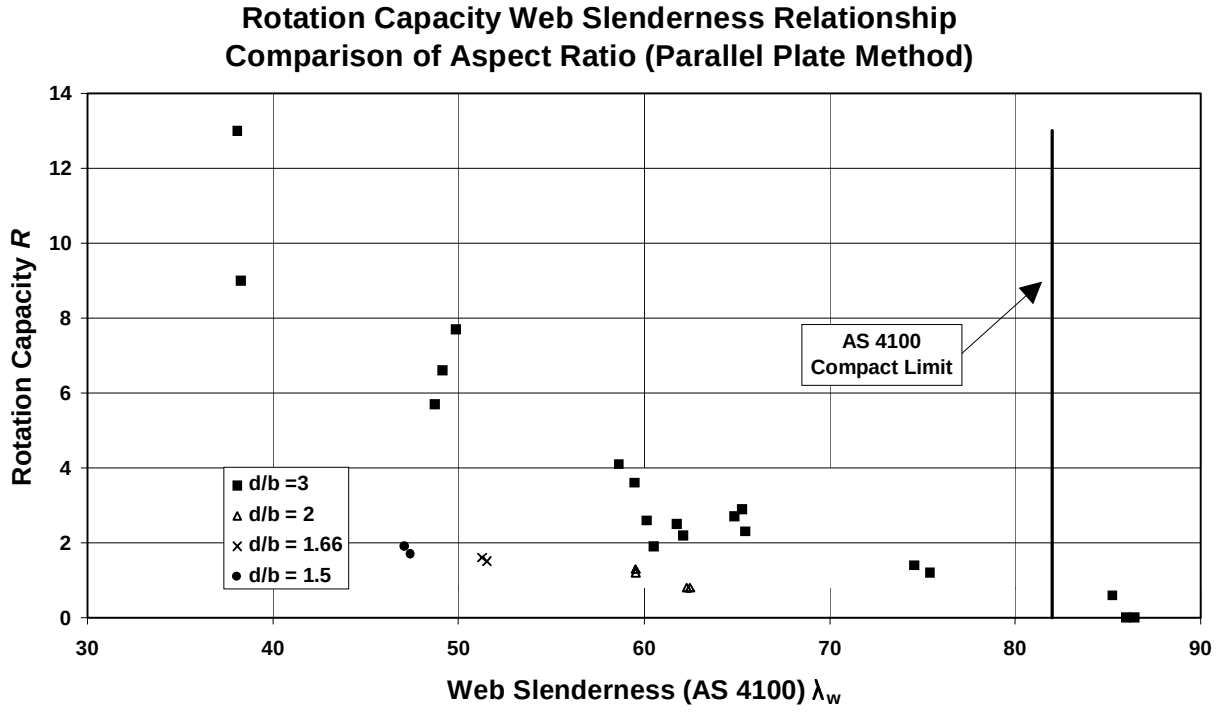

Figure 10: Web Slenderness - Rotation Capacity Curve: Effect of Aspect Ratio

Figure 11 shows approximate iso-rotation curves for the bending tests, taking into account both the flange and web slenderness. Since some tests were repeated, the rotation capacity shown in Figure 11 is the average rotation from the two (or three) tests performed on a given RHS size. To include the effects of flange buckling, the results of Hasan and Hancock (1988) and Zhao and Hancock (1991) are also included in Figure 10. Most of these tests were performed on SHS, with an aspect ratio of 1.0, and several RHS with an aspect ratio of 2.0 were also tested. All tests used the parallel plate method of loading.

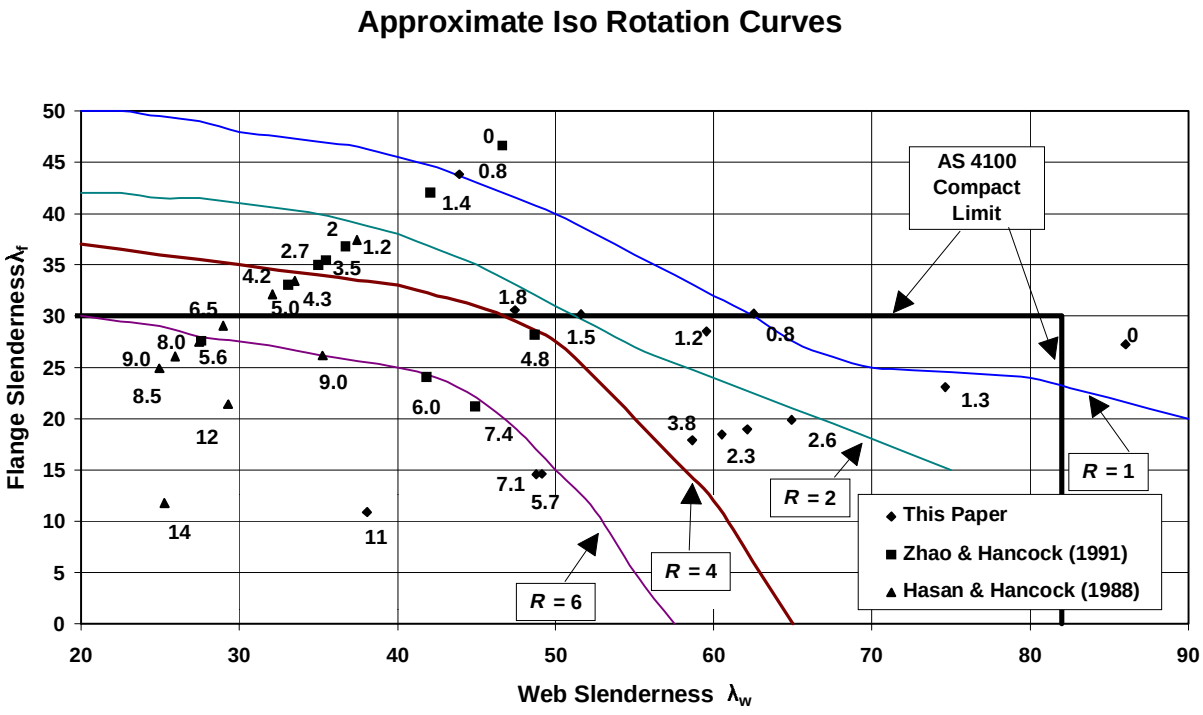

Figure 11: Iso-Rotation Curves

The iso-rotation curves in Figure 11 give the best indication as to the behaviour of the specimens. There is a definite interaction between the flange and the web so that the flange and web slenderness values required to reach a given *R* are correlated. The sections with higher aspect ratio have a relatively stiffer flange which provides restraint against web buckling. A section with a similar web but having a less stiff flange has less restraint against buckling and hence a lower rotation capacity.

Figure 11 indicates that the Compact flange limit accurately models the behaviour for RHS and SHS with stocky webs which buckle predominately in the flange. However there is a significant region for members with more slender webs in which the standard is non-conservative. A simple linear interaction formula may be appropriate and is shown in Figure 12. Similar proposals would be suitable for Eurocode 3 and the AISC LRFD.

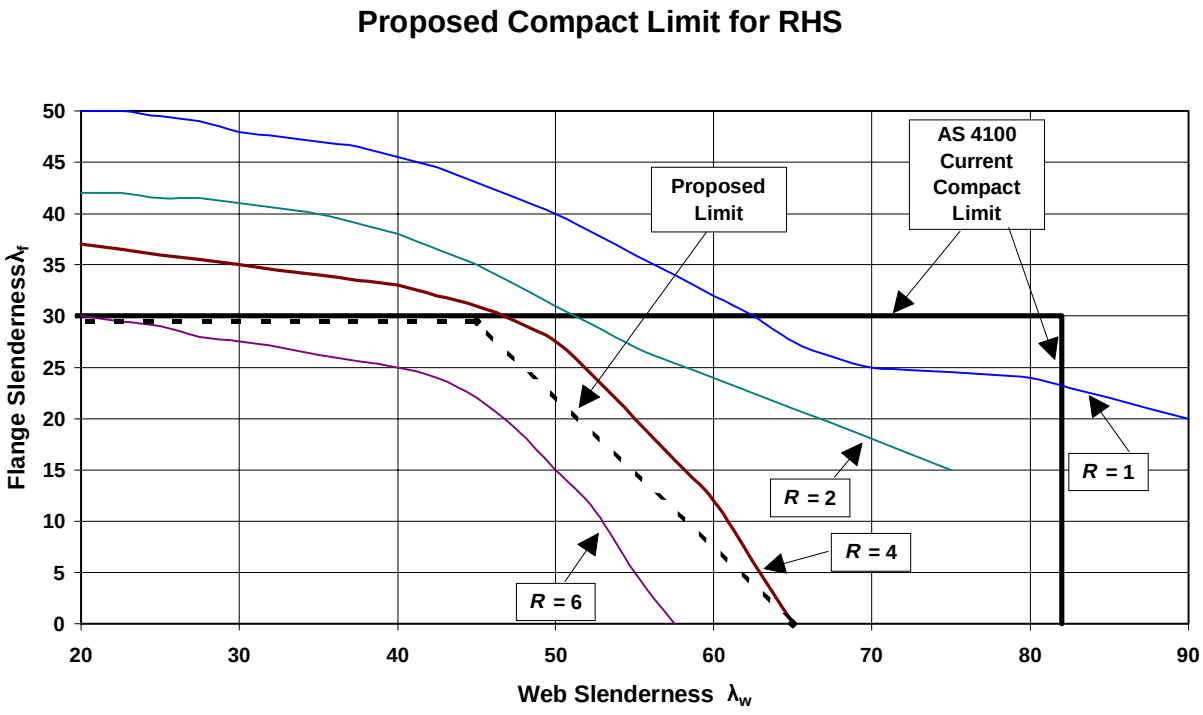

Figure 12: Proposal for New Compact Limits for RHS (AS 4100)

The cold-formed RHS do not satisfy the ductility requirements of AS 4100 or Eurocode 3 for plastic design (refer to Appendix C). However local instability (web buckling) was the failure mode of the sections, not material failure. Section BS01B, which did not experience local buckling, exhibited large rotations and strains, indicating that ductility may not present a problem. Hence the limitation on cold-formed RHS for plastic design may be incorrectly based.

3 CONCLUSIONS

The results of the plastic bending tests on a range of cold-formed RHS with different plate slendernesses, aspect ratio and yield stress grade have been presented. The major finding of the study is that the Compact or Class 1 web slenderness limits for RHS, which were based on tests of I-section beams, are non-conservative for RHS. Many Compact or Class 1 sections which satisfy the requirements of the Australian Standard AS 4100, Eurocode 3 and the American Institute of Steel Construction LRFD Specification do not exhibit the rotation capacity suitable for plastic design. There is considerable interaction between the flange and the web in the failure mode so that the flange and web slenderness limits must be correlated. This has been identified in the iso-rotation plot from which a simple linear interaction for the Compact limits of RHS has been proposed.

4 ACKNOWLEDGEMENTS

This research project is funded by CIDECT (Comité International pour le Developpement et l'Étude de la Construction Tubulaire). Tube specimens were provided by BHP Steel Structural and Pipeline Products (formerly Tubemakers of Australia Limited). The experiments were carried out in the J. W. Roderick Laboratory for Materials and Structures, Department of Civil Engineering, the University of Sydney. The first author is funded by an Australian Postgraduate Award from the Commonwealth of Australia Department of Employment, Education, Training and Youth Affairs, supplemented by the Centre for Advanced Structural Engineering and the University of Sydney.

5 REFERENCES

AISC, (1994), *Metric Load and Resistance Factor Design Specification for Structural Steel Buildings*, (AISC LRFD), American Institute of Steel Construction, Chicago, Il.

ASTM, (1993), "Cold-Formed Welded and Seamless Carbon Steel Structural Tubing in Rounds and Shapes", *ASTM A 500*, American Society for Testing and Materials, Philadelphia, Pa.

CASE, (1992), "Tests on Rectangular Hollow Sections to Investigate the Effect of Variation of Yield Stress Around a Section", *Investigation Report S885*, Centre for Advanced Structural Engineering, School of Civil and Mining Engineering, University of Sydney.

British Standards Institute, (1990), British Standard *BS5950 Part 1: Code of Practice for Design in Simple and Continuous Construction: hot-rolled sections, Structural use of Steelwork in Building*, London, United Kingdom.

Canadian Standards Association, (1994), Canadian Standard *S16.1-94 Limit States Design of Steel Structures*, Etobicoke, Ontario, Canada.

Dwyer T. J., and Galambos T.V., (1965), "Plastic Behaviour of Tubular Beam-Columns", *Journal of the Structural Division*, American Society of Civil Engineers, Vol. 91, No. ST4, pp 153-168.

European Committee for Standardisation, (1992), *Design of Steel Structures: Part 1.1 - General Rules and Rules for Buildings*, (known as "Eurocode 3"), DD ENV. 1993-1-1, Eurocode 3 Editorial Group.

Hasan S. W., and Hancock G. J., (1988), "Plastic Bending Tests of Cold-Formed Rectangular Hollow Sections", *Research Report*, No. R586, School of Civil and Mining Engineering, The University of Sydney, Sydney.

Johnston B. G. (ed), (1976), *Guide to Stability Design Criteria for Metal Structures*, Appendix B: Technical Memorandums of the Column Research Council, John Wiley, Sydney, Australia.

Key P. W., and Hancock G. J., (1993), "A Theoretical Investigation of the Column Behaviour of Cold-Formed Square Hollow Sections", *Thin-Walled Structures*, Vol. 16, Nos 1-4, pp 31 - 64.

Korol R. M., and Hudoba J., (1972), "Plastic Behaviour of Hollow Structural Sections", *Journal of the Structural Division*, American Society of Civil Engineers, Vol. 98, No. ST5, pp 1007-1023.

Standards Australia, (1991), Australian Standard *AS 1163 Structural Steel Hollow Sections*, Standards Australia, Sydney.

Standards Australia, (1990), Australian Standard *AS 4100 Steel Structures*, Standards Australia, Sydney.

Standards Australia, (1991), Australian Standard *AS 1391 Methods for Tensile Testing of Metals*, Standards Australia, Sydney.

Sedlacek G. And Feldmann M., (1995), *The b/t ratios Controlling the Applicability of Analysis models in Eurocode 3, Part 1.1*, Background Document 5.09 for Chapter 5 of Eurocode 3, Part 1.1, Aachen, Germany.

Tubemakers, (1994), *Design Capacity Tables for DuraGal Steel Hollow Sections*, Tubemakers of Australia Limited, Structural Products Division, Newcastle, N.S.W.

Zhao X. L. and Hancock G. J., (1990), "T-Joints in Rectangular Hollow Sections Subject to Combined Actions", *Journal of Structural Engineering*, ASCE, Vol 117, No. 8, pp 2258-2277.

Zhao X.L. & Hancock G.J. (1991), "Tests to Determine Plate Slenderness Limits for Cold-Formed Rectangular Hollow Sections of Grade C450", *Steel Construction*, Journal of Australian Institute of Steel Construction, 25 (4), Nov 1991, pp 2-16.

Zhao X. L. and Hancock G. J., (1992), "Square and Rectangular Hollow Sections Subject to Combined Actions", *Journal of Structural Engineering*, ASCE, Vol 118, No. 3, pp 648-668.

Zhao X. L., Hancock G. J., and Trahair N. S., (1995), "Lateral Buckling Tests of Cold-Formed RHS Beams", *Journal of Structural Engineering*, ASCE, Vol. 121, No. 11, pp 1565-1573.

6 NOTATION

A_g Gross cross section area
A_{gn} Nominal gross cross section area
b Width of RHS, or width of plate
d Depth of RHS
E Young's modulus of elasticity
E_n Nominal Young's modulus of elasticity
e_f Strain after failure
e_u Strain at which ultimate tensile strength (f_u) occurs
e_y Yield strain
f_o Elastic local buckling stress
f_u Ultimate tensile strength
f_{un} Nominal ultimate tensile strength
f_y Yield stress
f_{yn} Nominal yield stress
I Second moment of area
k Plate buckling coefficient
L_1 Length between loading plates
L_2 Length between supports
L_{sc} Length of stub column
M_{max} Maximum bending moment
M_p Plastic bending moment
M_{pn} Nominal plastic bending moment (based on nominal dimensions and nominal yield stress)
M_y Bending moment at first yield
N_{max} Maximum load in stub column test
N_s Stub column capacity
N_y Yield load ($=A_g f_y$)
R Rotation capacity
r_e External corner radius of RHS
r_y Radius of gyration about y axis
S_o Original cross sectional area of tensile coupon
t Thickness of RHS, or thickness of plate
δ "Bow-out" imperfection
κ Curvature
κ_p Plastic curvature ($= M_p/EI$)
λ_f Flange slenderness
λ_w Web slenderness
ν Poisson's ratio

APPENDIX A EFFECT OF LOADING METHOD

A.1 LOADING METHODS

Section 2.5.1 describes the plastic bending tests on RHS using the parallel plate method (see Figure 3). This setup has been used at the University of Sydney for bending tests on RHS for many years (Hasan and Hancock (1988), Zhao and Hancock (1991)). Some of the bending tests were repeated using alternate loading arrangements to detect if the different methods significantly affect the rotation capacity of the RHS.

A.1.1 Parallel Plate

In this procedure (already described in detail in Section 2.5.1), load was transferred from the spreader beam via a set of half rounds and a thick steel plate. This plate bore upon the loading plates which were welded onto the webs of the RHS so that they were parallel to the webs. The welds were vertical over the full length of the web.

A.1.2 Perpendicular Plate

For the perpendicular plate method, the loading plates were welded perpendicular to the web of the RHS as shown in Figure A.1. Two plates were welded on each side at each loading point. Care was taken to ensure full contact for the bearing between these plates and the load transfer plate. In all other respects the loading mechanism is the same as the first. This method was used to see whether the parallel plate method inadvertently strengthened the section.

A.1.3 Pin Loading

The pin loading system involved a steel pin through the neutral axis of the RHS. A hole was drilled through the RHS and short channel sections either side of the RHS and a pin inserted. Load was transferred by bearing from the spreader beam to the channel sections, and in turn from the channel to the pin and the bending specimen. The pin allowed rotation of the beam. Teflon pads between the spreader beam and the channels allowed longitudinal movement. The webs of both the RHS and the channels were reinforced with additional plates to avoid local bearing failure. Figure A.2 demonstrates this loading technique.

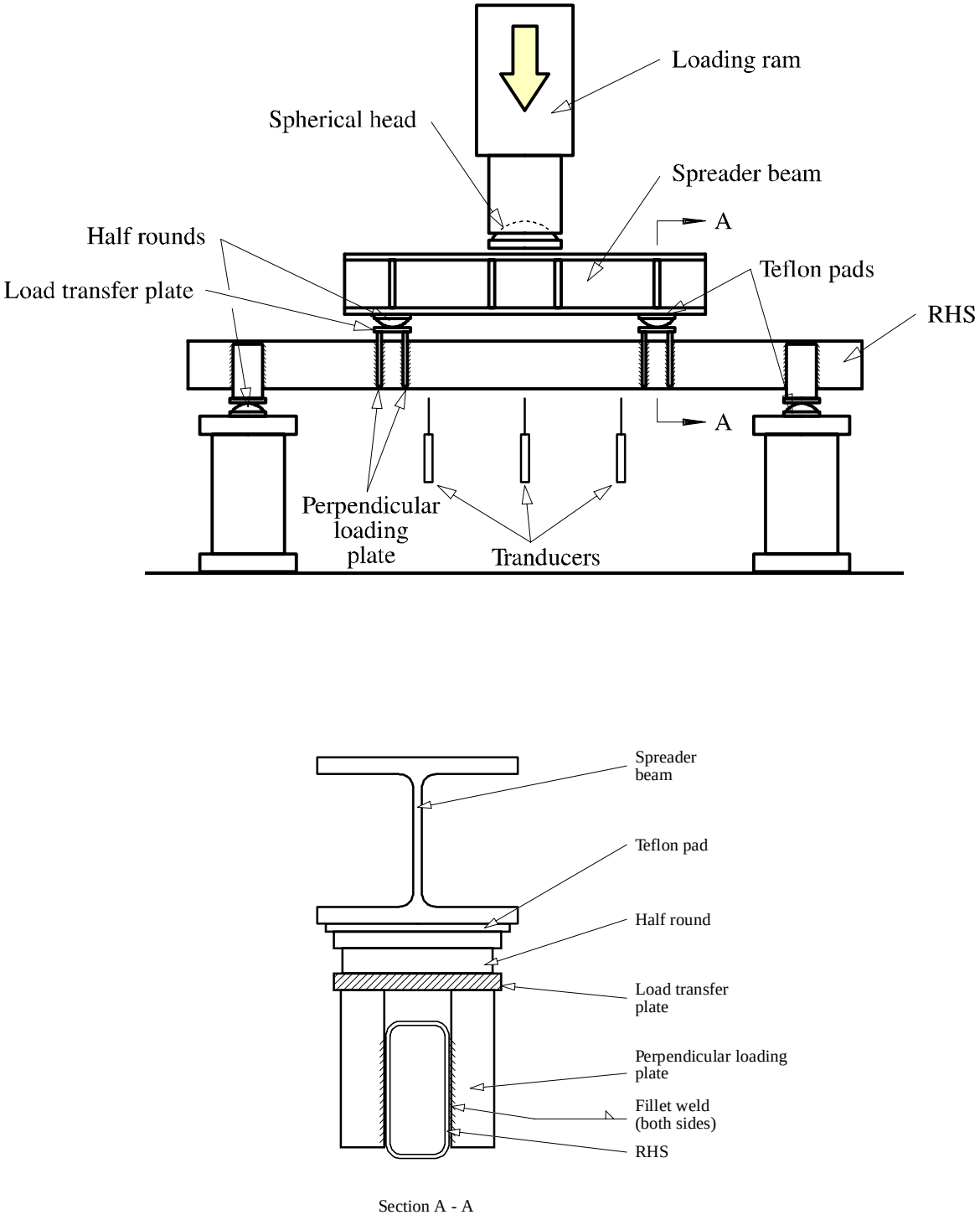

Figure A.1: The Perpendicular Plate Loading Method

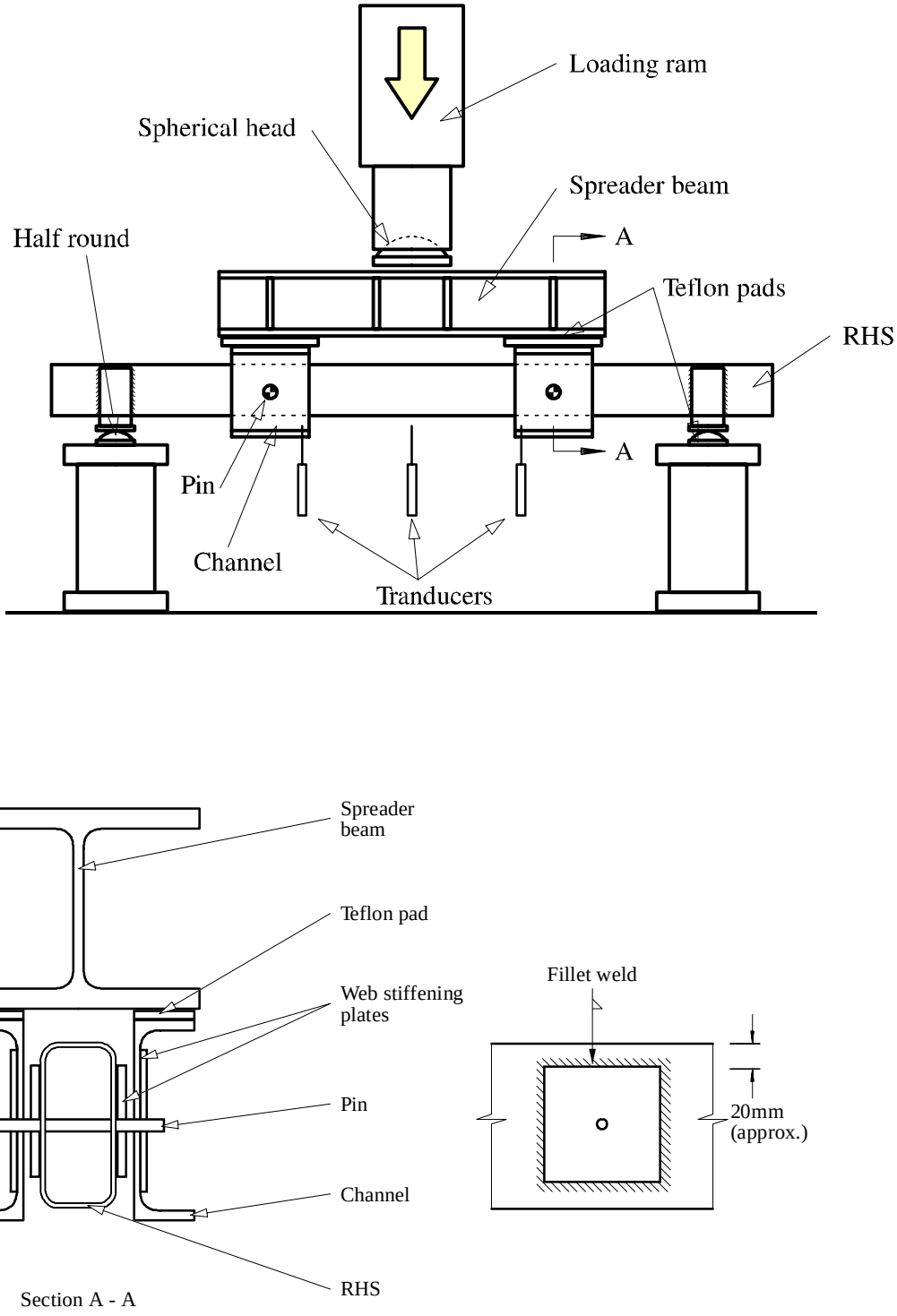

Figure A.2: The Pin Loading Method

A.2 RESULTS

The results of the bending tests with the alternative methods are given in Table A.1 which lists the ratio M_{max}/M_p and R for each test. This table repeats the results of the parallel plate tests in Table 5. There are two additional columns in Table A.1, each called the "Rotation ratio". The rotation ratio is defined as the rotation capacity using either the perpendicular or pin method divided by the average rotation capacity achieved in the parallel tests for that section size and grade.

All specimens experienced mainly web local buckling, except the square hollow sections (100 × 100 × 3.0 C450) which failed by mainly flange local buckling. The local buckle in specimen BS09A - 75 × 25 × 1.6 C450 (loaded by the perpendicular method) occurred adjacent to the loading plate. This restrained the buckle and hence there was not a rapid shedding of load associated with this failure. No specimen failed due to insufficient material ductility.

The moment-curvature relations and the measured dimensions for each specimen are given in Appendix B. Each graph shows all curves for a given size RHS, and it is possible to compare directly each method on this range of RHS. Figure A.3 plots the web slenderness against the rotation capacity and compares each loading method.

On average the perpendicular plate method gave an extra 16% rotation capacity. The pin loading method produced, on average, an extra 19% rotation capacity. However these averages have been boosted by three tests (BS04A - 150 × 50 × 2.5 C450 - perpendicular, BS06A - 100 × 50 × 2.0 C450 - perpendicular, and BS17A - 100 × 50 × 2.0 C450 - pin) which had rotation ratios of 1.69, 1.63, and 2.0 respectively. For all the other tests, there was no significant effect on the rotation capacity. These three specimens exhibit Non-Compact or Class 2 behaviour (M_p is reached but the rotation capacity is insufficient). The loading method did not change the behaviour to Compact. M_{max} was barely affected by altering the loading arrangement.

Section	Slenderness (AS 4100)		Parallel Plate		Perpendicular Plate			Pin Loading		
	Web λ_w	Flange λ_f	$\frac{M_{max}}{M_p}$	Rotation capacity R	$\frac{M_{max}}{M_p}$	Rotation capacity R	Rotation ratio	$\frac{M_{max}}{M_p}$	Rotation capacity R	Rotation ratio
150 × 50 × 4.0 C450	49	14	1.27 1.19	6.6 7.7				1.24	7.2	1.01
150 × 50 × 2.5 C450	75	23	1.02 1.00	1.4 1.2	1.08	2.2	1.69	1.11	1.1	0.85
100 × 50 × 2.0 C450	63	30	1.07 1.01	0.8 0.8	1.07	1.3	1.63	1.08	1.6	2.0
75 × 25 × 1.6 C450	62	19	1.08 1.13	2.2 2.5	1.09	2.5	1.06			
150 × 50 × 3.0 C350	59	18	1.21 1.15	4.1 3.6	1.18	3.2	0.83	1.21	3.6	0.94
125 × 75 × 3.0 C350	52	30	1.03 1.03	1.5 1.6	1.02	1.4	0.90			
125 × 75 × 2.5 C350	60	35						1.06	1.1	
100 × 100 × 3.0 C450	44	44	1.02	0.8	0.95	0.7*	0.88	1.03	0.9	1.13
Average							1.16			1.19

Note: * for 100 × 100 × 3.0 a value of R is given as κ_b/κ_p -1, where κ_b is the curvature at which local buckling occurred since this specimen had similar failure curvature to the other 100 × 100 × 3.0 specimens but just failed to reach M_p.

Table A.1: Summary of Bending Test Results

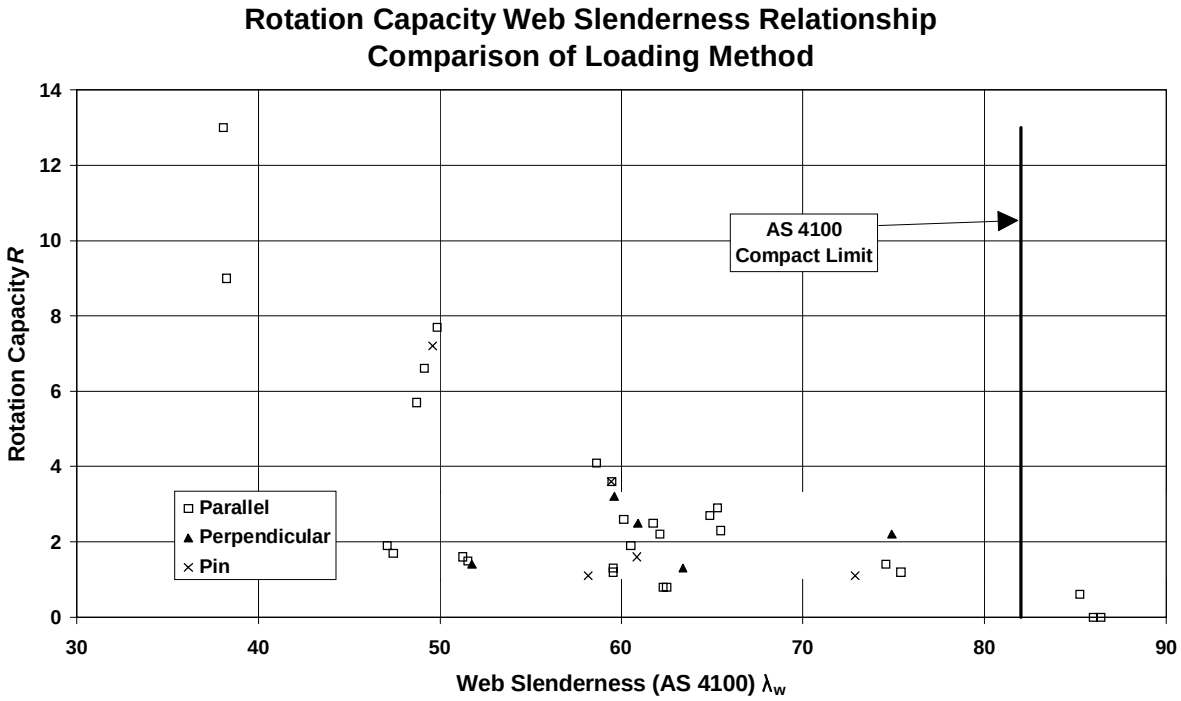

Figure A.3: Web Slenderness - Rotation Capacity: Effect of Loading Method

APPENDIX B PLASTIC BENDING TESTS

This section contains the non-dimensional moment-curvature relationships for each plastic bending test. The measured dimensions of each RHS are given in Table B.1 Since there were up to four tests performed on one particular size and stress grade of RHS, all tests for the one size RHS are shown on the one graph.

Specimen	Cut from section	Loading method	d (mm)	b (mm)	t (mm)	r_e (mm)	f_y (MPa)	M_{pn} (kNm)	M_p (kNm)	M_{max} (kNm)	$\frac{M_{max}}{M_p}$	R
BS01B	150×50×5.0	Parallel	151.04	50.25	4.92	9.9	441	35.49	35.51	43.80	1.23	13.0
BS01C	C450	Parallel	150.92	50.41	4.90	10.7	441	35.49	35.14	41.10	1.17	9.0
BS02B	150×50×4.0	Parallel	150.43	50.27	3.92	6.8	457	29.45	30.32	38.60	1.27	6.6
BS02C	C450	Parallel	150.44	50.40	3.87	7.3	457	29.45	29.86	35.50	1.19	7.7
BS02A		Pin	150.42	50.11	3.89	7.3	457	29.45	29.93	37.30	1.24	7.2
BS03A	150×50×3.0	Parallel	150.47	50.22	2.97	5.9	444	23.14	22.76	26.20	1.15	2.7
BS03B	C450	Parallel	150.79	50.01	2.95	5.8	444	23.14	22.68	26.30	1.16	2.3
BS03C		Parallel	150.80	50.34	2.96	5.7	444	23.14	22.81	25.80	1.13	2.9
BS04B	150×50×2.5	Parallel	150.43	50.15	2.60	4.6	446	19.58	20.30	20.80	1.02	1.4
BS04C	C450	Parallel	150.39	50.41	2.57	4.6	446	19.58	20.13	20.20	1.00	1.2
BS04A		Perp.	150.35	50.23	2.59	4.8	446	19.58	20.18	21.80	1.10	2.2
BS16A		Pin	150.31	50.40	2.64	5.3	440	19.58	20.28	22.60	1.11	1.1
BS05A	150×50×2.3	Parallel	150.65	50.64	2.25	4.6	444	18.13	17.73	17.40	0.98	0.0
BS05B	C450	Parallel	150.51	50.57	2.28	4.2	444	18.13	17.96	18.20	1.01	0.6
BS05C		Parallel	150.37	50.70	2.26	4.8	444	18.13	17.71	17.30	0.98	0.0

Table B.1: Summary of Results/Dimensions for Bending Tests

Specimen	Cut from section	Loading method	d (mm)	b (mm)	t (mm)	r_e (mm)	f_y (MPa)	M_{pn} (kNm)	M_p (kNm)	M_{max} (kNm)	$\frac{M_{max}}{M_p}$	R
BS06B	100×50×2.0	Parallel	100.45	50.70	2.06	3.8	449	8.33	8.70	9.30	1.07	0.8
BS06C	C450	Parallel	100.49	50.55	2.07	3.9	449	8.33	8.71	8.80	1.01	0.8
BS06A		Perp.	100.46	50.24	2.04	4.7	449	8.33	8.47	9.30	1.07	1.3
BS17A		Pin	100.45	50.22	2.04	3.4	423	8.33	7.91	8.75	1.08	1.6
BS07B	75×50×2.0	Parallel	75.48	50.10	1.94	4.4	411	5.38	4.80	5.00	1.04	1.7
BS07C	C450	Parallel	75.63	50.31	1.95	4.4	411	5.38	4.86	4.96	1.02	1.9
BS08B	75×25×2.0	Parallel	75.31	25.28	1.98	3.7	457	3.74	3.82	4.24	1.11	5.7
BS08C	C450	Parallel	75.33	25.23	1.95	4.0	457	3.74	3.75	4.25	1.13	*
BS09B	75×50×1.6	Parallel	75.24	25.12	1.54	3.1	439	3.07	2.84	3.16	1.08	2.2
BS09C	C450	Parallel	74.90	25.20	1.54	3.4	439	3.07	2.82	3.25	1.13	2.5
BS09A		Perp.	74.98	25.08	1.56	3.9	439	3.07	2.83	3.10	1.09	2.5
BS10B	75×50×1.6	Parallel	75.27	25.12	1.55	3.4	422	2.39	2.81	2.90	1.03	1.9
BS10C	C350	Parallel	75.19	25.25	1.56	3.4	422	2.39	2.82	2.82	1.00	2.6
BS11B	150×50×3.0	Parallel	150.46	50.13	3.00	6.2	370	18.00	19.11	23.20	1.21	4.1
BS11C	C350	Parallel	150.50	50.19	2.96	6.5	370	18.00	18.84	21.70	1.15	3.6
BS20A		Perp.	150.45	50.51	3.00	6.8	382	18.00	19.69	23.20	1.18	3.2
BS20B		Pin	150.38	50.51	3.00	6.3	382	18.00	19.79	23.90	1.21	3.6
BS12B	100×50×2.0	Parallel	100.91	50.43	2.06	3.6	400	6.48	7.77	7.70	1.00	1.1
BS12C	C350	Parallel	100.83	50.52	2.05	3.8	400	6.48	7.75	7.75	1.00	1.3

Table B.1 (continued): Summary of Results/Dimensions for Bending Tests

Specimen	Cut from section	Loading method	d (mm)	b (mm)	t (mm)	r_e (mm)	f_y (MPa)	M_{pn} (kNm)	M_p (kNm)	M_{max} (kNm)	$\frac{M_{max}}{M_p}$	R
BS13B	125×75×3.0 C350	Parallel	125.56	75.84	2.92	6.6	397	16.54	18.42	18.90	1.03	1.5
BS13C		Parallel	125.40	75.74	2.93	6.9	397	16.54	18.40	19.10	1.04	1.6
BS13A		Perp.	125.40	75.56	2.91	7.1	397	16.54	18.20	18.70	1.03	1.4
BS21A	125×75×2.5 C350	Pin	125.40	75.10	2.53	3.9	374	13.99	15.32	16.25	1.06	1.1
BS19A	100×100×5.0 C450	Parallel	100.43	100.27	2.88	5.2	445	18.54	17.86	18.16	1.02	0.8
BS19B		Pin	100.53	100.33	2.91	5.0	445	18.54	18.09	17.30	0.95	0.7
BS19C		Perp.	100.53	100.25	2.86	5.2	445	18.54	17.78	18.40	1.03	0.9

Table B.1 (continued): Summary of Results/Dimensions for Bending Tests

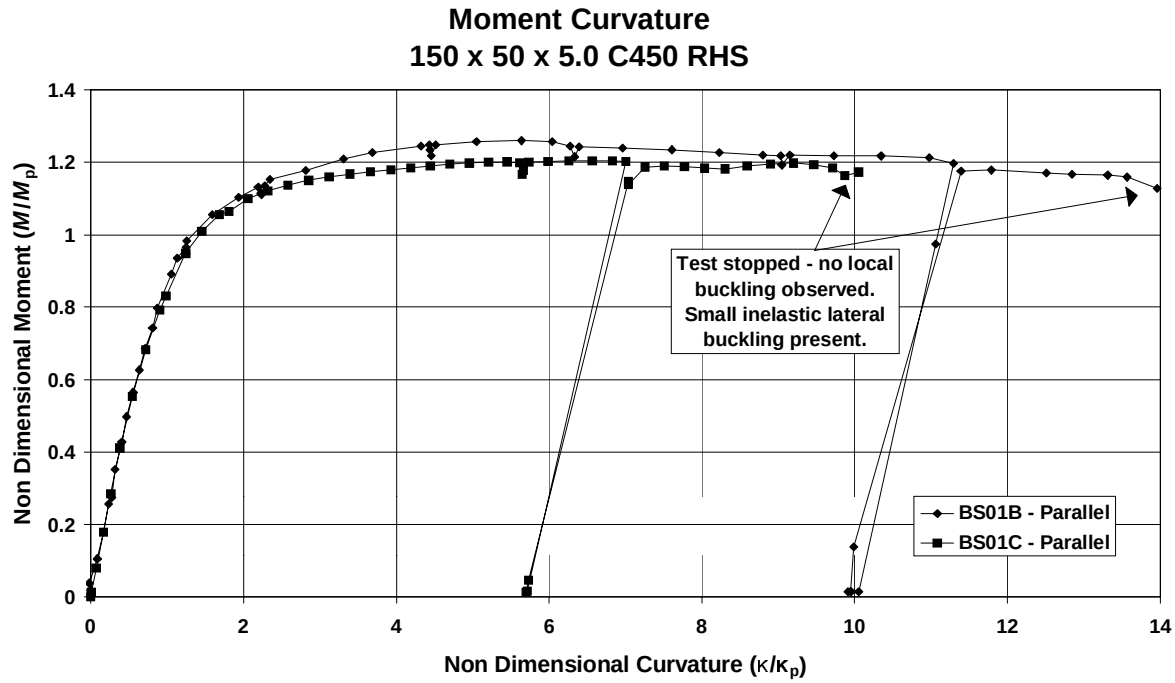
Moment Curvature
150 x 50 x 5.0 C450 RHS
Non Dimensional Moment (M/Mp)
Non Dimensional Curvature (κ/κp)
Test stopped - no local buckling observed. Small inelastic lateral buckling present.
BS01B - Parallel
BS01C - Parallel

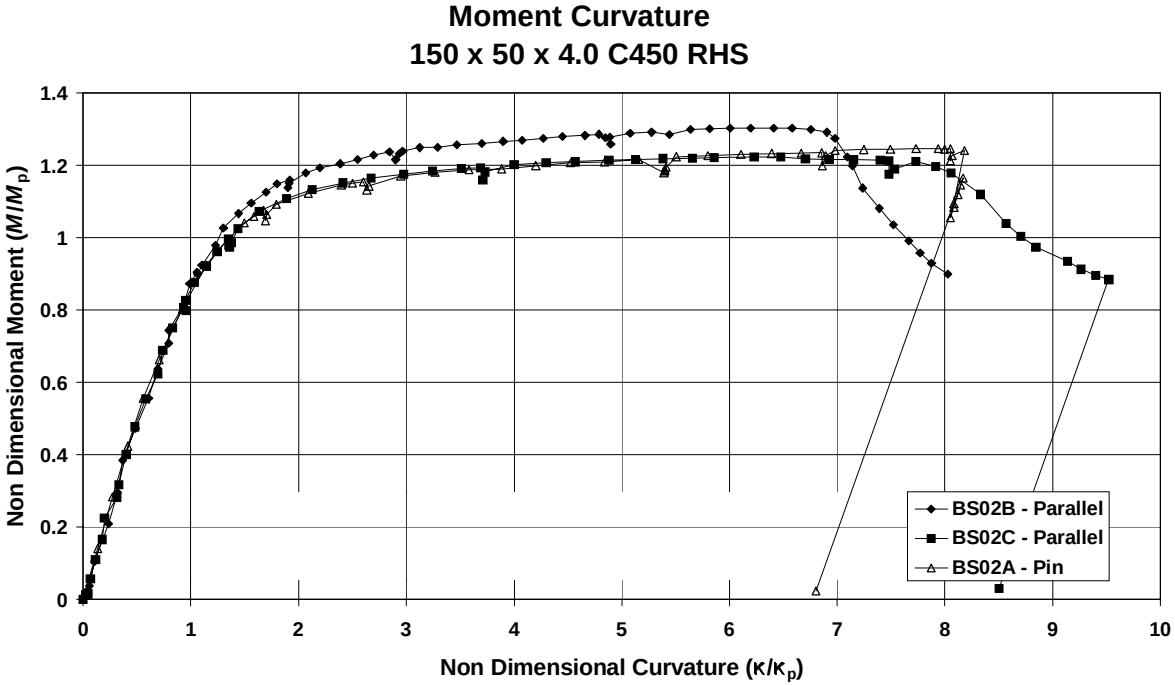
Moment Curvature
150 x 50 x 4.0 C450 RHS
Non Dimensional Moment (M/Mp)
Non Dimensional Curvature (κ/κp)
BS02B - Parallel
BS02C - Parallel
BS02A - Pin

Moment Curvature
150 x 50 x 3.0 C450 RHS

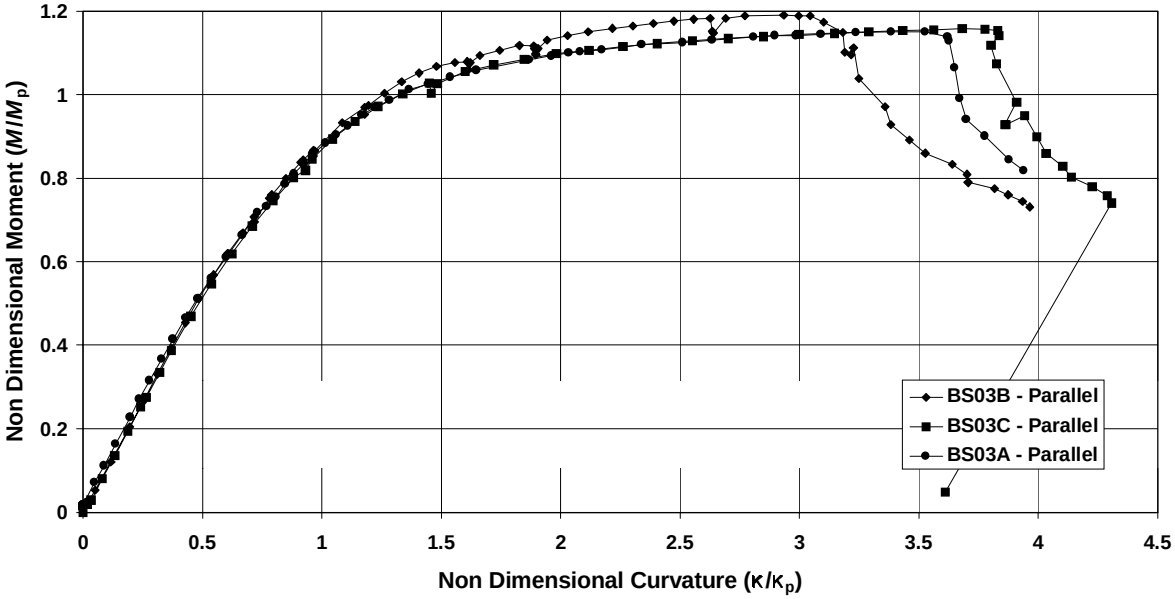

Moment Curvature
150 x 50 x 2.5 C450 RHS

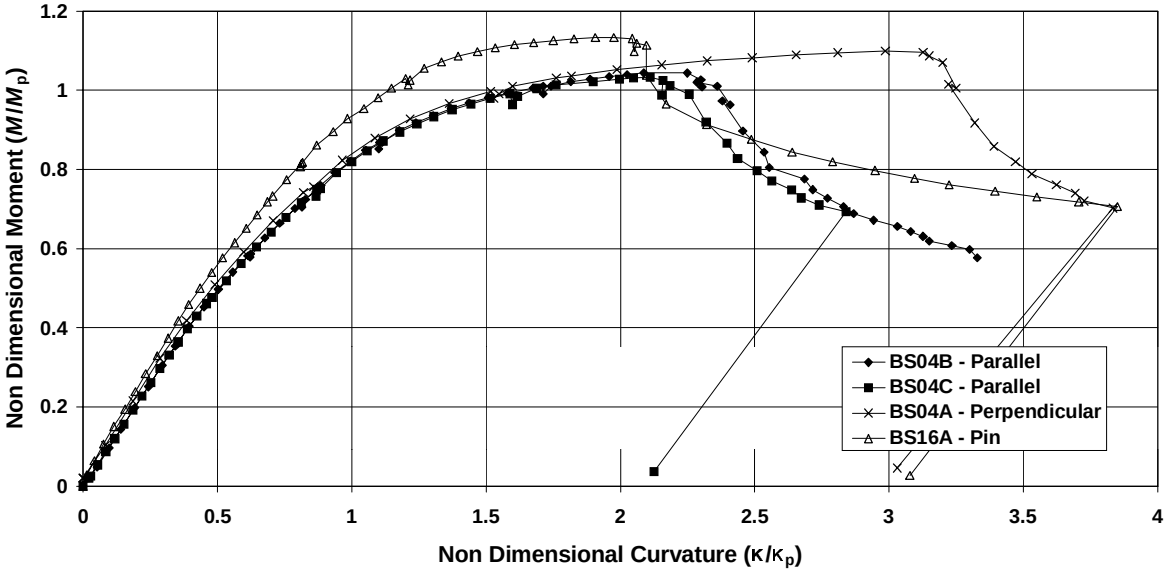

Moment Curvature
150 x 50 x 2.3 C450 RHS

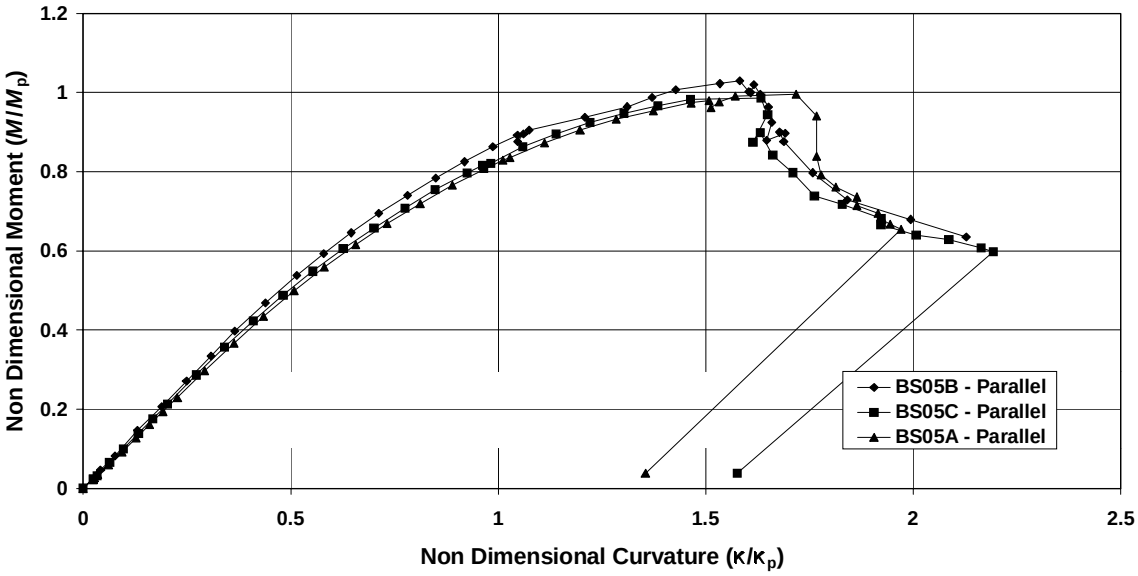

Moment Curvature
100 x 50 x 2.0 C450 RHS

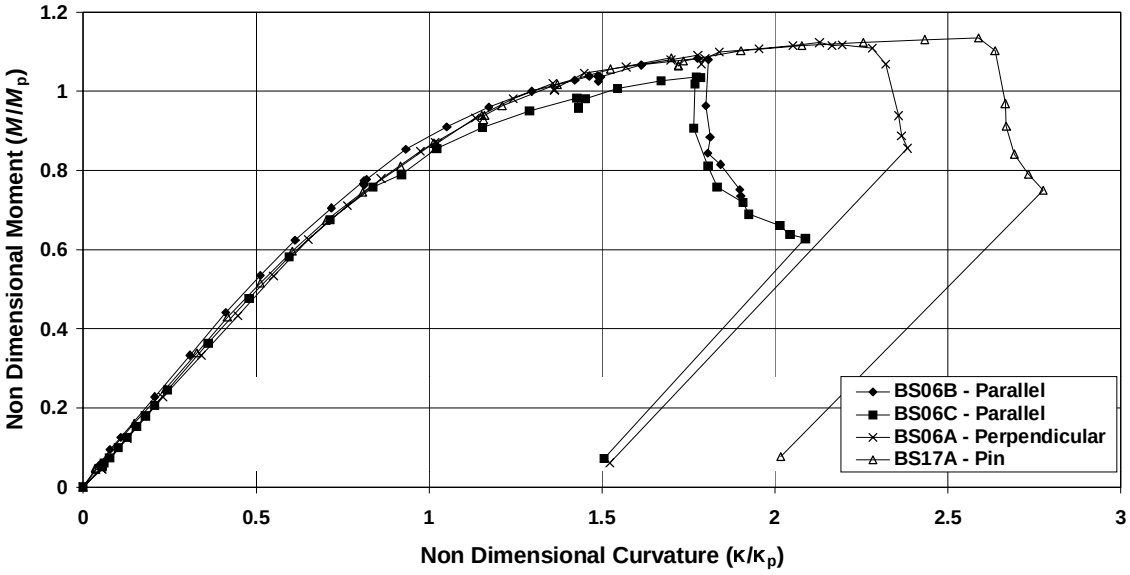

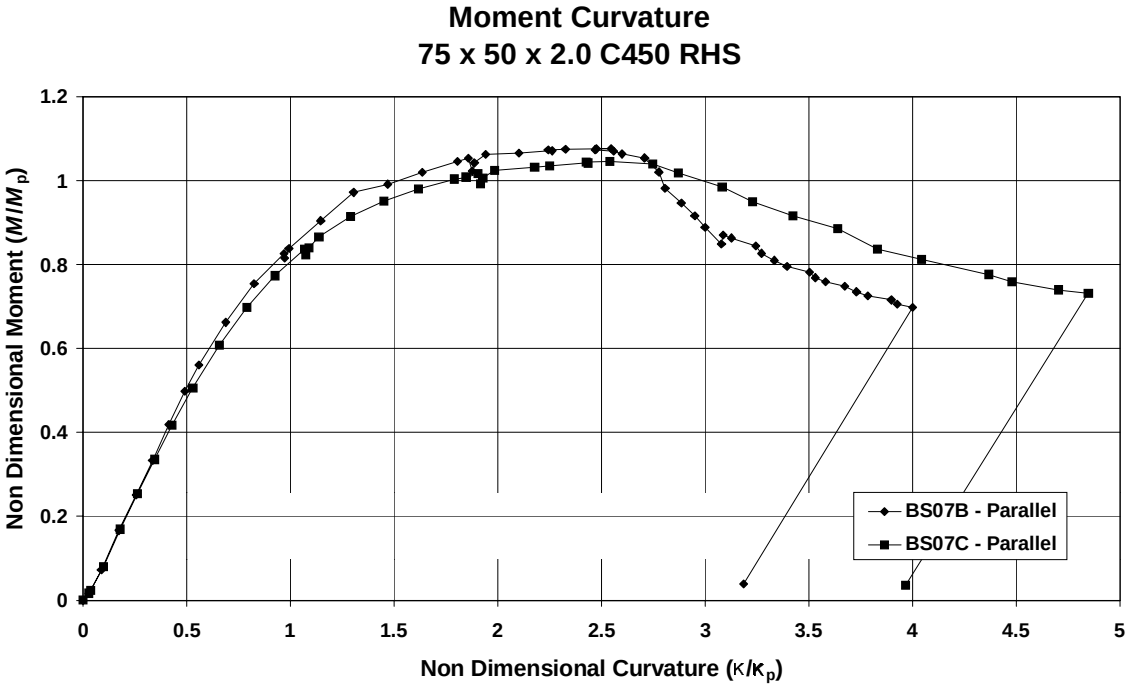
Moment Curvature
75 x 50 x 2.0 C450 RHS
Non Dimensional Moment (M/Mp)
Non Dimensional Curvature (κ/κp)
BS07B - Parallel
BS07C - Parallel
0
0.2
0.4
0.6
0.8
1
1.2
0
0.5
1
1.5
2
2.5
3
3.5
4
4.5
5

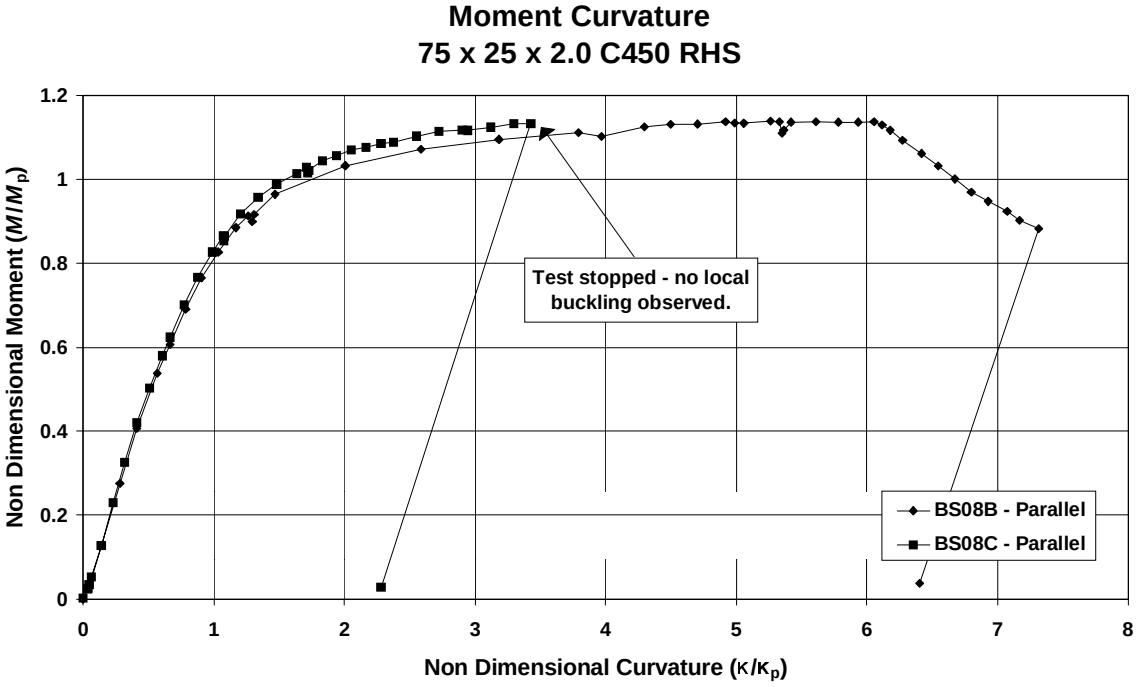
Moment Curvature
75 x 25 x 2.0 C450 RHS
Non Dimensional Moment (M/Mp)
Non Dimensional Curvature (κ/κp)
Test stopped - no local buckling observed.
BS08B - Parallel
BS08C - Parallel
0
0.2
0.4
0.6
0.8
1
1.2
0
1
2
3
4
5
6
7
8

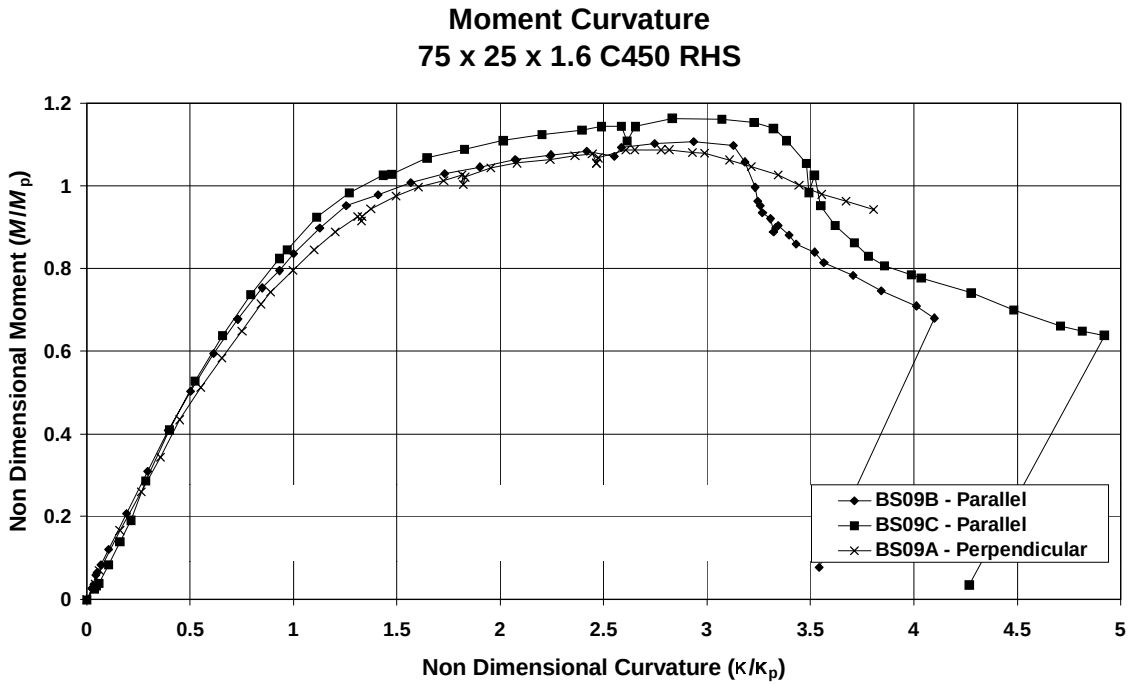
Moment Curvature
75 x 25 x 1.6 C450 RHS
Non Dimensional Moment (M/Mp)
Non Dimensional Curvature (κ/κp)
BS09B - Parallel
BS09C - Parallel
BS09A - Perpendicular

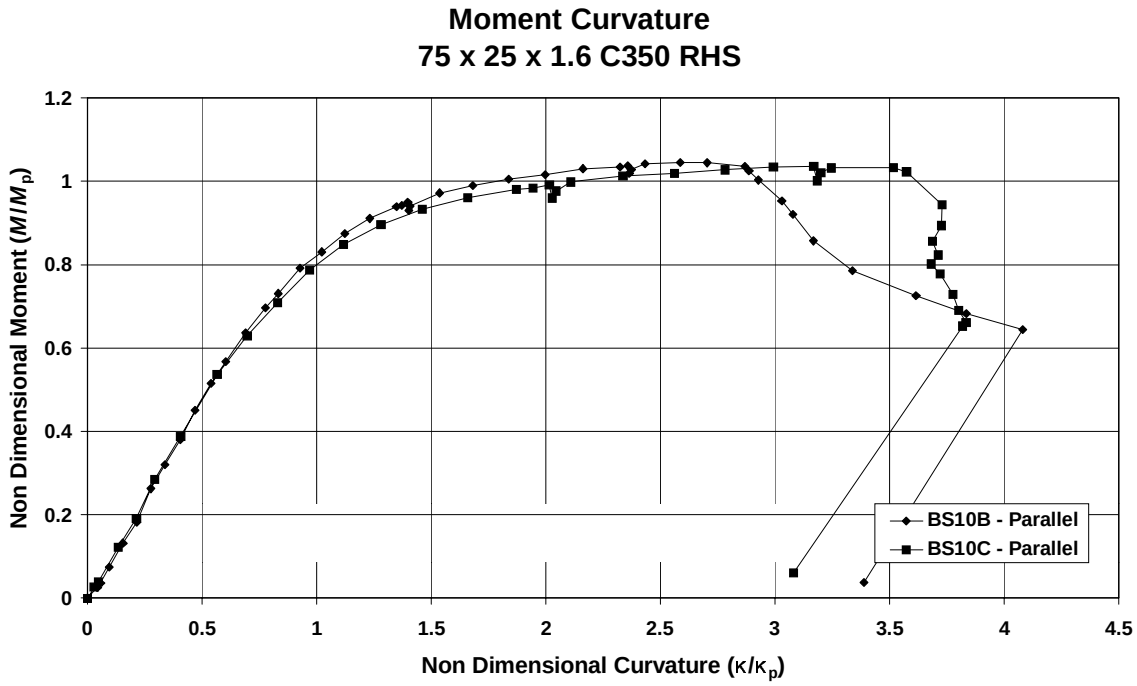
Moment Curvature
75 x 25 x 1.6 C350 RHS
Non Dimensional Moment (M/Mp)
Non Dimensional Curvature (κ/κp)
BS10B - Parallel
BS10C - Parallel

Moment Curvature
150 x 50 x 3.0 C350 RHS

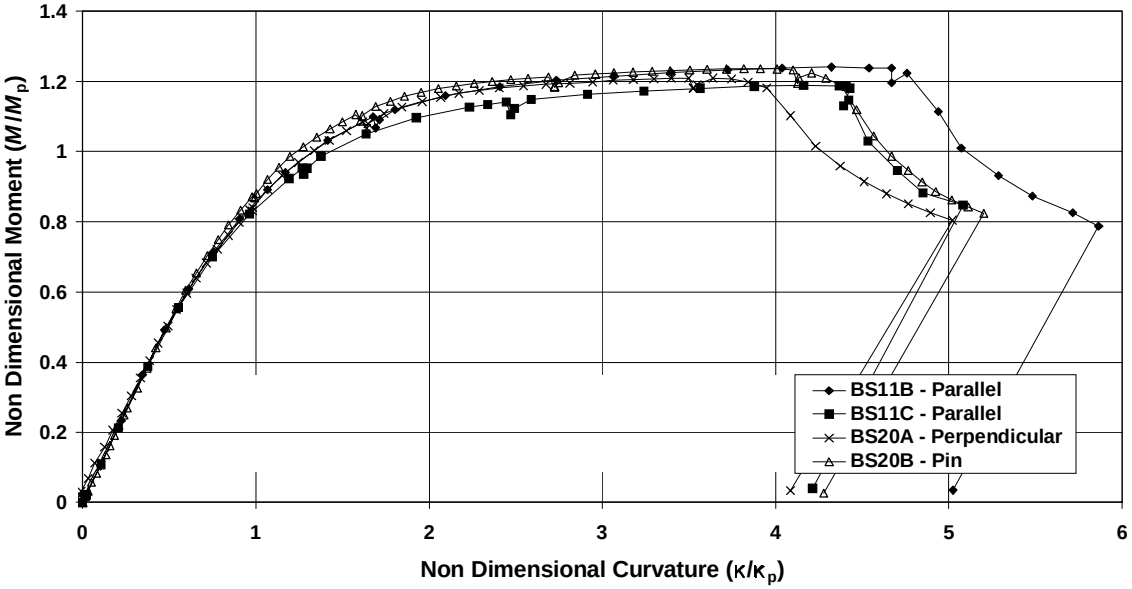

Moment Curvature
100 x 50 x 2.0 C350 RHS

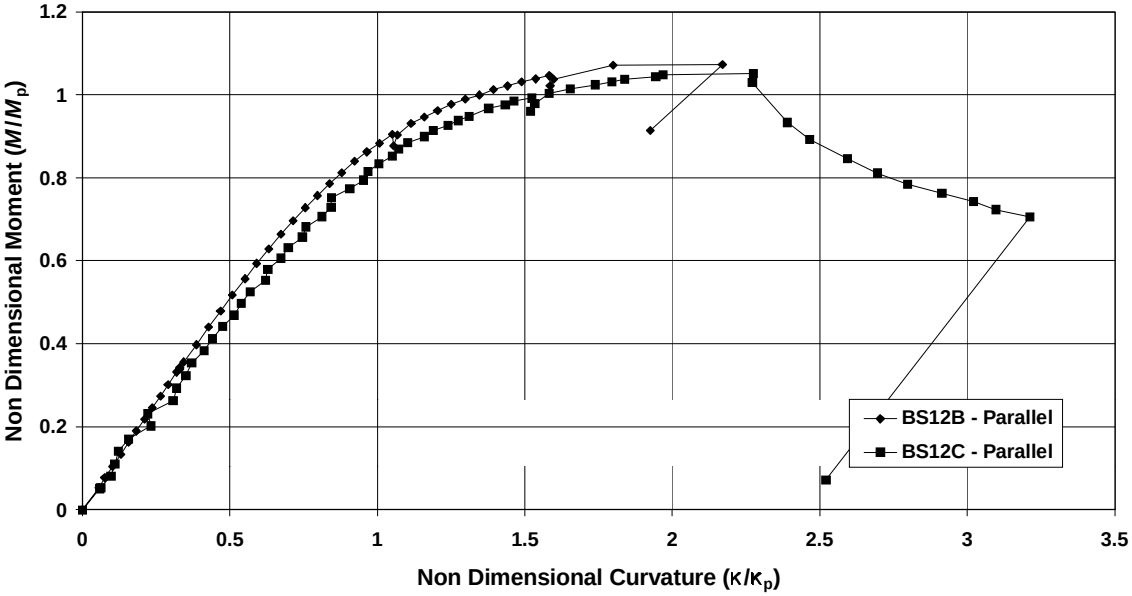

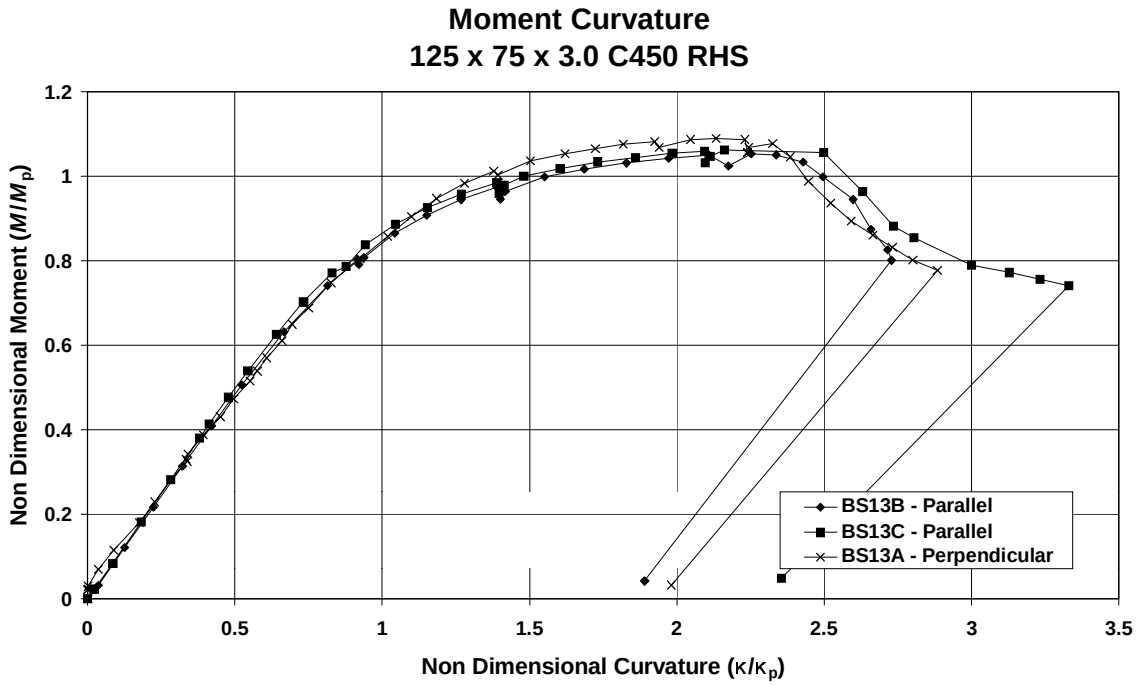
Moment Curvature
125 x 75 x 3.0 C450 RHS
Non Dimensional Moment (M/Mp)
Non Dimensional Curvature (κ/κp)
BS13B - Parallel
BS13C - Parallel
BS13A - Perpendicular
0
0.2
0.4
0.6
0.8
1
1.2
0.5
1.5
2
2.5
3
3.5

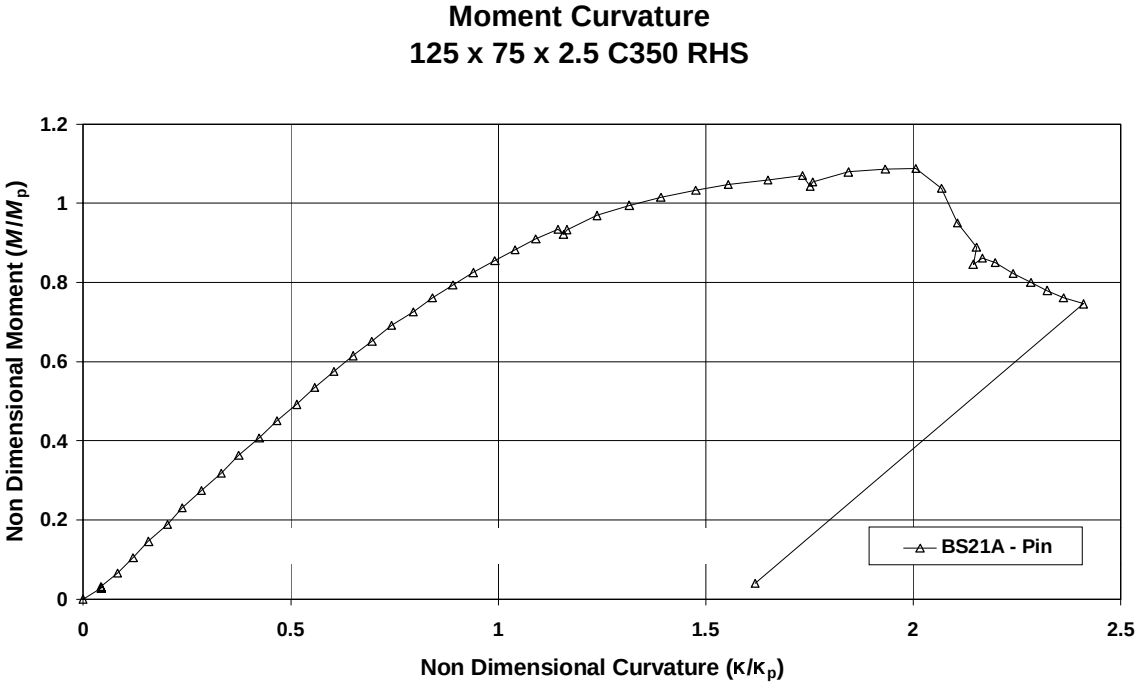
Moment Curvature
125 x 75 x 2.5 C350 RHS
Non Dimensional Moment (M/Mp)
Non Dimensional Curvature (κ/κp)
BS21A - Pin
0
0.2
0.4
0.6
0.8
1
1.2
0.5
1.5
2
2.5

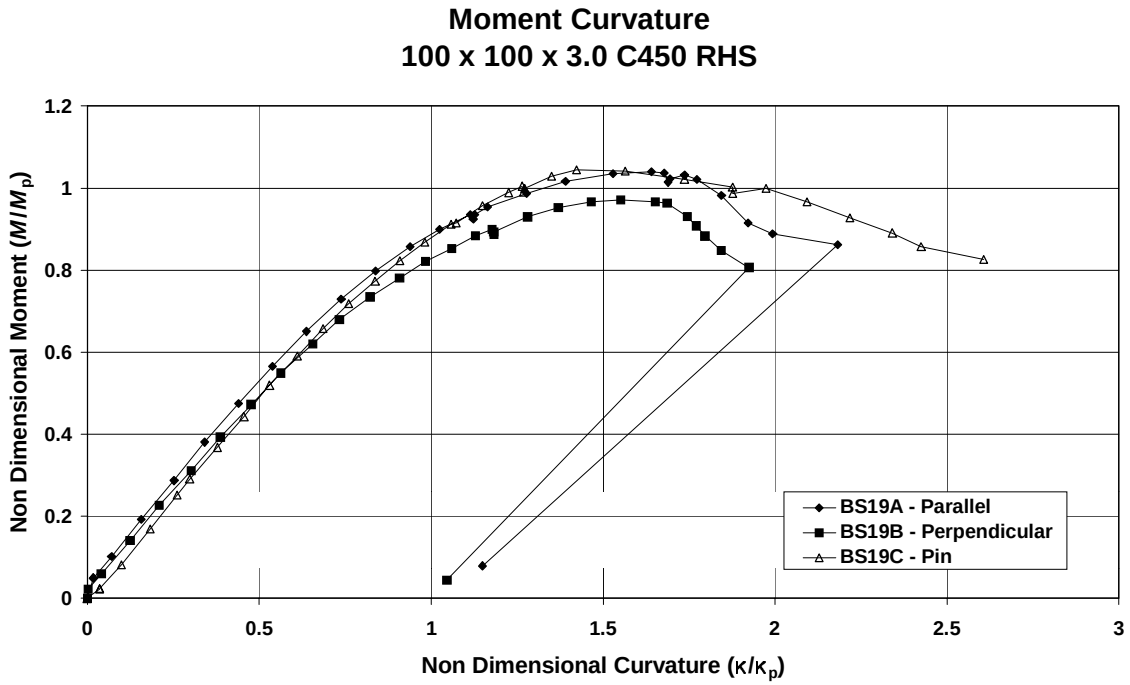
Moment Curvature
100 x 100 x 3.0 C450 RHS
Non Dimensional Moment (M/Mp)
Non Dimensional Curvature (κ/κp)
1.2
1
0.8
0.6
0.4
0.2
0
0
0.5
1
1.5
2
2.5
3
BS19A - Parallel
BS19B - Perpendicular
BS19C - Pin

APPENDIX C TENSILE COUPON TESTS

C.1 PROCEDURE

Three coupons were taken from the flats of each tube. One was cut from the face opposite the weld, and one from each side adjacent to the weld. A coupon was also taken from each of the four corners of most RHS. Figure 1 shows the position of these faces with respect to the weld.

The tensile coupons were prepared and tested to Australian Standard AS 1391 (Standards Australia (1991)). The flat coupons were instrumented with linear strain gauges. An extensometer was used to measure strain for the corner coupons. The coupons were tested in a 250 kN capacity INSTRON Universal Testing Machine with friction grips to apply the loading. A SPECTRA data acquisition system recorded the load and strain gauge readings. A constant strain rate of approximately 1.3×10^{-4} s^{-1} for the flats and 1.0×10^{-4} s^{-1} for the corners was used. Near the yield and ultimate stresses, the machine was halted for one minute to obtain a value of the static stress.

C.2 RESULTS

Values of the yield stress (f_y), ultimate stress (f_u) and percentage elongation after failure (e_f) on a gauge length of $5.65\sqrt{S_o}$ were obtained from each test (S_o is the original area of the coupon). As the yielding was gradual, the yield stress quoted is the 0.2% proof stress. The stress-strain curve was linear only for small strains. The Young's modulus of elasticity (E) was calculated by averaging the slope of the curve over this initial region. An important parameter in the ductility requirements for plastic design is the ratio f_u/f_y, which is also tabulated. For the corner coupons it was not possible to determine a value of E with great precision since an extensometer was used, so it is assumed that E = 200 GPa for the corners.

Results are summarised in Table C.2. The stresses listed are *static* values, while the graphs depict both static and dynamic stresses. (The static stresses were those obtained after the machine has been stopped for one minute. The dynamic stresses were recorded while the testing machine is still moving.) For low strain (typically $\leq$ 30000 μstrain) the strain was the average from the gauges (or the extensometer reading for the corner coupons). Above this, the gauges failed and strain was calculated as the change in length divided by the original length (65 mm for the flat coupons and 90 mm for corners).

The "approximate" strain cannot be reliably compared to the strain gauge strain since there was some extension of the sample and the testing machine outside the assumed gauge length. However along the reasonably flat yield plateau the load was approximately constant and most extension would have occurred within the assumed gauge length. On each stress-strain curve, the approximate location of this changeover point is marked by a solid line.

The average of the yield stress values from both of the adjacent faces is used in the calculation of section capacities (plastic moment (M_p) and yield load (N_y)). The mean of the Young's modulus of elasticity from both of the adjacent faces is used in stiffness calculations. These average values are also listed in Table 3.

The yield stress of the face opposite the weld is on average 10% higher than that of the adjacent faces. This has been previously documented (CASE (1992)) and is a result of the forming process. The corners of the RHS have even higher yield stress due to the extra working at those locations but reduced ductility. The yield stress of the corners is on average approximately 20% higher than that of the adjacent faces.

One measure of material ductility is the ratio e_u/e_y, where e_u is the strain at which the ultimate tensile strength (f_u) is reached and e_y is the yield strain. Since the ultimate stress nearly always occurred after the strain gauges broke, it was not possible to obtain a precise value of e_u and hence a range of ratios is reported. Using the approximate strain described above, the ratios obtained are given in Table C.1.

Specimen		Range of e_u/e_y values
Grade C450	Flats	10 - 20
	Corners	2 - 5
Grade C350	Flats	15 - 30
	Corners	2 - 5

Table C.1: Range of e_u/e_y values

Since considerable rotations can occur in plastic design, large strains occur. Certain material ductility requirements are specified for plastic design, given in Section 1.2. None of the sections tested fulfil all the material requirements of either AS 4100 or Eurocode 3. The requirement that $f_u/f_y > 1.2$ was never satisfied, while the strain after fracture, $e_f > 15$ %, was achieved for approximately 90 % of the coupons tested (including corners). Eurocode 3 specifies $e_u/e_y > 20$, and as mentioned above, this could not be measured precisely. The range of values obtained for this ratio indicate that this was rarely achieved for the flats of the C450 specimens, and was satisfied considerably more often for the flats of the C350 samples. No corner coupons fulfilled this requirement.

Spec-imen	Cut from section	Posi-tion	E (GPa)	f_y (MPa)	f_u (MPa)	$\frac{f_u}{f_y}$	e_f (%)	E^1 (GPa)	f_y^1 (MPa)
TS01D	150 × 50 × 5.0 C450	Adj 1	198	425	492	1.16	18.0	198	441
		Adj 2	198	457	498	1.09	16.2		
		Opp	213	505	543	1.07	15.6		
		C1	200[2]	520	556	1.07	20.0		
		C2	200[2]	480	566	1.18	16.7		
		C3	200[2]	495	566	1.14	16.7		
		C4	200[2]	500	560	1.12	18.3		
TS02D	150 × 50 × 4.0 C450	Adj 1	219	460	537	1.17	20.3	212	457
		Adj 2	205	454	516	1.14	18.3		
		Opp	198	514	580	1.13	15.7		
		C1	200[2]	563	616	1.09	17.2		
		C2	200[2]	545	601	1.10	16.0		
		C3	200[2]	550	608	1.11	16.0		
		C4	200[2]	570	613	1.08	18.0		
TS03D	150 × 50 × 3.0 C450	Adj 1	210	445	520	1.17	19.9	206	444
		Adj 2	201	442	506	1.14	16.6		
		Opp	218	514	585	1.14	13.2		
		C1[3]							
		C2	200[2]	540	588	1.09	20.0		
		C3	200[2]	545	594	1.09	20.0		
		C4	200[2]	540	611	1.13	20.0		
TS04D	150 × 50 × 2.5 C450	Adj 1	202	445	527	1.18	15.2	204	446
		Adj 2	206	446	518	1.16	16.3		
		Opp	204	485	560	1.15	13.1		
		C1	200[2]	540	600	1.11	25.0		
		C2	200[2]	530	585	1.10	20.0		
		C3	200[2]	545	596	1.09	20.0		
		C4	200[2]	540	588	1.09	17.5		
TS05D	150 × 50 × 2.3 C450	Adj 1	207	453	528	1.17	16.3	205	444
		Adj 2	204	434	508	1.17	18.3		
		Opp	191	480	547	1.14	14.5		
		C1	200[2]	535	585	1.09	17.5		
		C2	200[2]	470	523	1.11	17.5		
		C3	200[2]	490	526	1.07	21.0		
		C4	200[2]	480	530	1.10	18.5		
TS06D	100 × 50 × 2.0 C450	Adj 1	194	445	492	1.11	12.9	202	449
		Adj 2	209	452	505	1.12	10.9		
		Opp	182	480	540	1.13	9.17		
		C1	200[2]	490	538	1.10	17.5		
		C2	200[2]	490	540	1.10	15.0		
		C3	200[2]	510	560	1.10	20.0		
		C4	200[2]	500	547	1.09	20.0		

Table C.2: Summary of Tensile Test Results

ec-imen	Cut from section	Posi-tion	E (GPa)	f_y (MPa)	f_u (MPa)	$\frac{f_u}{f_y}$	e_f (%)	E^1 (GPa)	f_y^1 (MPa)
TS07D	75 × 50 × 2.0 C450	Adj 1	199	345	430	1.25	28.3	203	411[4]
		Adj 2	208	411	484	1.18	12.5		
		Opp	196	428	482	1.13	23.3		
		C1	200[2]	475	520	1.09	18.5		
		C2	200[2]	450	500	1.11	17.5		
		C3	200[2]	445	480	1.08	19.0		
		C4	200[2]	465	503	1.08	20.0		
TS08D	75 × 25 × 2.0 C450	Adj 1	202	438	507	1.16	14.2	203	457
		Adj 2	204	475	522	1.10	11.0		
		Opp	204	487	537	1.10	26.0		
		C1	200[2]	480	538	1.12	19.0		
		C2	200[2]	550	588	1.07	15.0		
		C3	200[2]	530	576	1.09	18.5		
		C4	200[2]	525	585	1.11	15.0		
TS09D	75 × 25 × 1.6 C450	Adj 1	194	450	506	1.12	26.0	193	439
		Adj 2	193	428	515	1.20	12.5		
		Opp	200	487	545	1.12	14.0		
		C1	200[2]	560	589	1.05	16.7		
		C2	200[2]	555	576	1.04	14.7		
		C3	200[2]	555	605	1.09	14.7		
		C4	200[2]	565	585	1.04	16.7		
TS10D	75 × 25 × 1.6 C350	Adj 1	205	421	460	1.09	16.1	202	422
		Adj 2	199	423	452	1.07	17.2		
		Opp	206	445	514	1.16	6.25		
		C1	200[2]	505	540	1.07	16.0		
		C2	200[2]	500	515	1.03	16.7		
		C3	200[2]	510	532	1.04	17.3		
		C4	200[2]	510	555	1.09	15.3		
TS11D	150 × 50 × 3.0 C350	Adj 1	207	370	433	1.17	32.6	205	370
		Adj 2	202	369	425	1.15	27.9		
		Opp	198	380	436	1.15	22.2		
		C1	200[2]	465	511	1.10	20.0		
		C2	200[2]	475	516	1.09	22.5		
		C3	200[2]	480	534	1.11	21.0		
		C4	200[2]	495	542	1.09	20.5		
TS12D	100 × 50 × 2.0 C350	Adj 1	205	395	454	1.15	21.1	203	400
		Adj 2	200	404	445	1.10	19.0		
		Opp	199	433	471	1.08	12.0		
		C1	200[2]	500	536	1.07	21.0		
		C2	200[2]	485	530	1.09	21.5		
		C3	200[2]	480	520	1.08	20.0		
		C4	200[2]	505	545	1.08	22.5		

Table C.2 (continued): Summary of Tensile Test Results

Spec-imen	Cut from section	Posi-tion	E (GPa)	f_y (MPa)	f_u (MPa)	$\frac{f_u}{f_y}$	e_f (%)	E^1 (GPa)	f_y^1 (MPa)
TS13D	125 × 75 × 3.0 C350	Adj 1	211	396	450	1.14	25.0	211	397
		Adj 2	210	397	448	1.13	28.4		
		Opp	203	403	453	1.12	19.1		
		C1	200[2]	470	510	1.09	23.0		
		C2	200[2]	475	518	1.09	22.5		
		C3	200[2]	475	508	1.07	24.0		
		C4	200[2]	470	520	1.11	22.5		
TS16D	150 × 50 × 2.5 C450	Adj 1	204	425	498	1.17	25.0	207	440
		Adj 2	209	455	515	1.13	28.3		
		Opp	200	507	560	1.10	20.0		
TS17D	100 × 50 × 2.0 C450	Adj 1	203	415	475	1.14	28.3	203	423
		Adj 2	203	432	482	1.17	23.3		
		Opp	206	462	516	1.12	18.3		
TS19D	100 × 100 × 3.0 C450	Adj 1	212	433	494	1.14	24.3	207	445
		Adj 2	202	457	510	1.12	24.3		
		Opp	199	482	525	1.09	21.4		
TS20D	150 × 50 × 3.0 C350	Adj 1	200	380	425	1.12	30.0	200	382
		Adj 2	200	383	435	1.14	31.4		
		Opp	206	403	455	1.13	27.1		
TS21D	125 × 75 × 2.5 C350	Adj 1	204	377	443	1.18	37.3	201	374
		Adj 2	199	370	438	1.18	31.7		
		Opp	203	420	453	1.08	30.0		

Notes: (1) The average of E and f_y for the two adjacent sides is used for the whole RHS.
(2) For corner coupons it is assumed that E = 200 GPa.
(3) Specimen TS03DC1 not tested.
(4) For TS07D f_y is from face Adjacent 2 only.
(5) Nominal strengths: Grade C450 specimens f_{yn} = 450 MPa and f_{un} = 500 MPa.
Grade C350 specimens f_{yn} = 350 MPa and f_{un} = 430 MPa.

.

Table C.2 (continued): Summary of Tensile Test Results

Stress Strain Curve
TS01D 150 x 50 x 5.0 C450

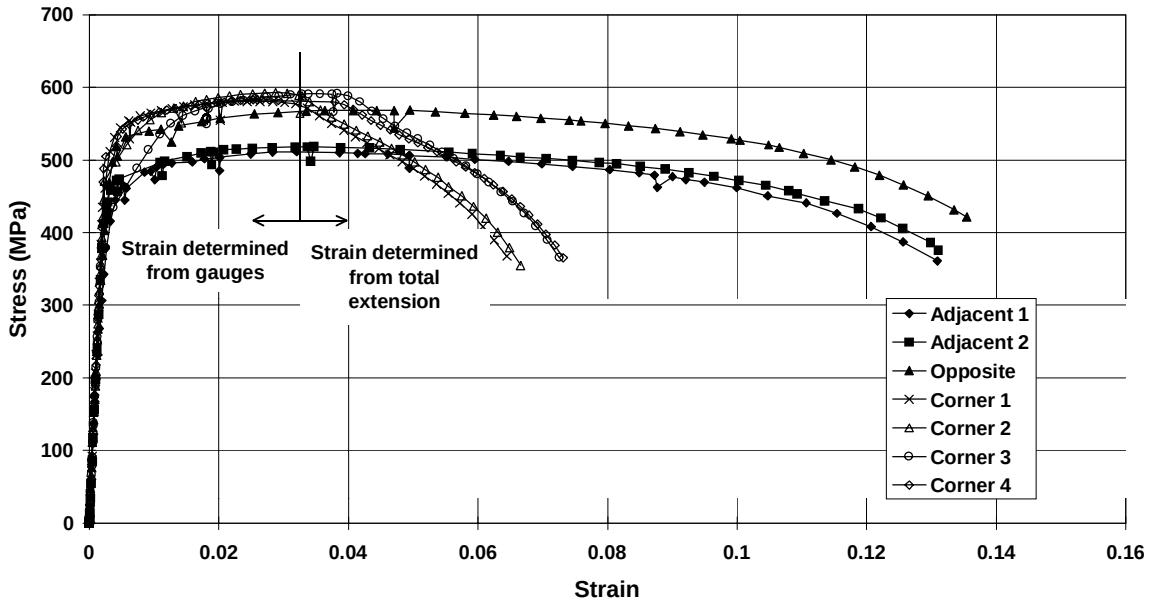

Stress Strain Curve
TS02D 150 x 50 x 4.0 C450

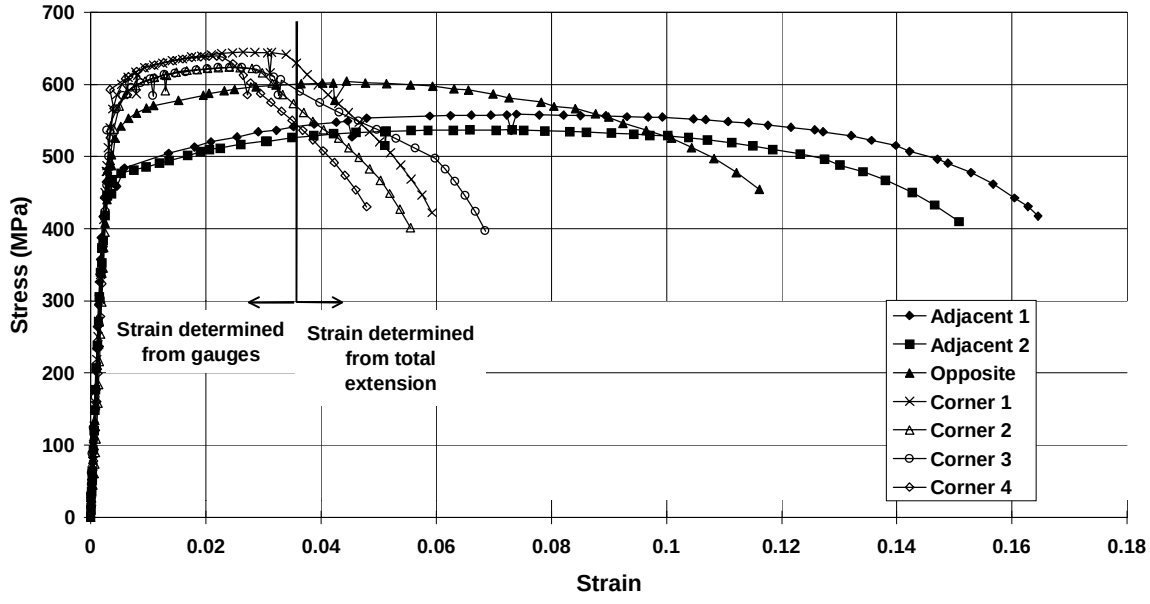

Stress Strain Curve
TS03D 150 x 50 x 3.0 C450

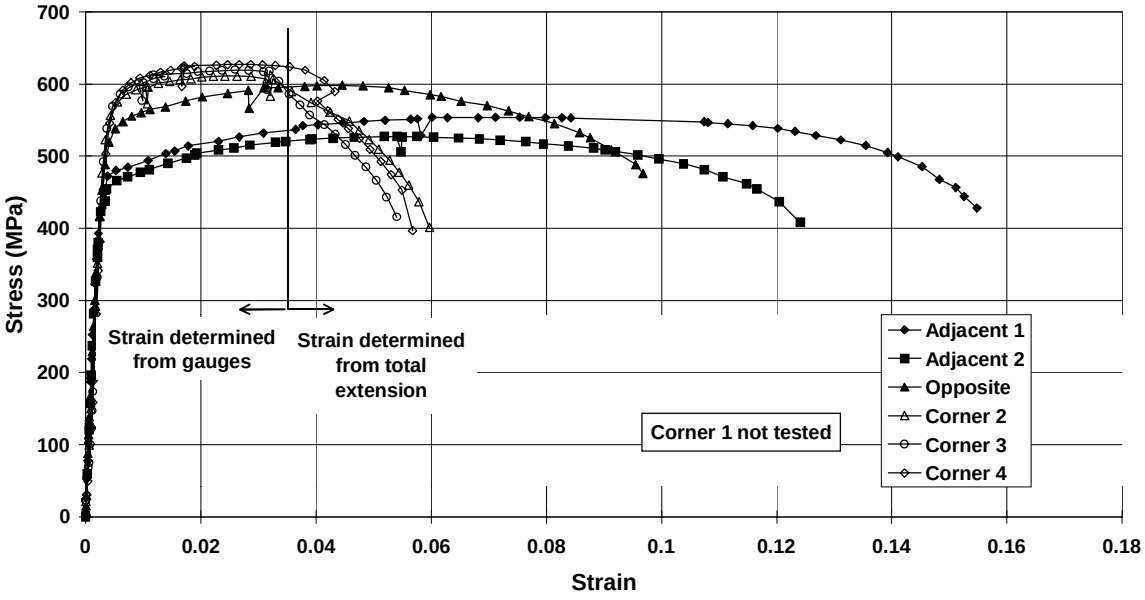

Stress Strain Curve
TS04D 150 x 50 x 2.5 C450

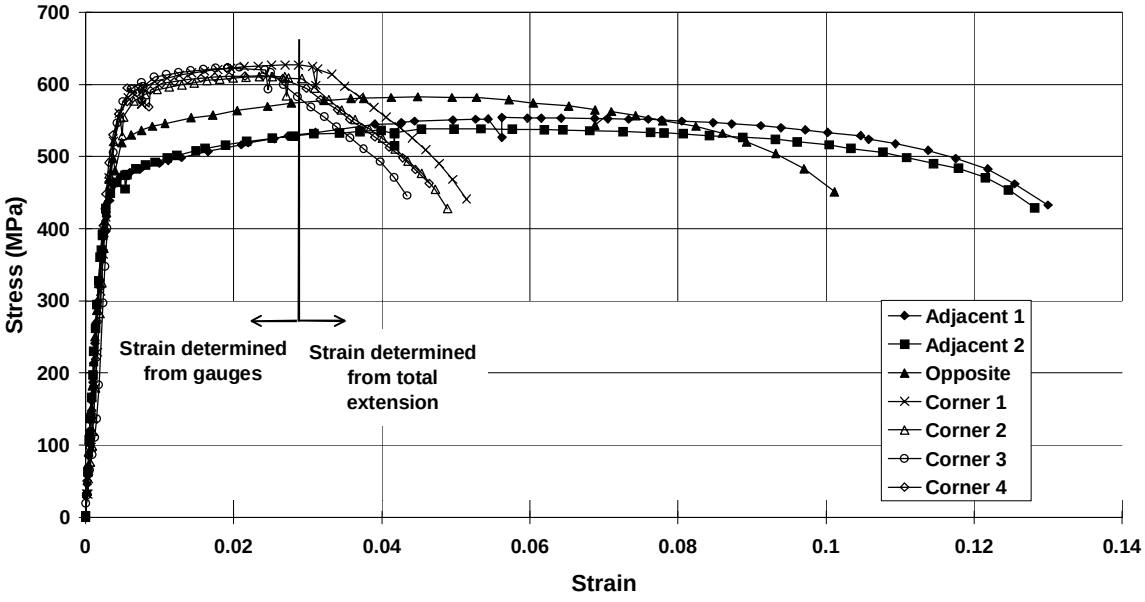

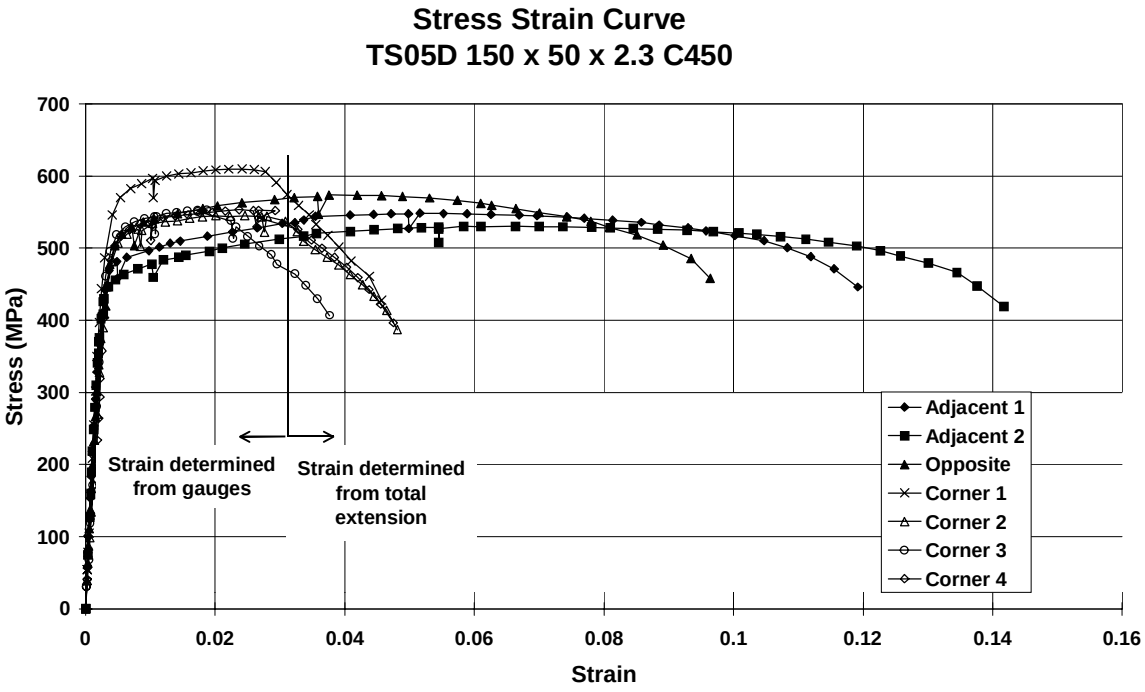
Stress Strain Curve
TS05D 150 x 50 x 2.3 C450
Stress (MPa)
Strain
Strain determined from gauges
Strain determined from total extension
Adjacent 1
Adjacent 2
Opposite
Corner 1
Corner 2
Corner 3
Corner 4

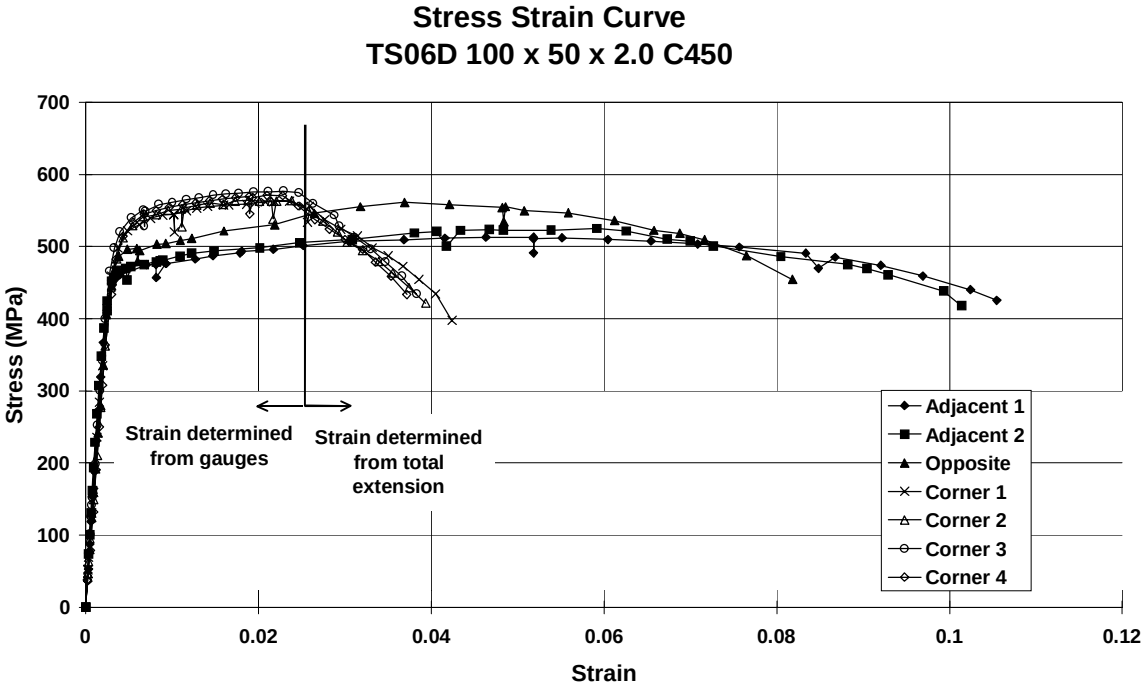
Stress Strain Curve
TS06D 100 x 50 x 2.0 C450
Stress (MPa)
Strain
Strain determined from gauges
Strain determined from total extension
Adjacent 1
Adjacent 2
Opposite
Corner 1
Corner 2
Corner 3
Corner 4

Stress Strain Curve
TS07D 75 x 50 x 2.0 C450

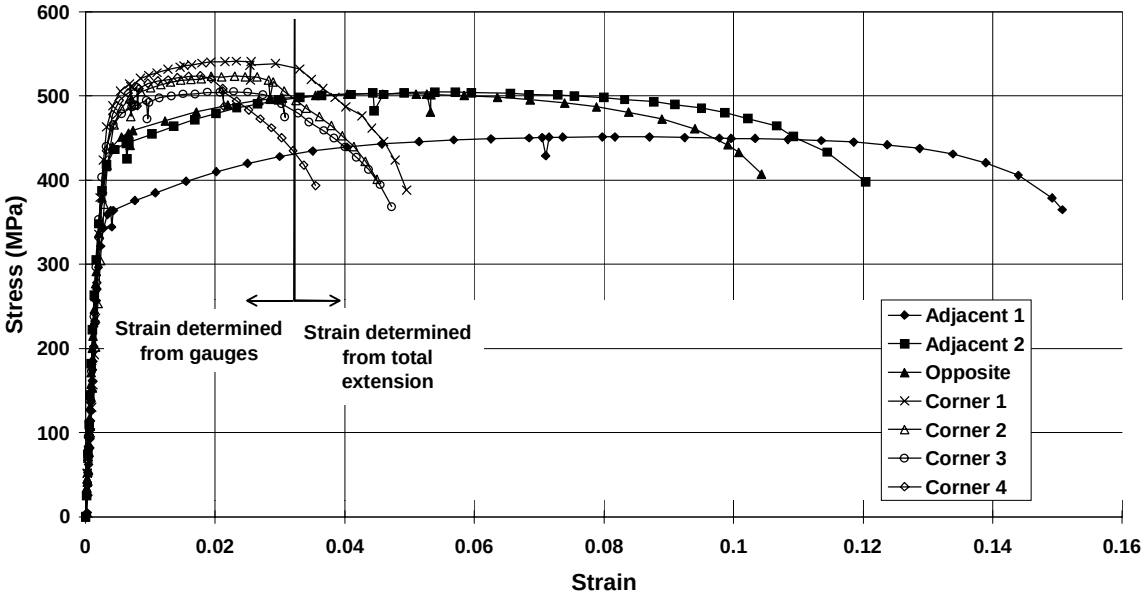

Stress Strain Curve
TS08D 75 x 25 x 2.0 C450

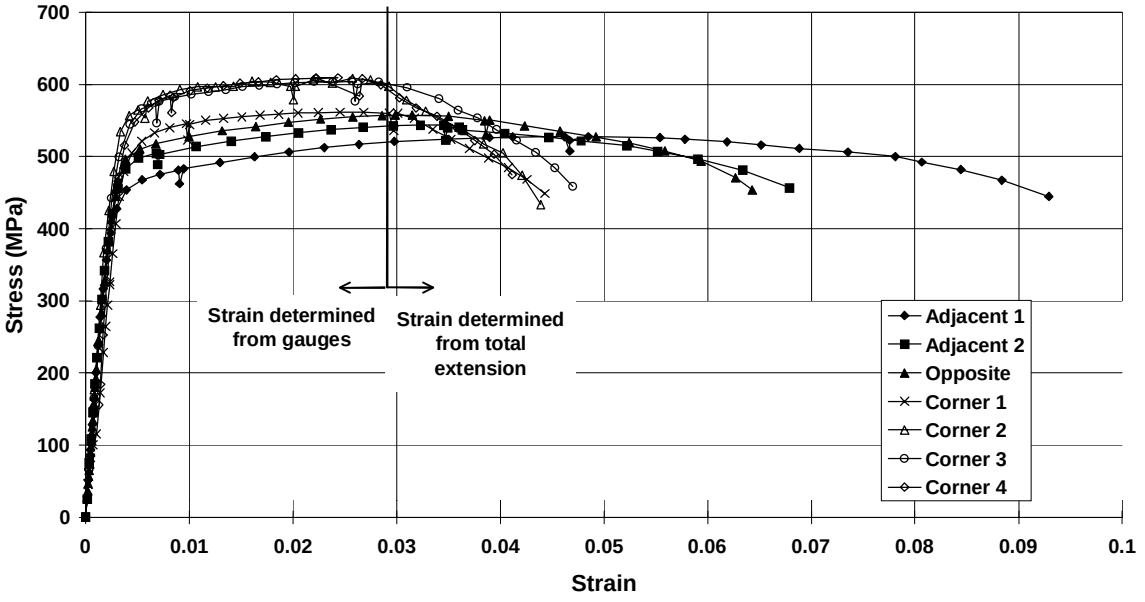

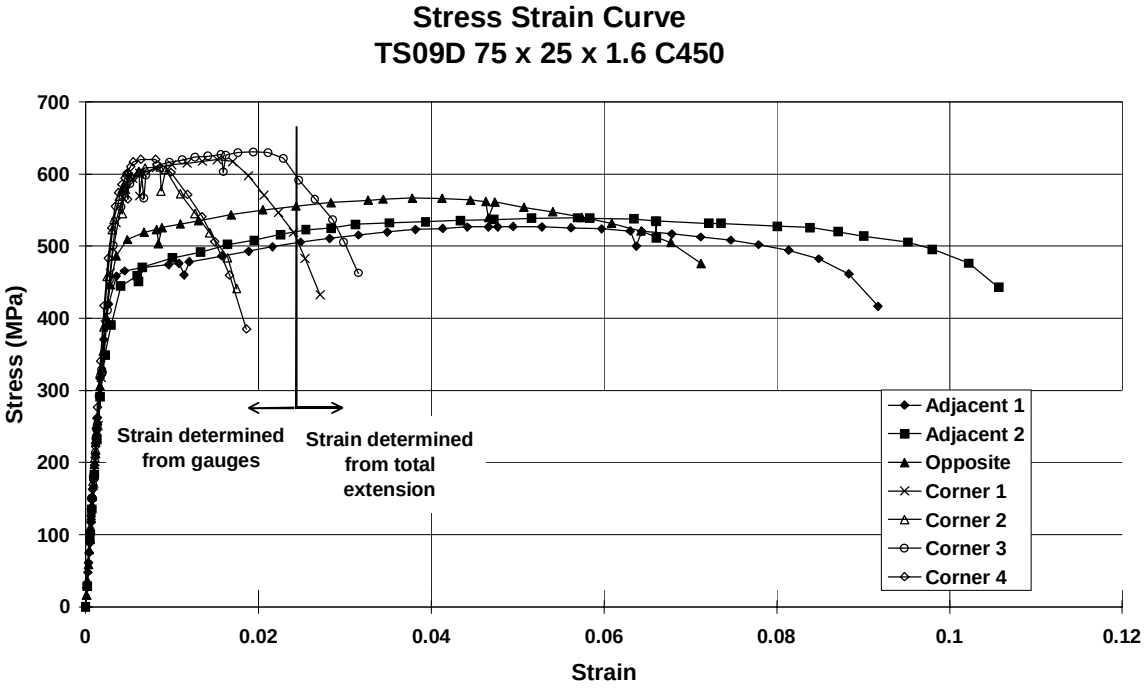
Stress Strain Curve
TS09D 75 x 25 x 1.6 C450
Stress (MPa)
Strain
Strain determined from gauges
Strain determined from total extension
Adjacent 1
Adjacent 2
Opposite
Corner 1
Corner 2
Corner 3
Corner 4

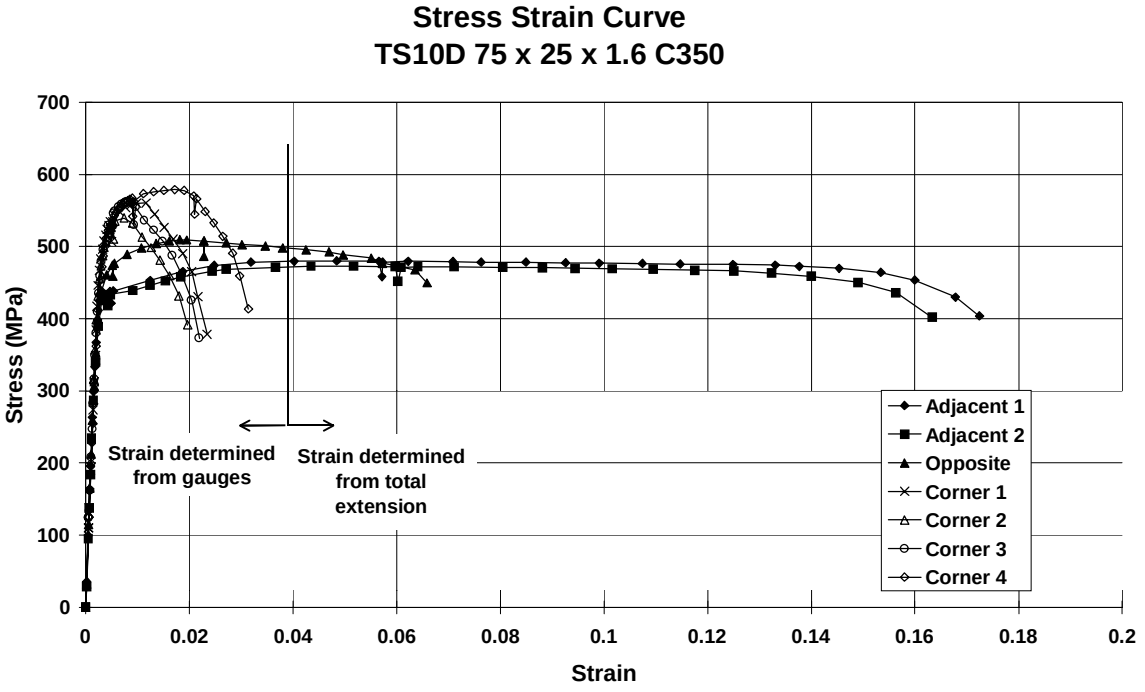
Stress Strain Curve
TS10D 75 x 25 x 1.6 C350
Stress (MPa)
Strain
Strain determined from gauges
Strain determined from total extension
Adjacent 1
Adjacent 2
Opposite
Corner 1
Corner 2
Corner 3
Corner 4

Stress Strain Curve
TS11D 150 x 50 x 3.0 C350

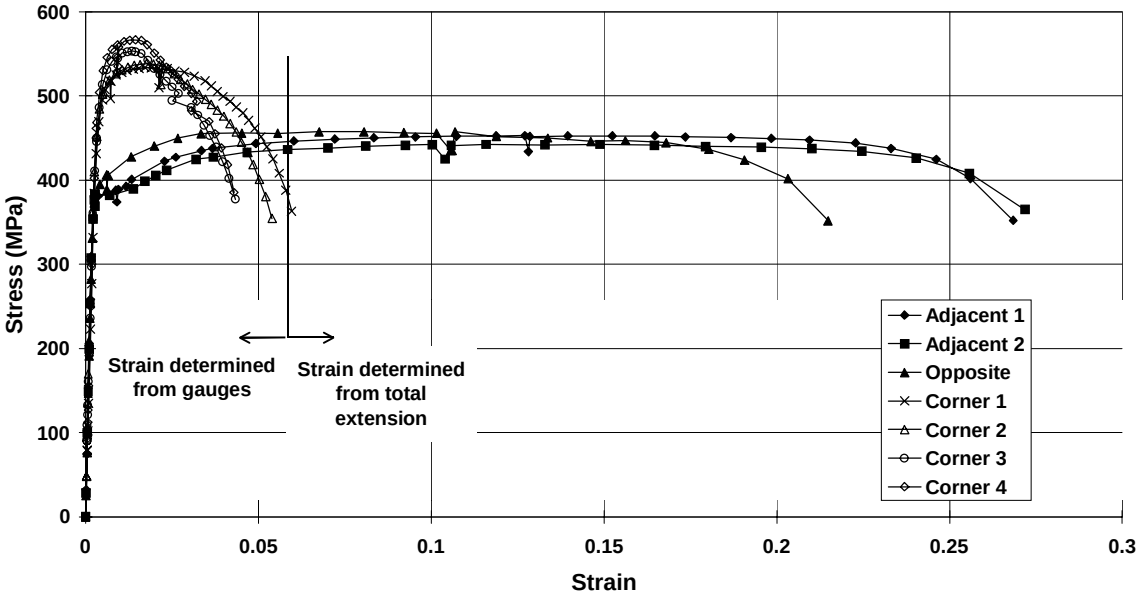

Stress Strain Curve
TS12D 100 x 50 x 2.0 C350

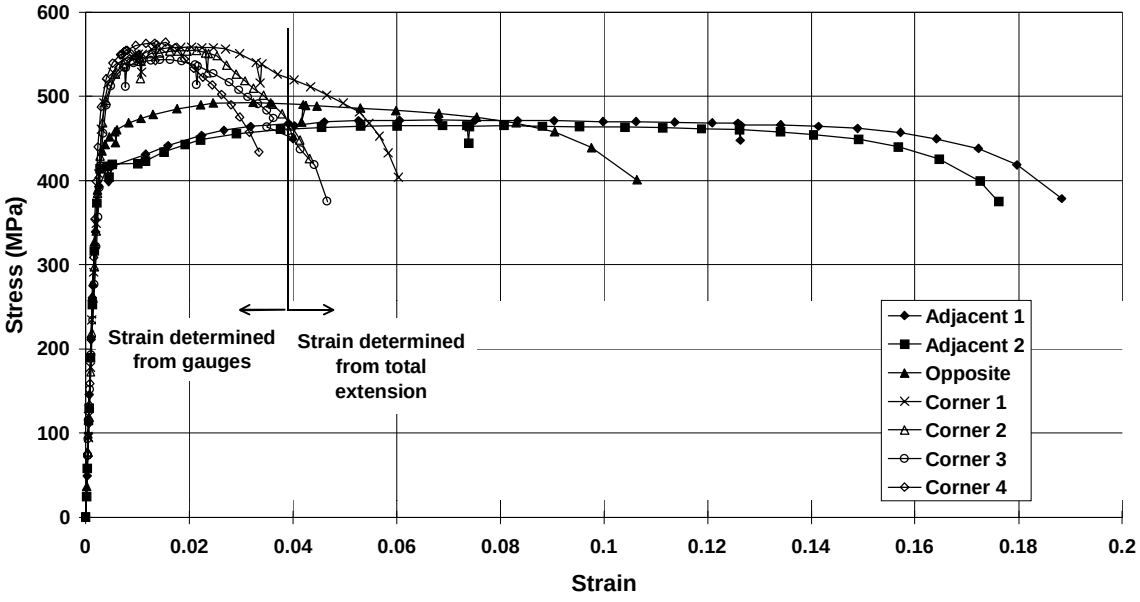

Stress Strain Curve
TS13D 125 x 75 x 3.0 C350

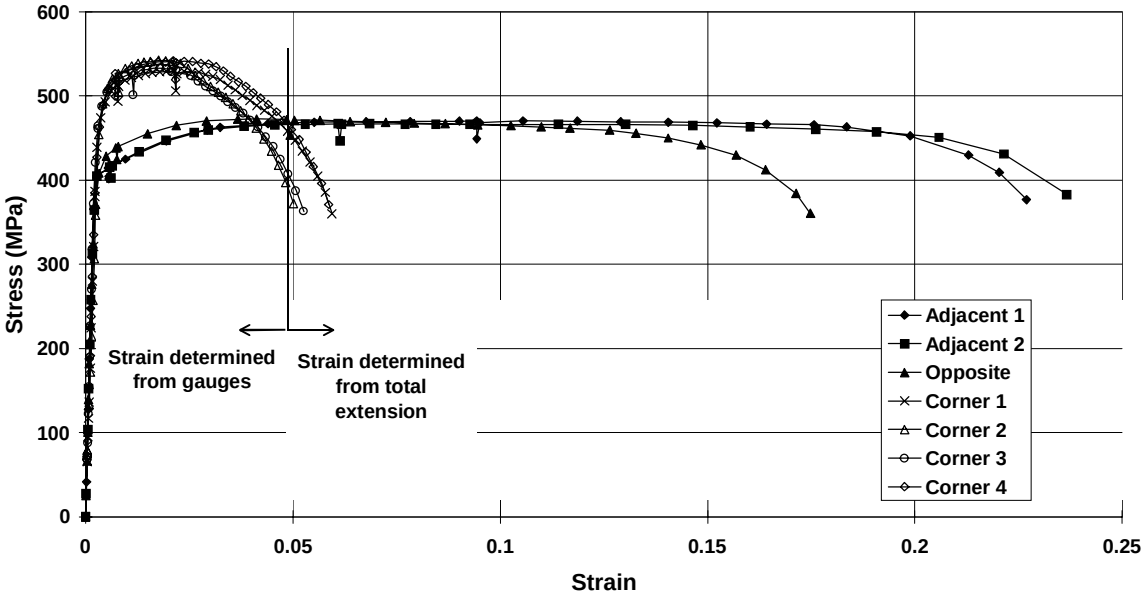

Stress Strain Curve
TS16D 150 x 50 x 2.5 C450

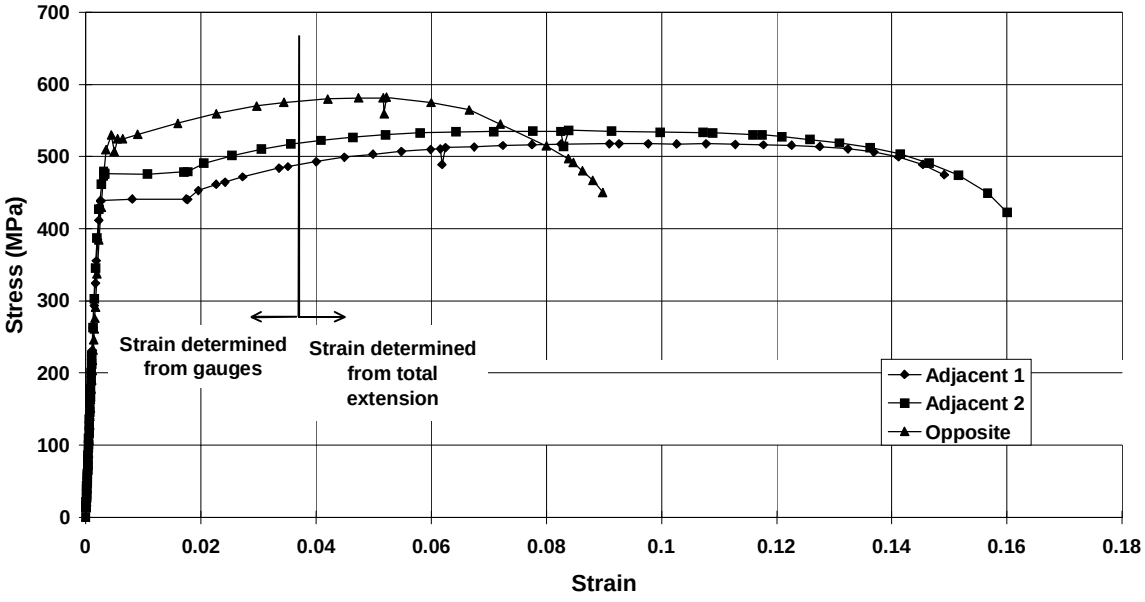

Stress Strain Curve
TS17D 100 x 50 x 2.0 C450

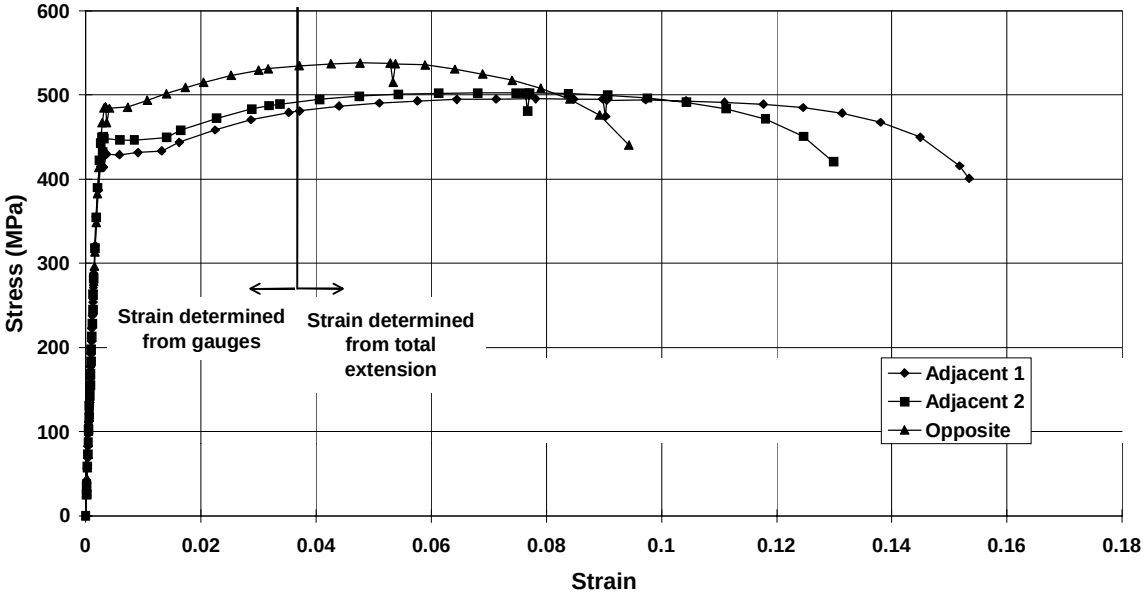

Stress Strain Curve
TS19D 100 x 100 x 3.0 C450

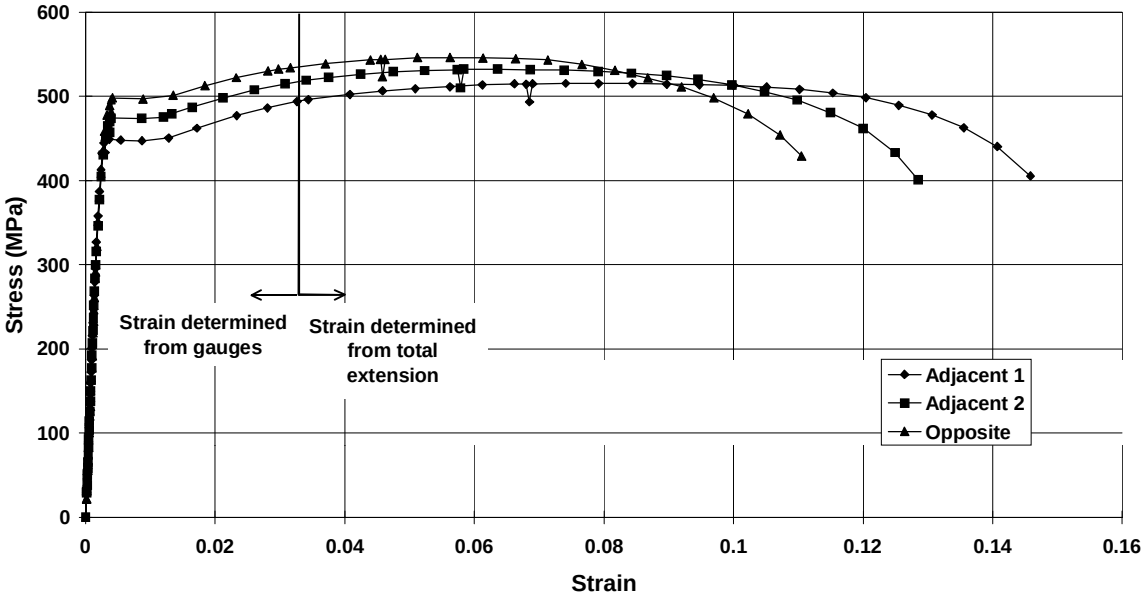

Stress Strain Curve
TS20D 150 x 50 x 3.0 C350

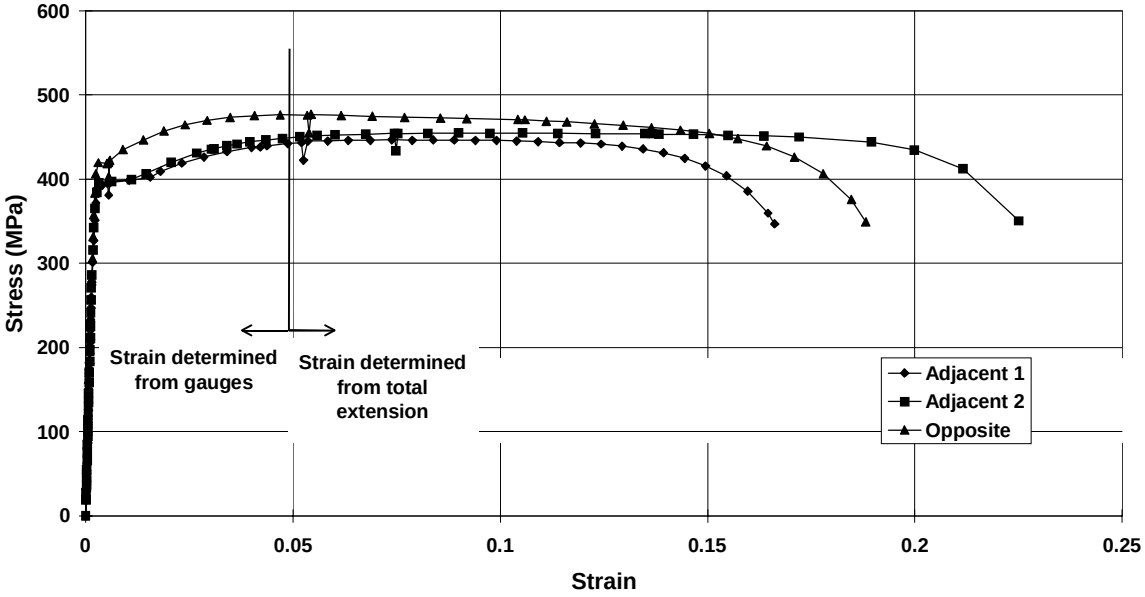

Stress Strain Curve
TS21D 125 x 75 x 2.5 C350

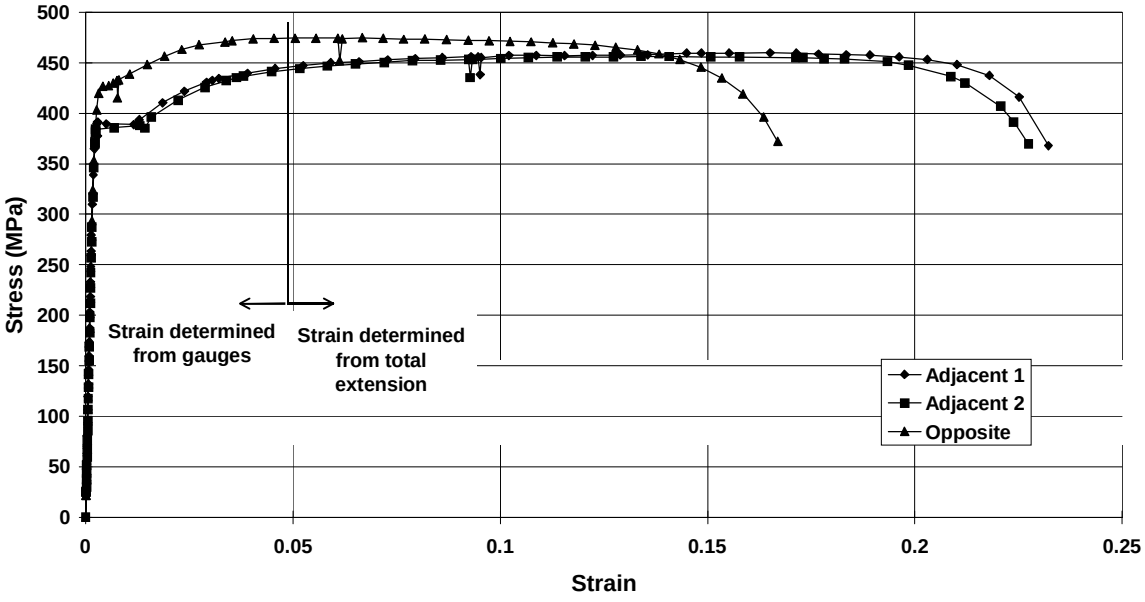

BLANK PAGE

APPENDIX D STUB COLUMN TESTS

D.1 PROCEDURE

Stub column tests were performed in a 2000 kN capacity DARTEC testing machine, using a servo-controlled hydraulic ram. The ends of each RHS sample were machined flat and perpendicular prior to test. The bottom platen was fixed against rotation. The top platen was mounted on a spherical seat which allowed complete contact between each end of the stub column and the platens. The test set up is shown in Figure D.1. Displacement transducers measured the axial shortening of the specimen. A SPECTRA data acquisition system recorded the transducer readings and the load at regular stages during each test. The test was halted for approximately one minute to obtain a value of the static load near the maximum.

The lengths of the stub columns were chosen using the guidelines set out by Johnston (1976). This specifies a minimum stub column length of $3d$ and a maximum length of $20r_y$. It was not always possible to adhere to these limits for the sections with an aspect ratio d/b of 3 since $3d > 20r_y$ for these samples. In these cases the length chosen was approximately $3d$.

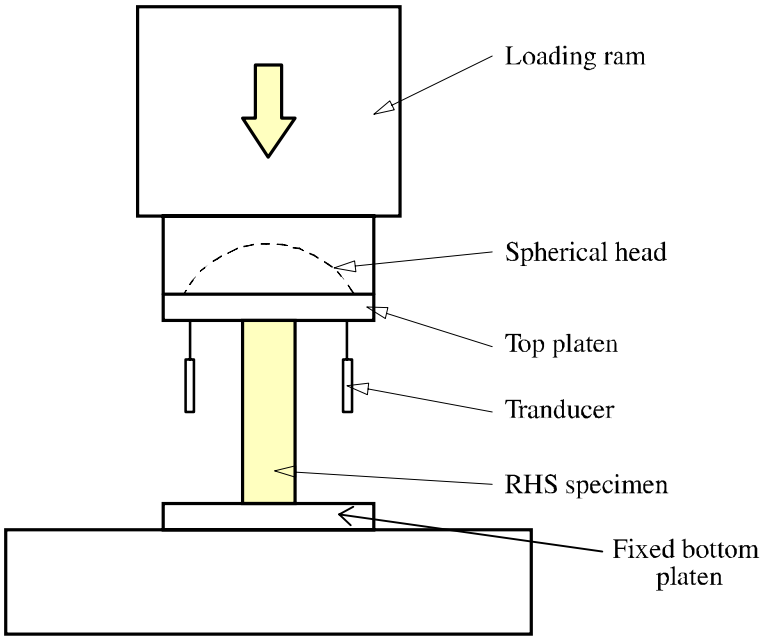

Figure D.1: Diagrammatic Representation of Stub Column Test

D.2 RESULTS

Each specimen experienced local buckling which initiated in the web. Compatibility of rotation at the corner produced deformation in the flange of the RHS. The load increased until local buckling occured, after which the load dropped with increased axial shortening.

Table D.1 sets out the results for each stub column test. The maximum static load (N_{max}) is compared to the yield load ($N_y = A_g f_y$) and the section capacity (N_s) (determined to AS 4100, Eurocode 3 and AISC LRFD), which includes the effect of local buckling by the use of effective widths. The yield stress used in calculations is the measured yield stress (Table 3) rather than the nominal yield stress. The ratios of these loads and the web slenderness are also tabulated. Table D.2 tabulates the dimensions of each test piece. Figure D.2 shows the relationship between these ratios and the web slenderness, as well as the yield slenderness limit (for AS 4100 only).

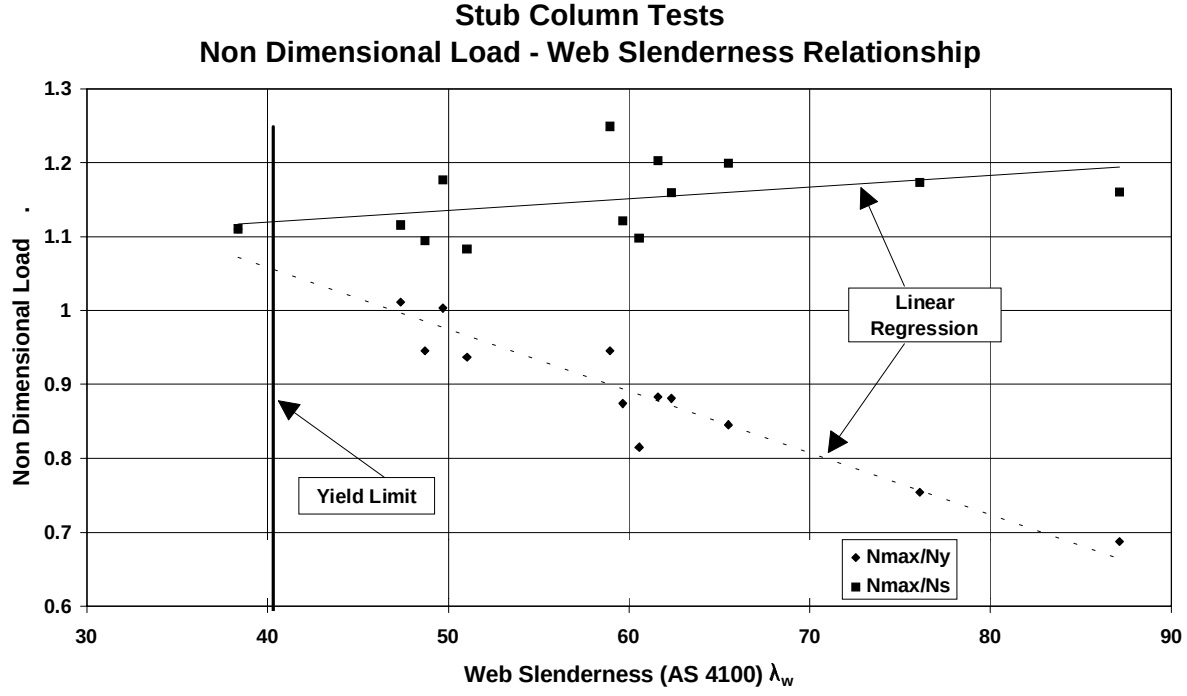

Figure D.2: Load - Slenderness Relation for Stub Column Tests

D.3 DISCUSSION

N_{max}/N_y is less than or equal to unity for all but one section when the web slenderness exceeds yield slenderness limit and N_{max}/N_y is greater than one when the web slenderness is less than the limit. This indicates that the web slenderness limit for pure compression is appropriate.

N_{max}/N_s is greater than 1.0 for all but one section (SCS10D for AISC LRFD only). This fact indicates that the effective width formulation in the determination of N_s is safe. The linear regression relationship for N_{max}/N_s in Figure D.2, which is in the region of 1.1 to 1.2, suggests that AS 4100 is slightly conservative in this formulation.

Specimen	Cut from Section	N_{max} (kN)	N_y (kN)	$\frac{N_{max}}{N_y}$	AS 4100			Eurocode 3			AISC LRFD		
					λ_w	N_s (kN)	$\frac{N_{max}}{N_s}$	λ_w	N_s (kN)	$\frac{N_{max}}{N_s}$	λ_w	N_s (kN)	$\frac{N_{max}}{N_s}$
Limit					40			42			1.40		
SCS01D	150 × 50 × 5.0 C450	878	790	1.11	38.4	790	1.11	38.2	790	1.11	1.22	790	1.11
SCS02D	150 × 50 × 4.0 C450	670	668	1.00	49.7	569	1.18	49.9	596	1.12	1.68	610	1.10
SCS03D	150 × 50 × 3.0 C450	422	499	0.845	65.5	352	1.20	66.2	387	1.09	2.23	394	1.07
SCS04D	150 × 50 × 2.5 C450	330	438	0.754	76.1	281	1.17	77.1	314	1.05	2.64	315	1.05
SCS05D	150 × 50 × 2.3 C450	263	383	0.687	87.1	227	1.16	88.5	255	1.03	2.99	259	1.01
SCS06D	100 × 50 × 2.0 C450	235	267	0.881	62.3	203	1.16	62.9	218	1.08	2.10	224	1.05
SCS07D	75 × 50 × 2.0 C450	190	188	1.01	47.4	170	1.12	47.5	175	1.08	1.56	180	1.05
SCS08D	75 × 25 × 2.0 C450	160	269	0.946	48.7	146	1.09	48.8	152	1.05	1.62	157	1.02
SCS09D	75 × 25 × 1.6 C450	114	129	0.904	61.6	95	1.22	62.1	103	1.10	2.08	106	1.08
SCS10D	75 × 25 × 1.6 C350	101	124	0.815	60.6	92	1.10	61.1	100	1.01	2.03	103	0.980
SCS11D	150 × 50 × 3.0 C350	397	420	0.945	58.9	318	1.25	59.5	343	1.15	2.00	351	1.13
SCS12D	100 × 50 × 2.0 C350	207	237	0.874	59.6	185	1.12	60.2	197	1.04	2.02	202	1.03
SCS13D	125 × 75 × 3.0 C350	418	446	0.936	51.0	386	1.08	51.3	402	1.04	1.70	412	1.01

Table D.1: Summary of Stub Column Test Results

Specimen	Cut from Section	d (mm)	b (mm)	t (mm)	r (mm)	A_g (mm^2)	$\frac{A_g}{A_n}$	L_{sc} (mm)
SCS01D	150 × 50 × 5.0 C450	150.99	50.11	4.89	11.8	1792	0.988	399.9
SCS02D	150 × 50 × 4.0 C450	150.38	50.17	3.88	7.1	1462	0.987	400.1
SCS03D	150 × 50 × 3.0 C450	150.64	50.09	2.94	5.8	1125	0.986	400.2
SCS04D	150 × 50 × 2.5 C450	150.25	50.03	2.55	4.0	982	1.024	400.2
SCS05D	150 × 50 × 2.3 C450	150.28	50.57	2.23	4.4	863	0.900	400.1
SCS06D	100 × 50 × 2.0 C450	100.38	50.43	2.07	4.4	595	1.036	300.0
SCS07D	75 × 50 × 2.0 C450	75.25	49.88	1.93	4.4	457	0.965	225.0
SCS08D	75 × 25 × 2.0 C450	75.24	25.06	1.98	4.1	371	0.992	224.9
SCS09D	75 × 25 × 1.6 C450	75.03	25.15	1.55	3.2	294	0.970	224.9
SCS10D	75 × 25 × 1.6 C350	75.21	25.10	1.55	3.4	294	0.969	224.8
SCS11D	150 × 50 × 3.0 C350	150.42	50.07	2.98	5.9	1137	0.997	224.8
SCS12D	100 × 50 × 2.0 C350	100.88	50.45	2.05	4.2	593	1.033	300.3
SCS13D	125 × 75 × 3.0 C350	125.32	75.60	2.94	6.3	1125	0.986	374.9

Table D.2: Dimensions of Stub Columns

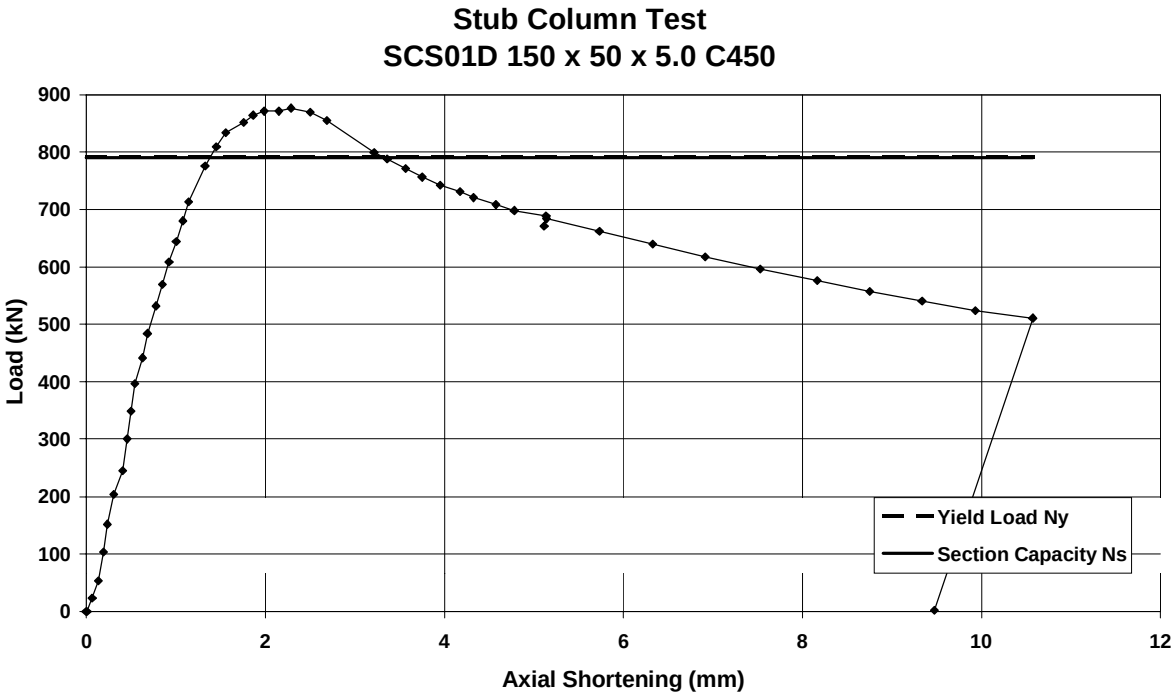
Stub Column Test
SCS01D 150 x 50 x 5.0 C450
Load (kN)
Axial Shortening (mm)
Yield Load Ny
Section Capacity Ns
0
100
200
300
400
500
600
700
800
900
0
2
4
6
8
10
12

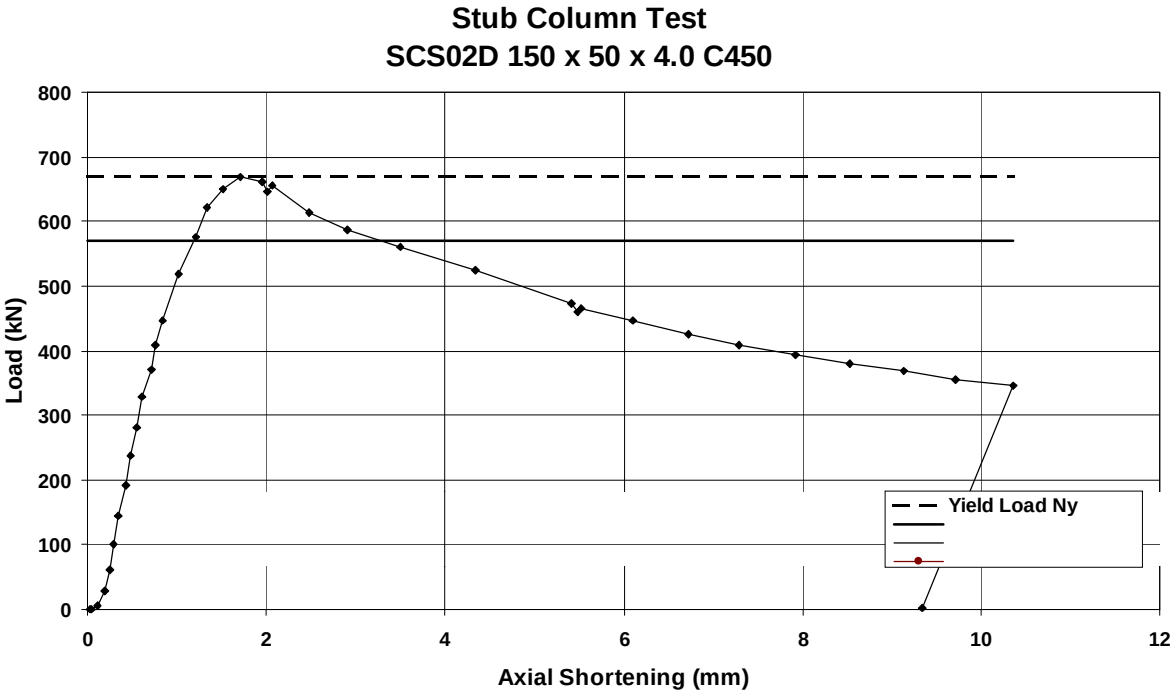
Stub Column Test
SCS02D 150 x 50 x 4.0 C450
Load (kN)
Axial Shortening (mm)
Yield Load Ny
0
100
200
300
400
500
600
700
800
0
2
4
6
8
10
12

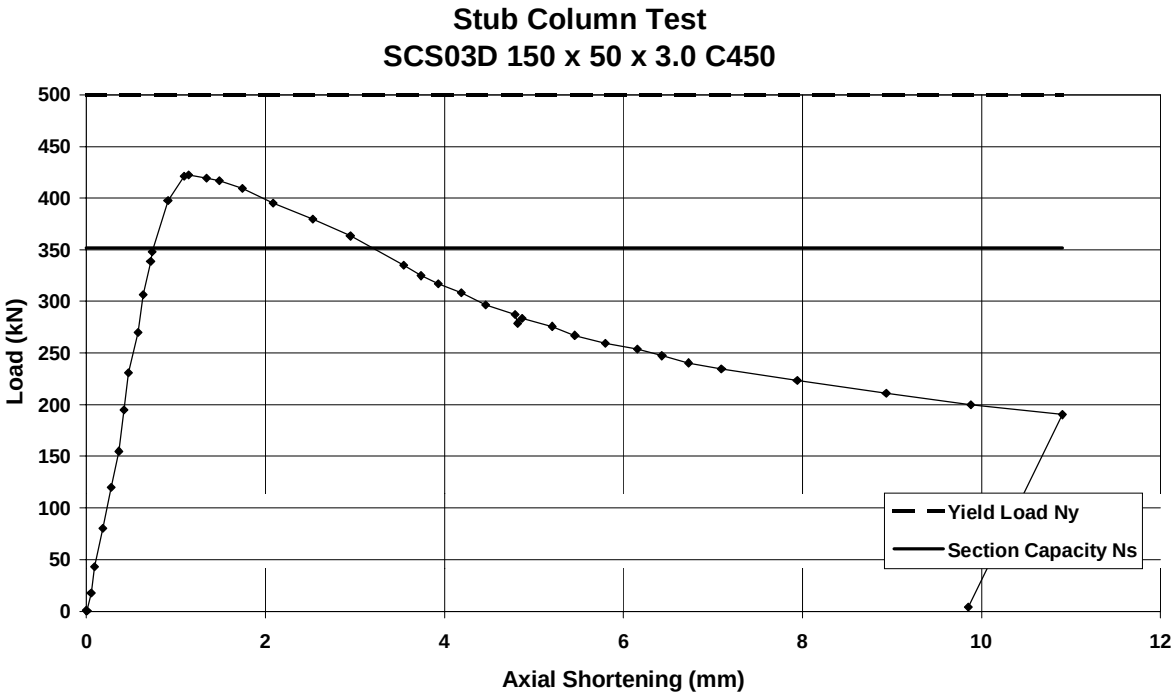
Stub Column Test
SCS03D 150 x 50 x 3.0 C450
Load (kN)
Axial Shortening (mm)
Yield Load Ny
Section Capacity Ns
0
50
100
150
200
250
300
350
400
450
500
0
2
4
6
8
10
12

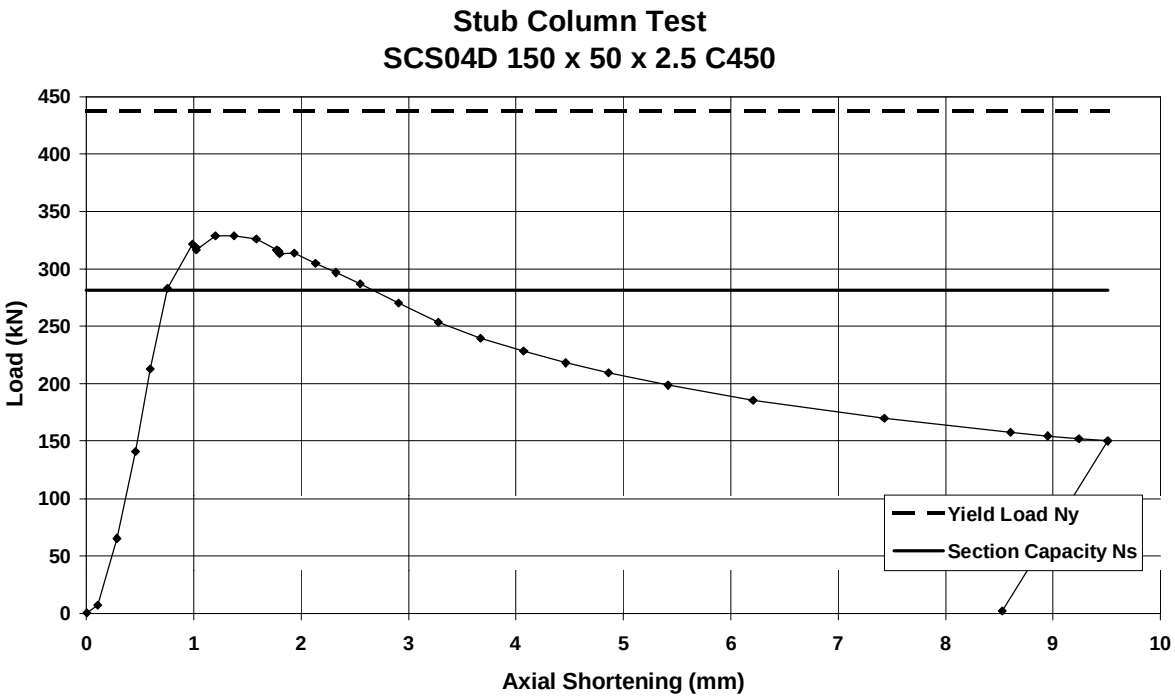
Stub Column Test
SCS04D 150 x 50 x 2.5 C450
Load (kN)
Axial Shortening (mm)
Yield Load Ny
Section Capacity Ns
0
50
100
150
200
250
300
350
400
450
0
1
2
3
4
5
6
7
8
9
10

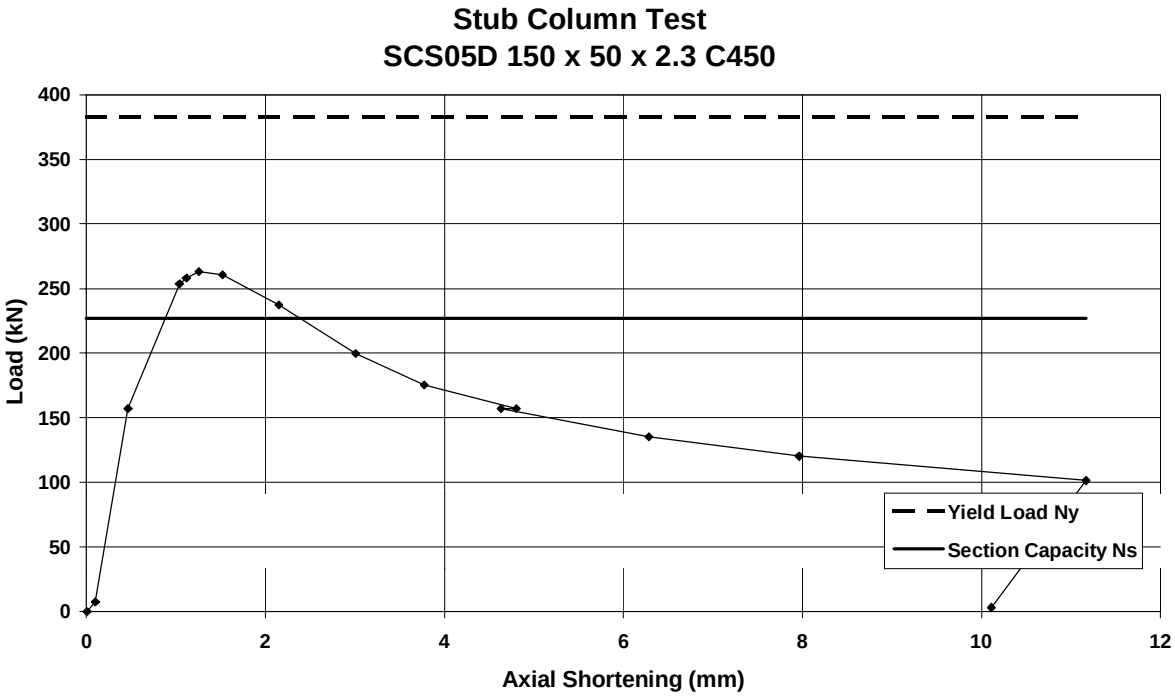
Stub Column Test
SCS05D 150 x 50 x 2.3 C450
Load (kN)
Axial Shortening (mm)
Yield Load Ny
Section Capacity Ns
0
50
100
150
200
250
300
350
400
0
2
4
6
8
10
12

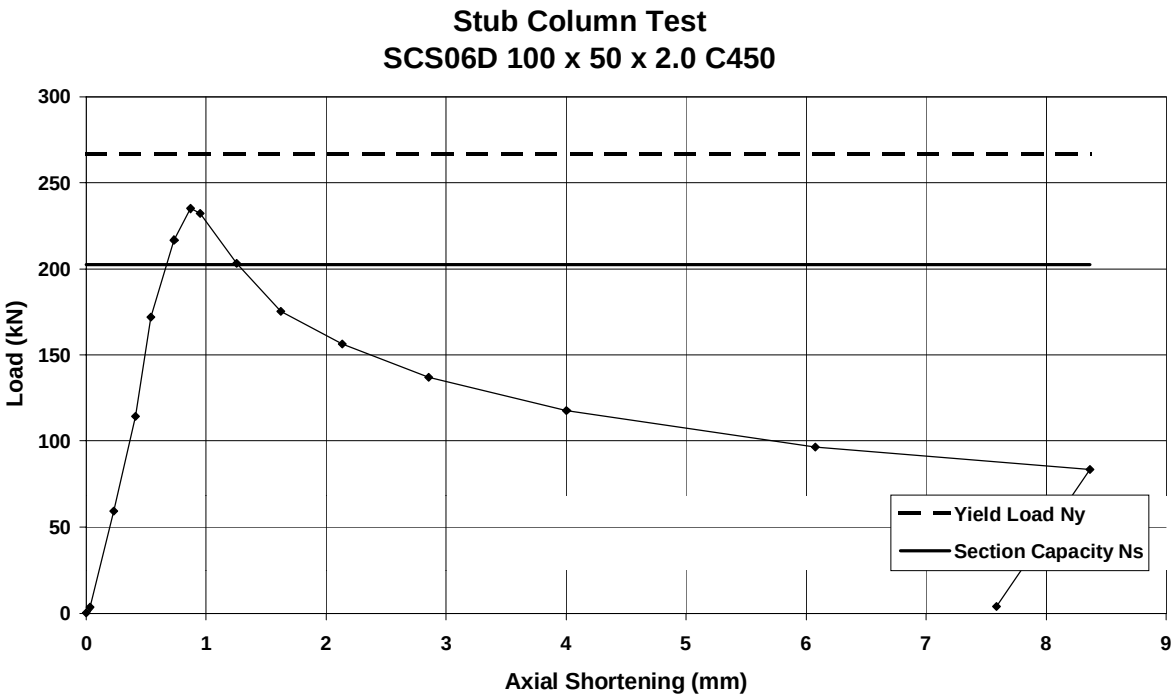
Stub Column Test
SCS06D 100 x 50 x 2.0 C450
Load (kN)
Axial Shortening (mm)
Yield Load Ny
Section Capacity Ns
0
50
100
150
200
250
300
0
1
2
3
4
5
6
7
8
9

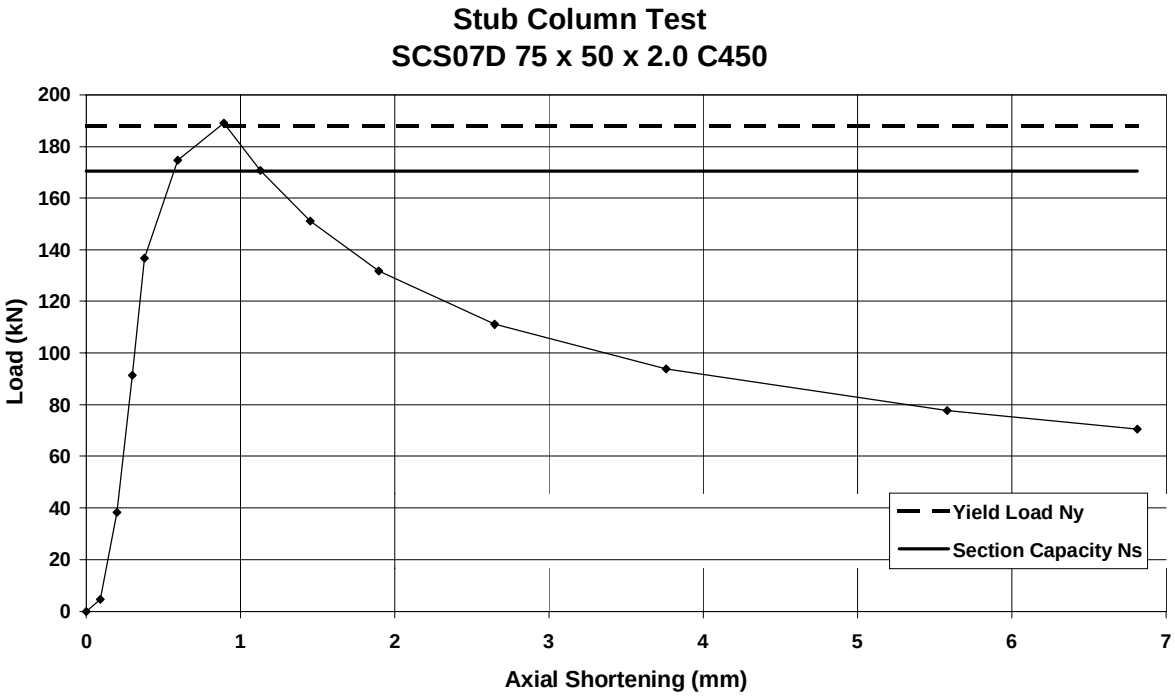
Stub Column Test
SCS07D 75 x 50 x 2.0 C450
Load (kN)
Axial Shortening (mm)
Yield Load Ny
Section Capacity Ns
0
20
40
60
80
100
120
140
160
180
200
0
1
2
3
4
5
6
7

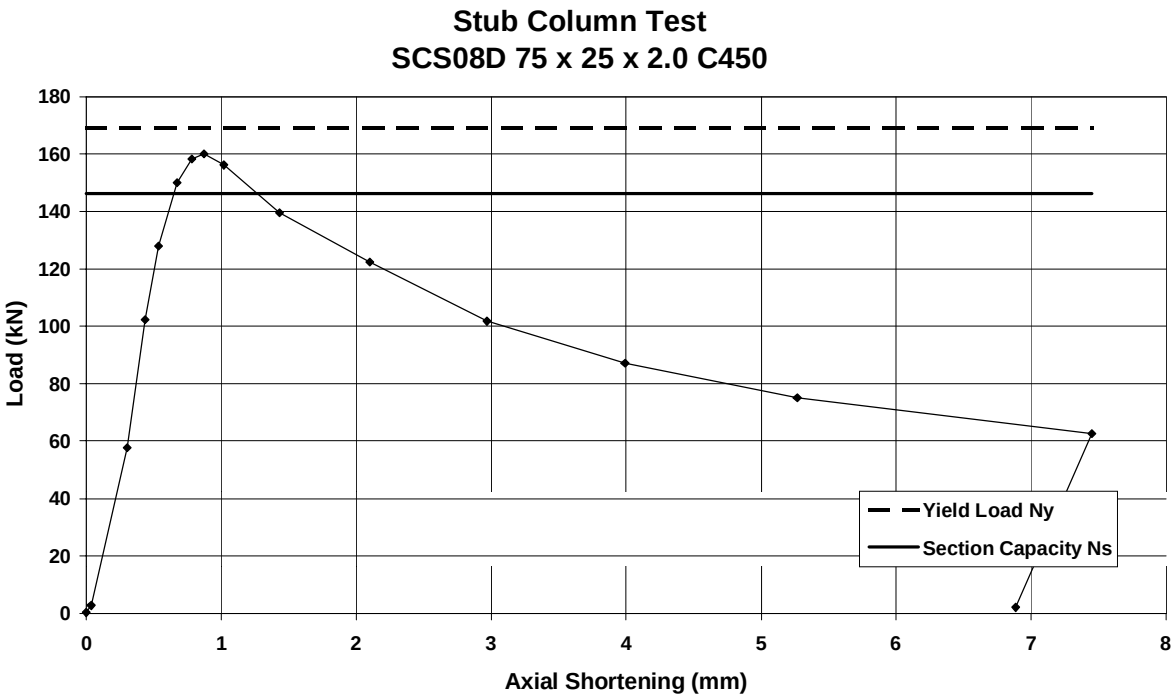
Stub Column Test
SCS08D 75 x 25 x 2.0 C450
Load (kN)
Axial Shortening (mm)
Yield Load Ny
Section Capacity Ns
0
20
40
60
80
100
120
140
160
180
0
1
2
3
4
5
6
7
8

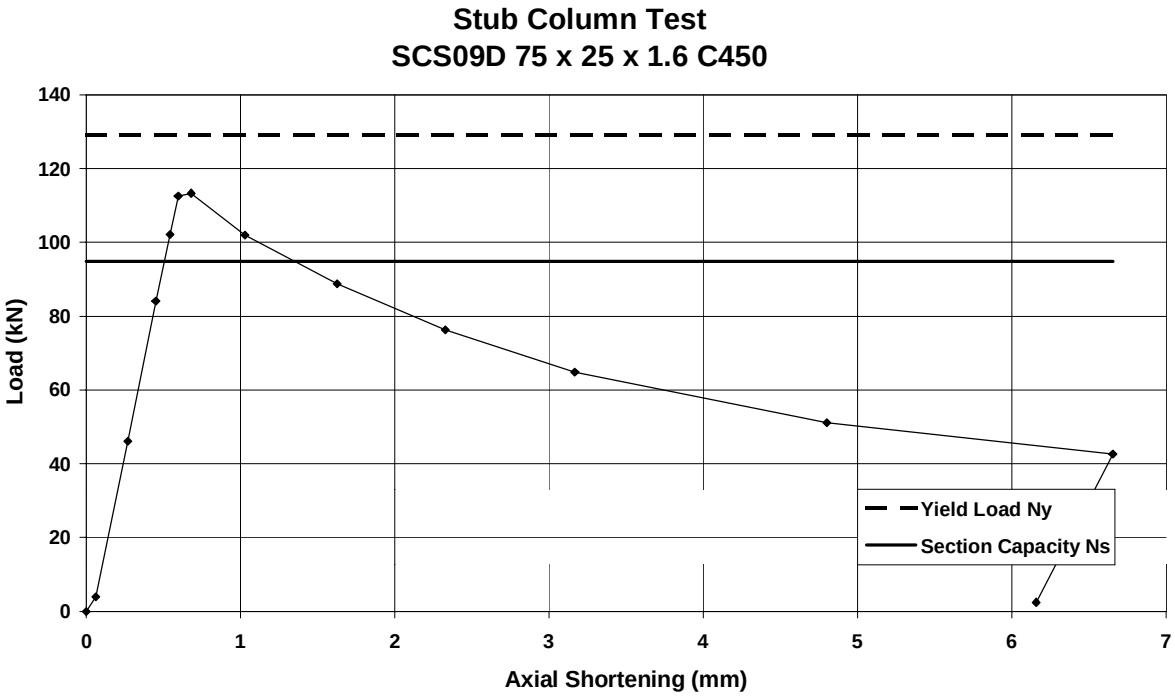
Stub Column Test
SCS09D 75 x 25 x 1.6 C450
Load (kN)
Axial Shortening (mm)
Yield Load Ny
Section Capacity Ns
0
20
40
60
80
100
120
140
0
1
2
3
4
5
6
7

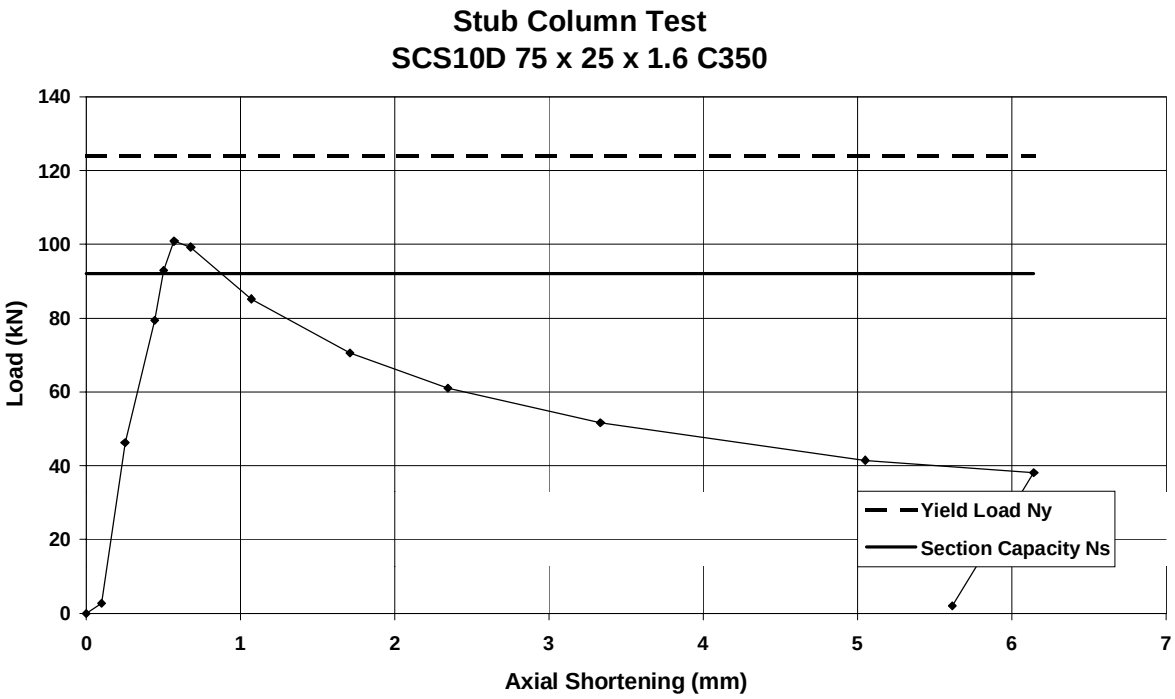
Stub Column Test
SCS10D 75 x 25 x 1.6 C350
Load (kN)
Axial Shortening (mm)
Yield Load Ny
Section Capacity Ns
0
20
40
60
80
100
120
140
0
1
2
3
4
5
6
7

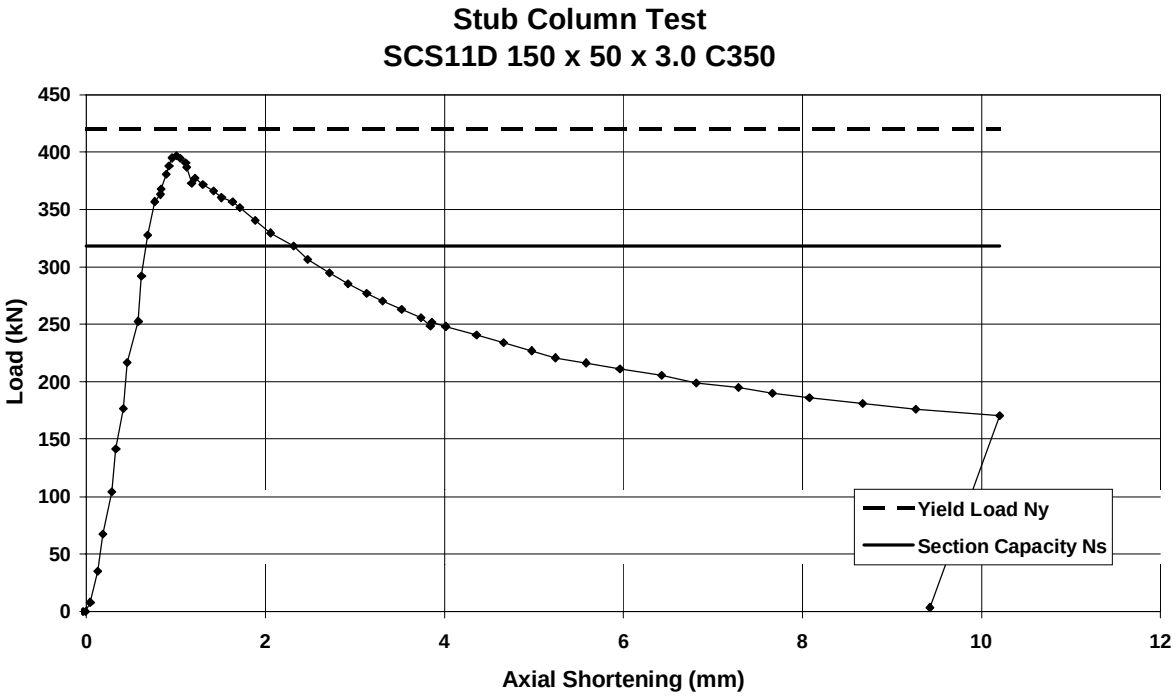
Stub Column Test
SCS11D 150 x 50 x 3.0 C350
Load (kN)
Axial Shortening (mm)
Yield Load Ny
Section Capacity Ns
0
50
100
150
200
250
300
350
400
450
0
2
4
6
8
10
12

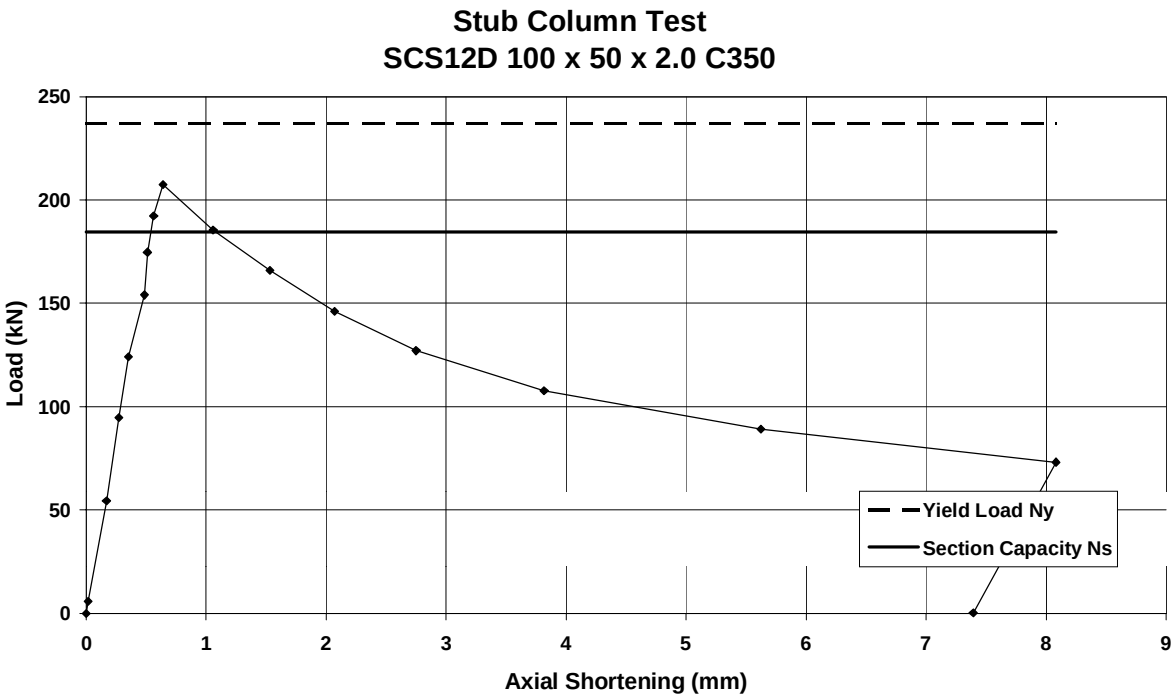
Stub Column Test
SCS12D 100 x 50 x 2.0 C350
Load (kN)
Axial Shortening (mm)
Yield Load Ny
Section Capacity Ns
0
50
100
150
200
250
0
1
2
3
4
5
6
7
8
9

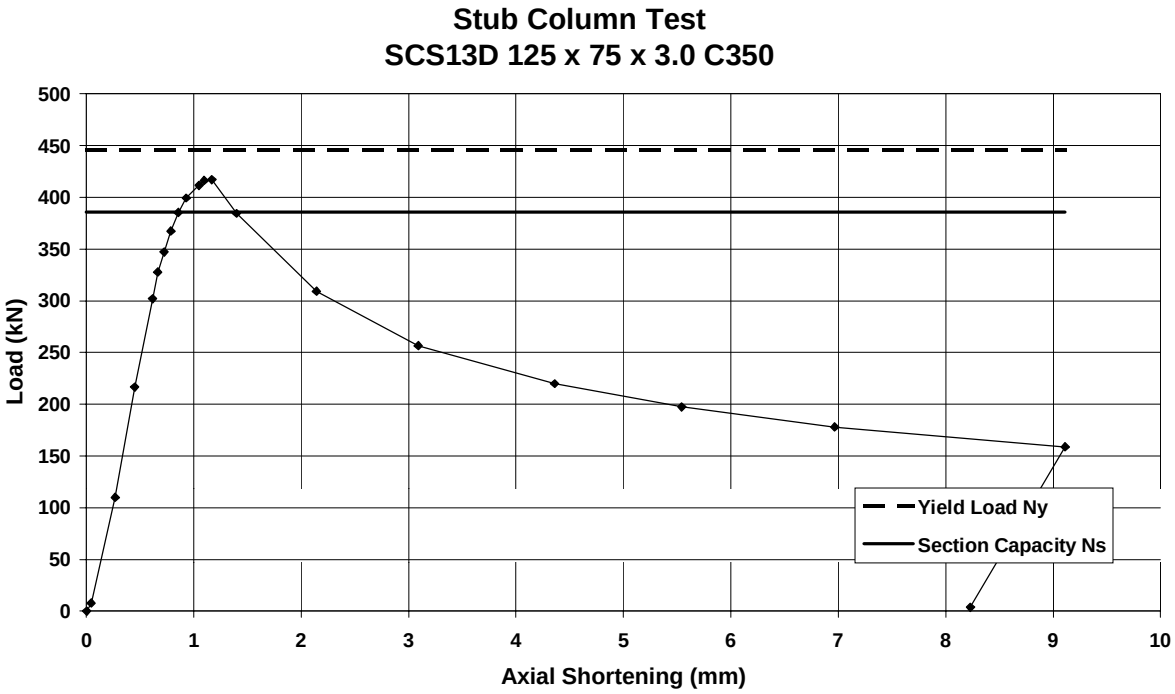
Stub Column Test
SCS13D 125 x 75 x 3.0 C350
Load (kN)
Axial Shortening (mm)
Yield Load Ny
Section Capacity Ns
0
50
100
150
200
250
300
350
400
450
500
0
1
2
3
4
5
6
7
8
9
10

APPENDIX E IMPERFECTION PROFILES

RHS are not perfect rectangular specimens. The cold-forming process, welding, handling and other factors can introduce geometric imperfections. Local imperfections can have a significant effect on the capacity. Hence the local imperfections of the RHS have been measured. These values will be important in future finite element modelling of the tests.

E.1 METHOD

Each sample was placed above an accurately machined and greased beam. A displacement transducer was moved along this machined beam, measuring the distance to the specimen at 25 mm intervals as shown in Figure E.1. Measurement was made along fourteen lines down the specimen (Figure E.1). By comparing the transducer readings along the edges of each face to those at the centre of each face, the "bow-out" imperfection (refer to Figure E.3) at the middle of each flange and third points of each web were obtained, to give a profile of the beam. The readings were made between the loading points (Figure 3). It was only possible to measure each specimen to within 100 mm of the centre of the loading points.

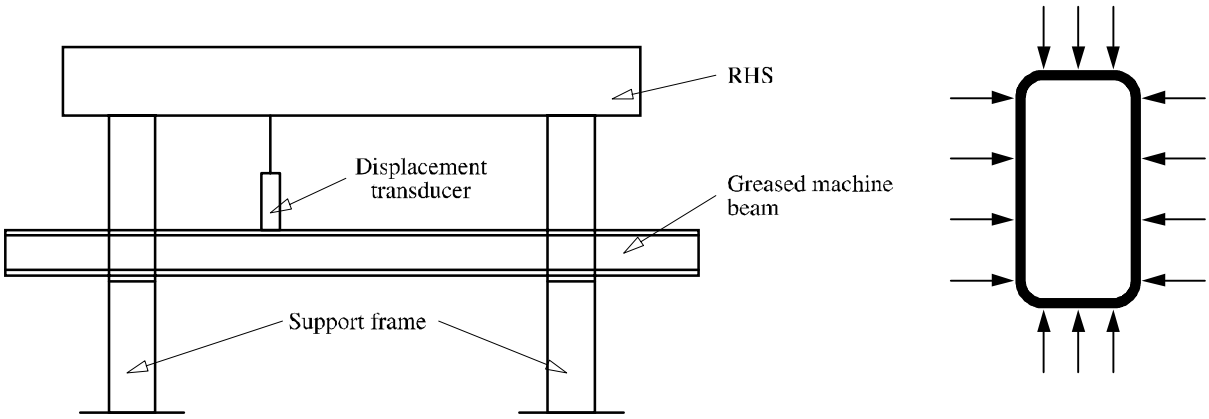

Figure E.1: Imperfection Measurement Rig and Measurement Locations

E.2 IMPERFECTION PROFILES

The figures in this section give the "bow-out" deformation along the length of the RHS specimen at six positions along the flange and web shown below in Figure E.2.

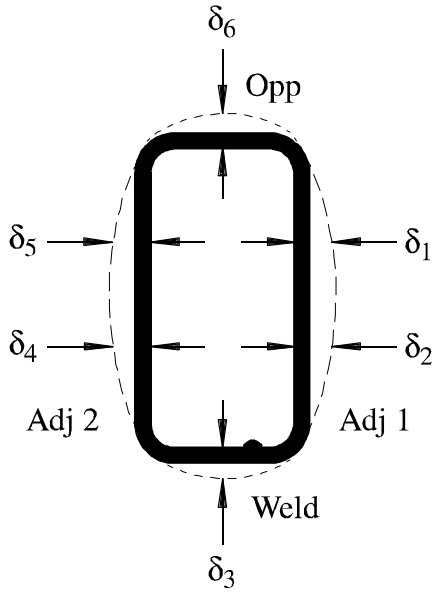

Figure E.2: Location of Imperfection Profile Measurements

It can be observed that the values of these imperfections are small (typically less than ± 1% of the depth (for web imperfections) or the width (for flange imperfections)). The stiffer faces of the RHS tend to exhibit a negative imperfection (an inwards bow), while the other faces exhibit an outwards bow. For example, a thick specimen, BS01C, exhibits inwards imperfection on all faces, and a thinner specimen exhibits bow-out on the less stiff webs but inwards bowing on the stiffer flanges.

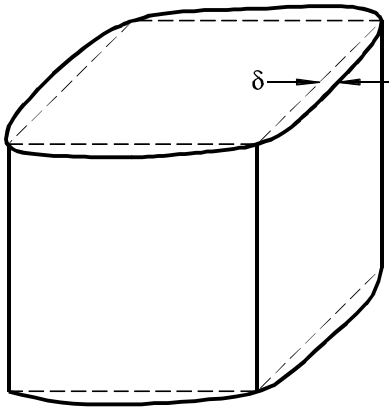

Figure E.3: Typical "Bow-Out" Imperfection of an RHS

The “bow-out” imperfection results from the cold-forming process. The sheet is initially rolled as a circle and then the centre of each face is pushed in by successive sets of rollers to form the rectangular shape. The same set of rollers is used for the same outer size of RHS and hence similar force forms the section into the rectangular shape. The thinner sections tend to “spring back” more after passing a set of rolls causing the “bow-out”.

This imperfection is generally approximately constant along the length of the beam. Any wave-like profile would represent a local imperfection. There is often some extra initial deformation near the loading plates, caused by welding of the loading plates and the clamping of the samples during this welding. There is more variability in the profile of the smaller specimens - it was more difficult to measure accurately these samples, and smaller values of these imperfections approach the precision of the displacement transducer. The profile of the weld face of the RHS was often difficult to measure precisely due to the seam of the join on the outside of the RHS.

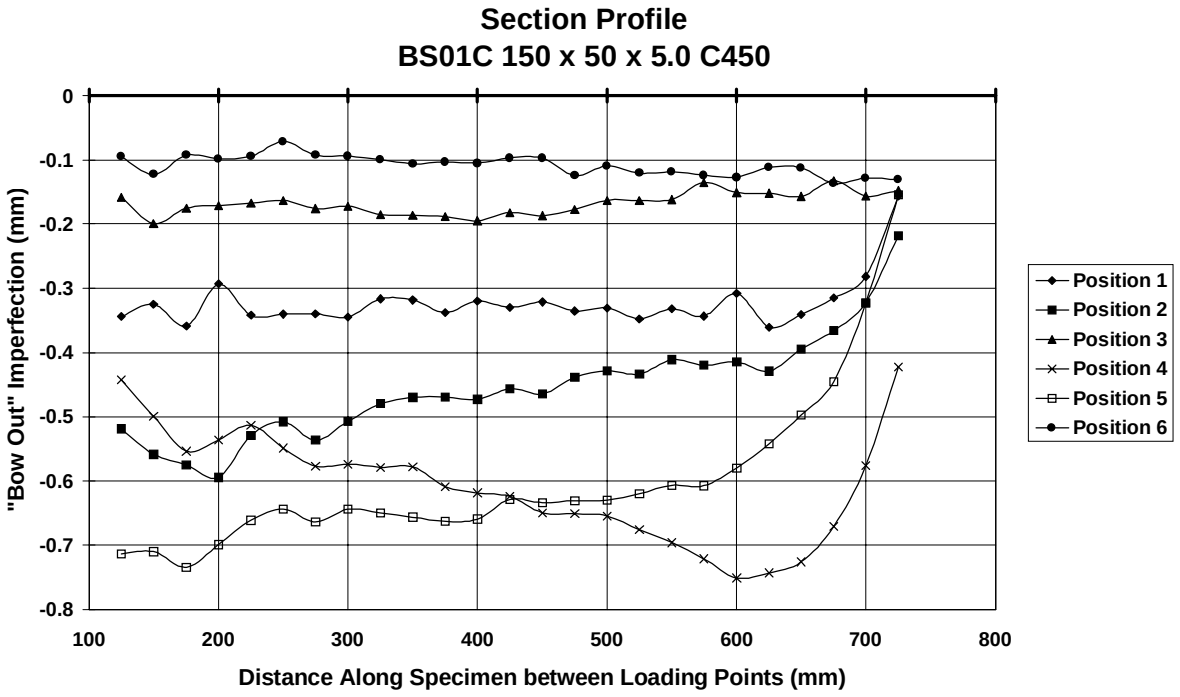
Section Profile
BS01C 150 x 50 x 5.0 C450
"Bow Out" Imperfection (mm)
0
-0.1
-0.2
-0.3
-0.4
-0.5
-0.6
-0.7
-0.8
100
200
300
400
500
600
700
800
Distance Along Specimen between Loading Points (mm)
Position 1
Position 2
Position 3
Position 4
Position 5
Position 6

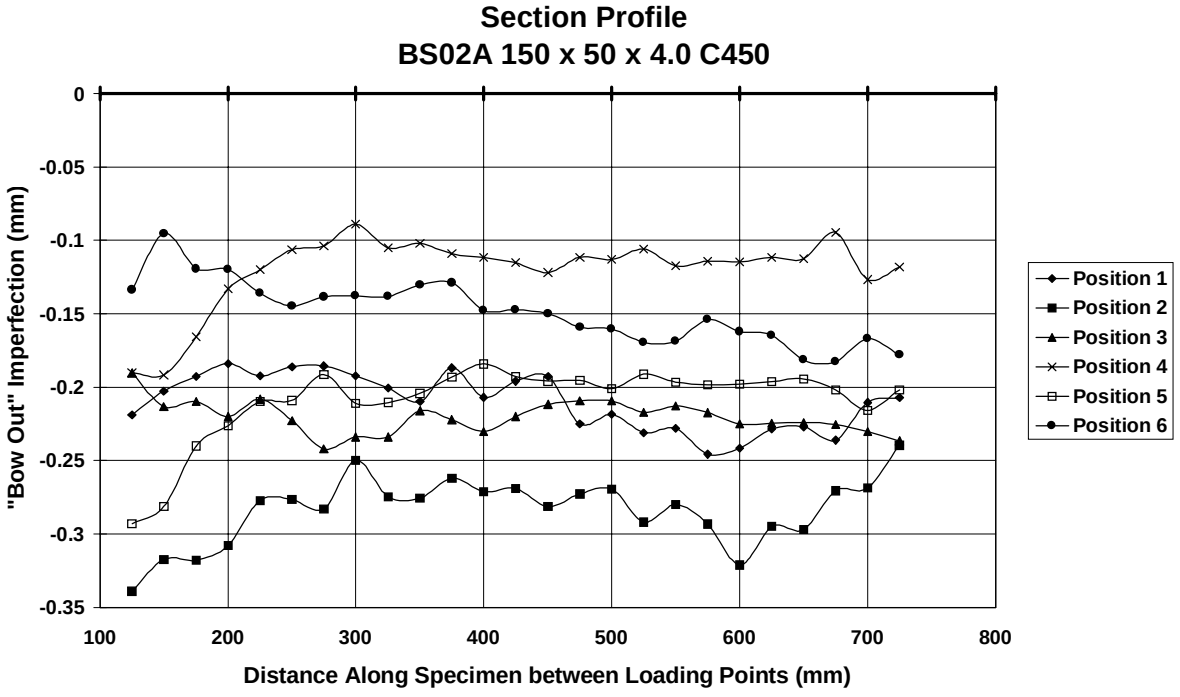
Section Profile
BS02A 150 x 50 x 4.0 C450
"Bow Out" Imperfection (mm)
0
-0.05
-0.1
-0.15
-0.2
-0.25
-0.3
-0.35
100
200
300
400
500
600
700
800
Distance Along Specimen between Loading Points (mm)
Position 1
Position 2
Position 3
Position 4
Position 5
Position 6

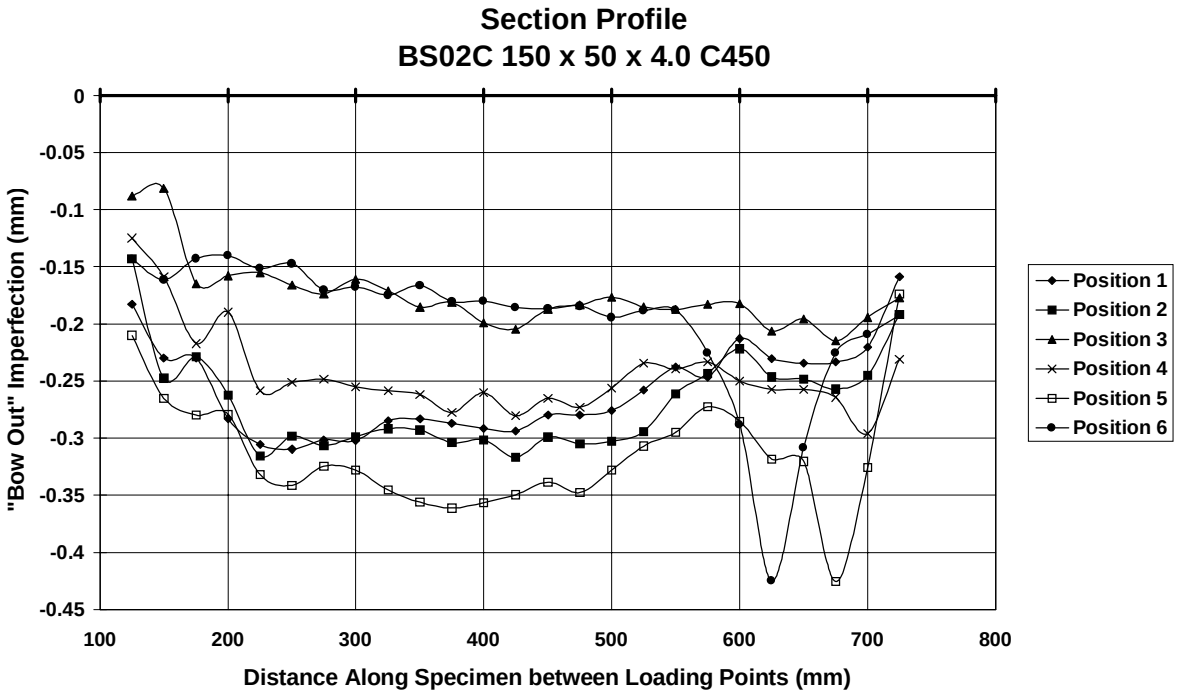
Section Profile
BS02C 150 x 50 x 4.0 C450
"Bow Out" Imperfection (mm)
0
-0.05
-0.1
-0.15
-0.2
-0.25
-0.3
-0.35
-0.4
-0.45
100
200
300
400
500
600
700
800
Distance Along Specimen between Loading Points (mm)
Position 1
Position 2
Position 3
Position 4
Position 5
Position 6

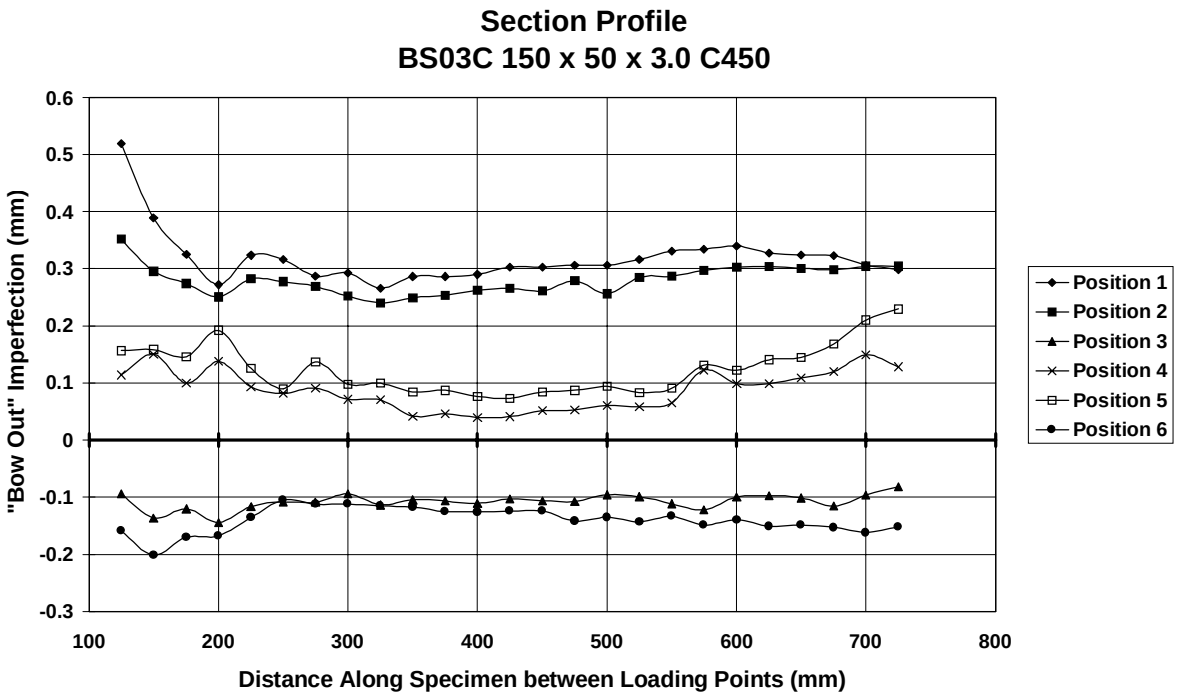
Section Profile
BS03C 150 x 50 x 3.0 C450
"Bow Out" Imperfection (mm)
0.6
0.5
0.4
0.3
0.2
0.1
0
-0.1
-0.2
-0.3
100
200
300
400
500
600
700
800
Distance Along Specimen between Loading Points (mm)
Position 1
Position 2
Position 3
Position 4
Position 5
Position 6

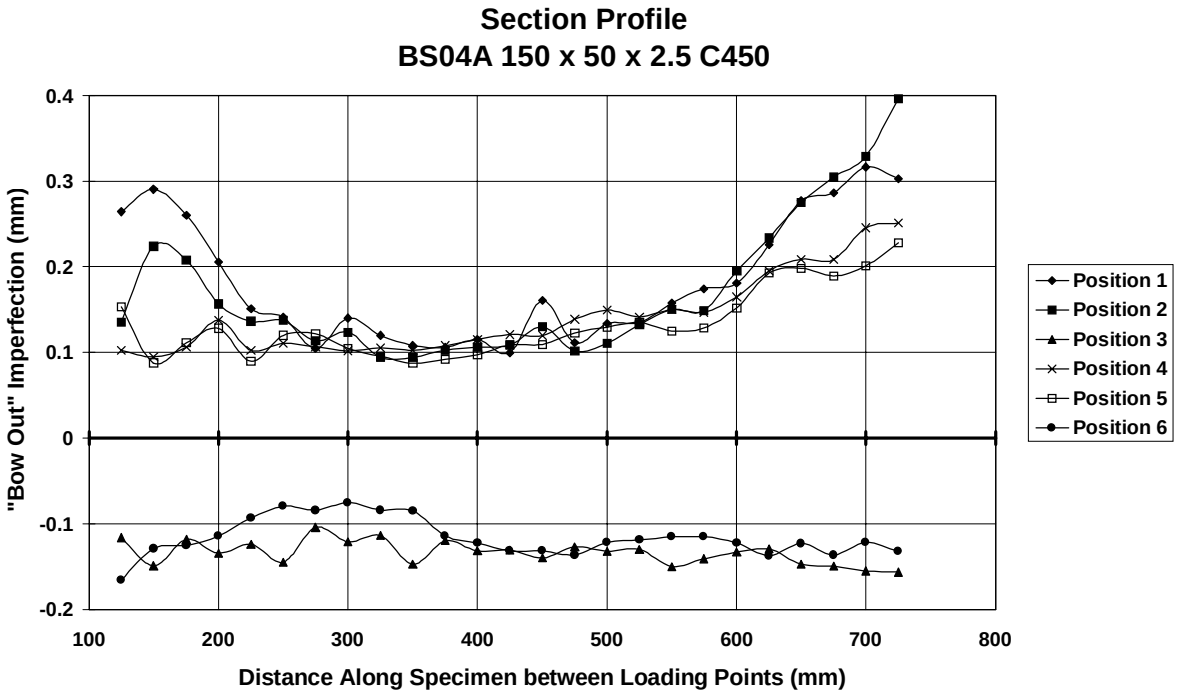
Section Profile
BS04A 150 x 50 x 2.5 C450
"Bow Out" Imperfection (mm)
0.4
0.3
0.2
0.1
0
-0.1
-0.2
100
200
300
400
500
600
700
800
Distance Along Specimen between Loading Points (mm)
Position 1
Position 2
Position 3
Position 4
Position 5
Position 6

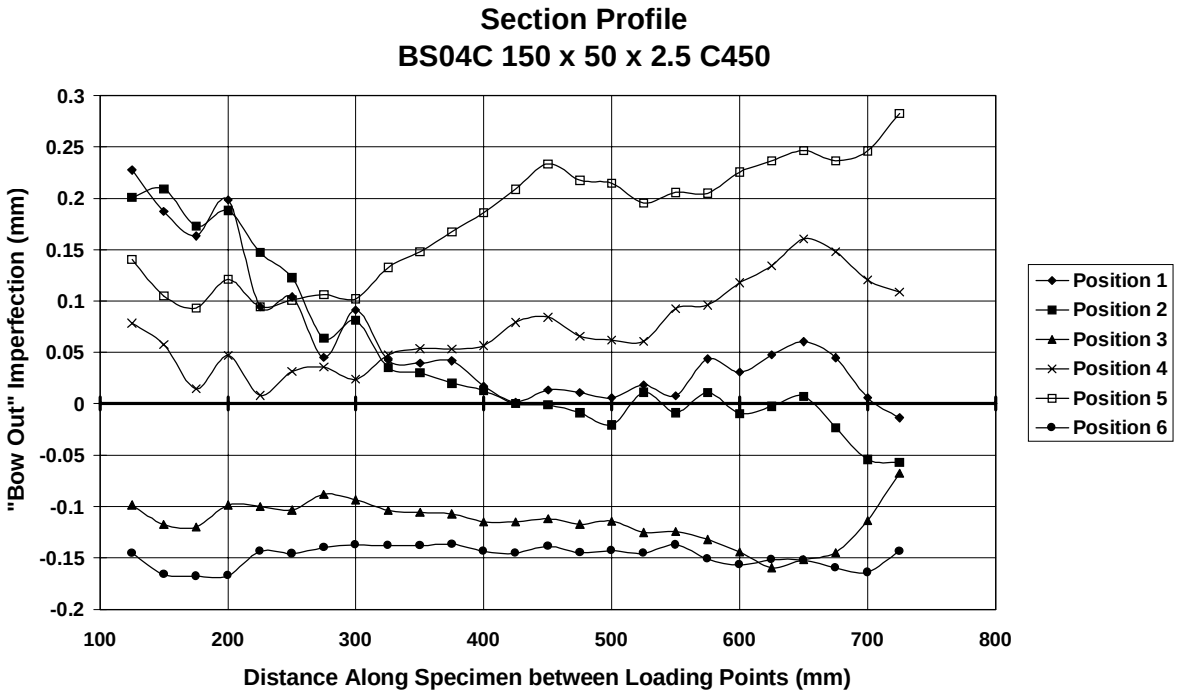
Section Profile
BS04C 150 x 50 x 2.5 C450
"Bow Out" Imperfection (mm)
0.3
0.25
0.2
0.15
0.1
0.05
0
-0.05
-0.1
-0.15
-0.2
100
200
300
400
500
600
700
800
Distance Along Specimen between Loading Points (mm)
Position 1
Position 2
Position 3
Position 4
Position 5
Position 6

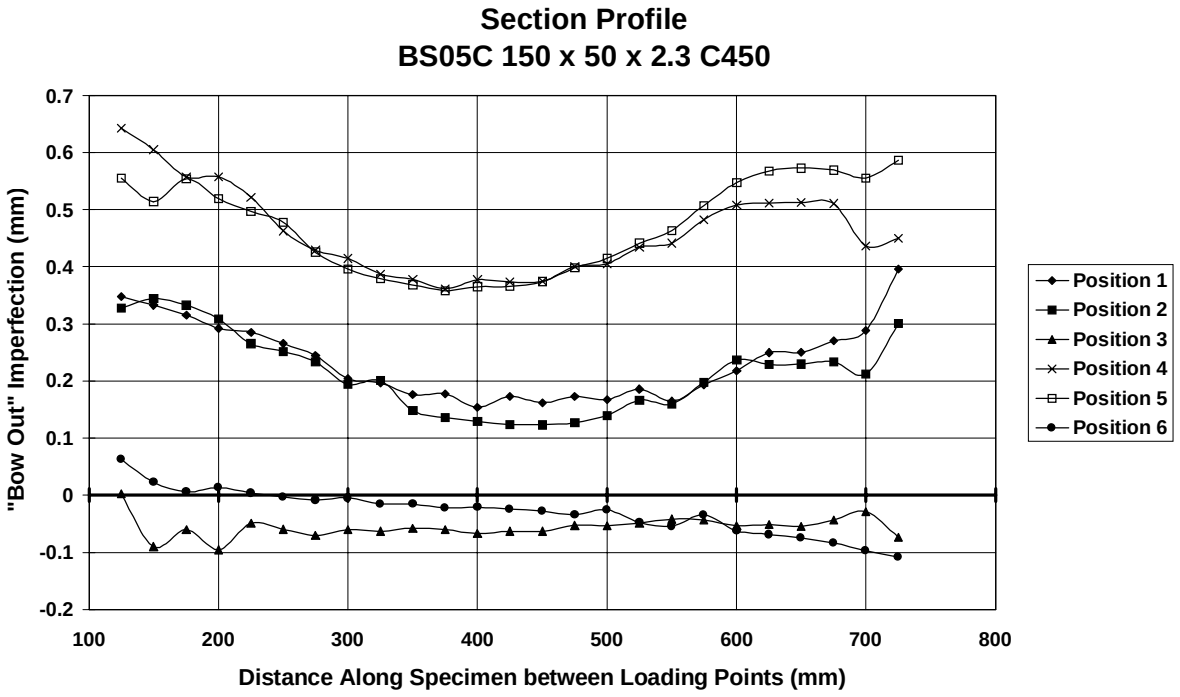
Section Profile
BS05C 150 x 50 x 2.3 C450
"Bow Out" Imperfection (mm)
0.7
0.6
0.5
0.4
0.3
0.2
0.1
0
-0.1
-0.2
100
200
300
400
500
600
700
800
Distance Along Specimen between Loading Points (mm)
Position 1
Position 2
Position 3
Position 4
Position 5
Position 6

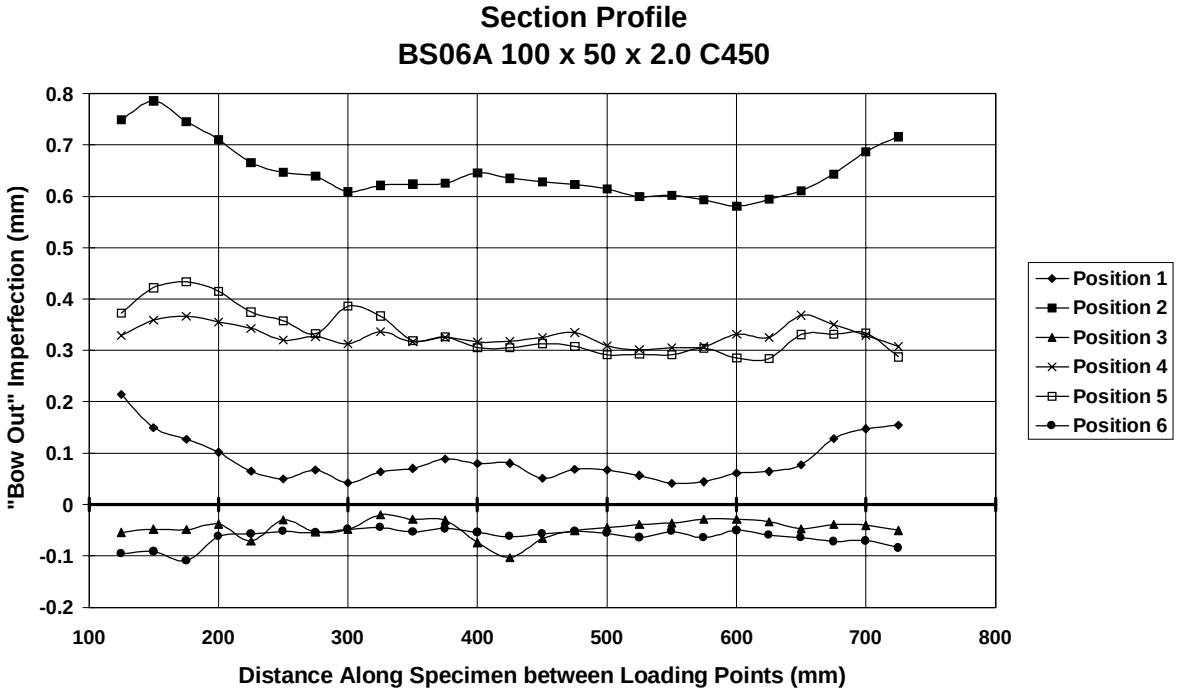
Section Profile
BS06A 100 x 50 x 2.0 C450
"Bow Out" Imperfection (mm)
0.8
0.7
0.6
0.5
0.4
0.3
0.2
0.1
0
-0.1
-0.2
100
200
300
400
500
600
700
800
Distance Along Specimen between Loading Points (mm)
Position 1
Position 2
Position 3
Position 4
Position 5
Position 6

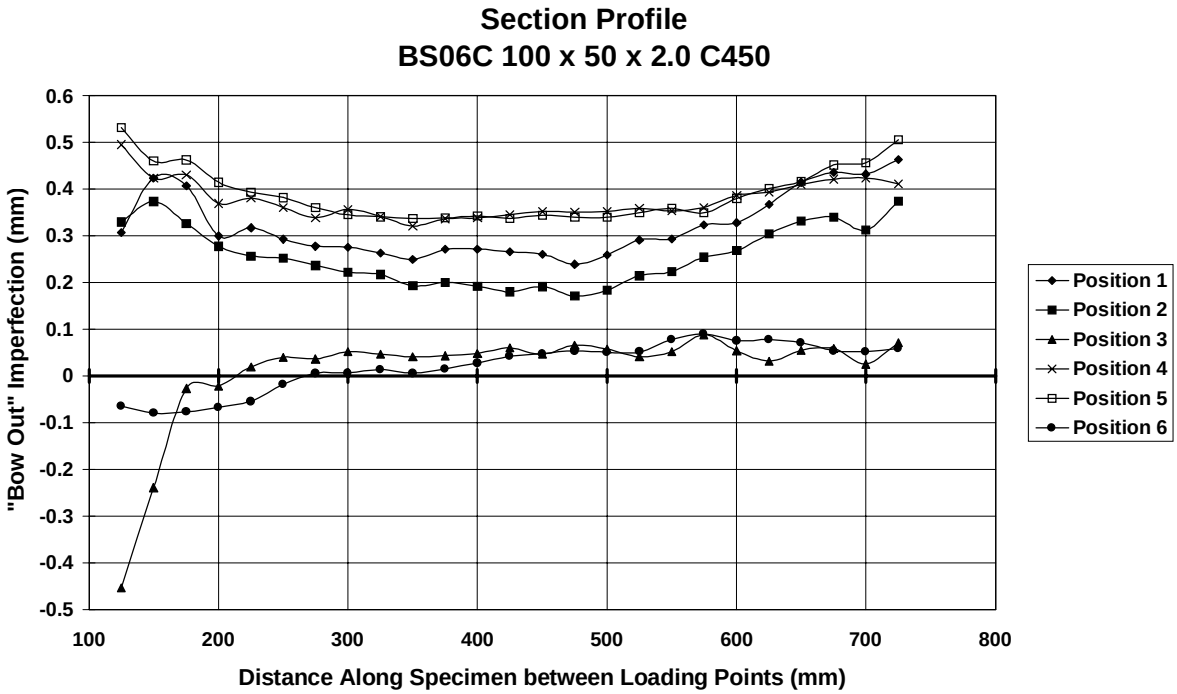
Section Profile
BS06C 100 x 50 x 2.0 C450
"Bow Out" Imperfection (mm)
0.6
0.5
0.4
0.3
0.2
0.1
0
-0.1
-0.2
-0.3
-0.4
-0.5
100
200
300
400
500
600
700
800
Distance Along Specimen between Loading Points (mm)
Position 1
Position 2
Position 3
Position 4
Position 5
Position 6

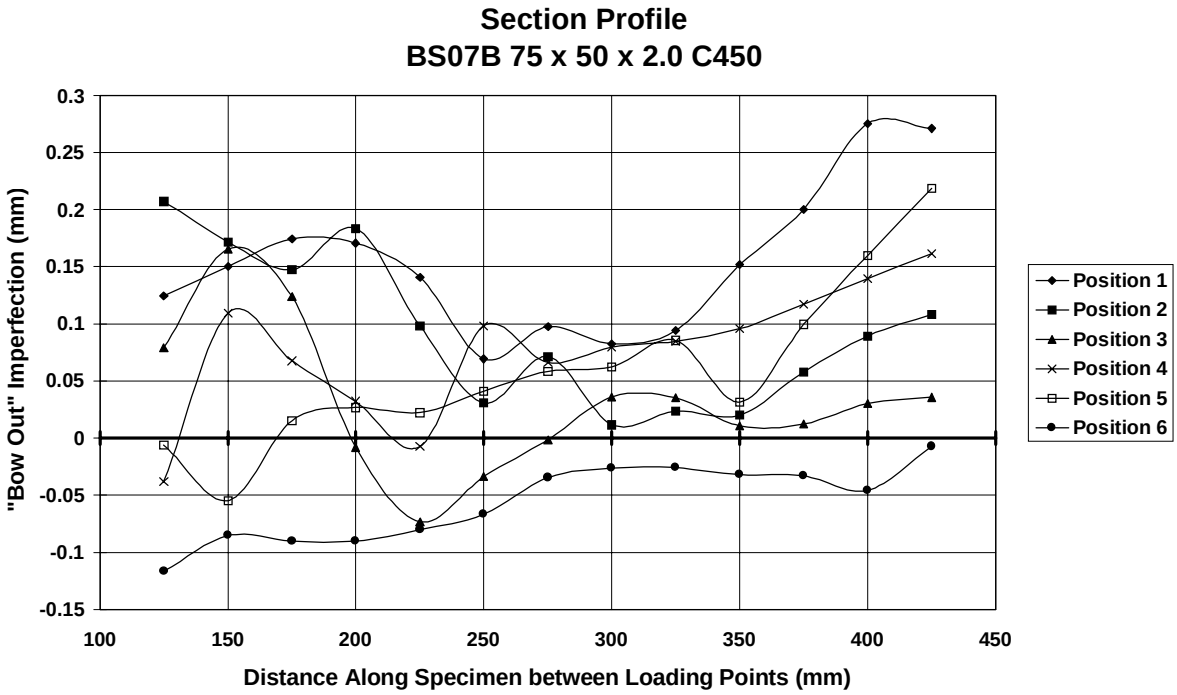
Section Profile
BS07B 75 x 50 x 2.0 C450
"Bow Out" Imperfection (mm)
0.3
0.25
0.2
0.15
0.1
0.05
0
-0.05
-0.1
-0.15
100
150
200
250
300
350
400
450
Distance Along Specimen between Loading Points (mm)
Position 1
Position 2
Position 3
Position 4
Position 5
Position 6

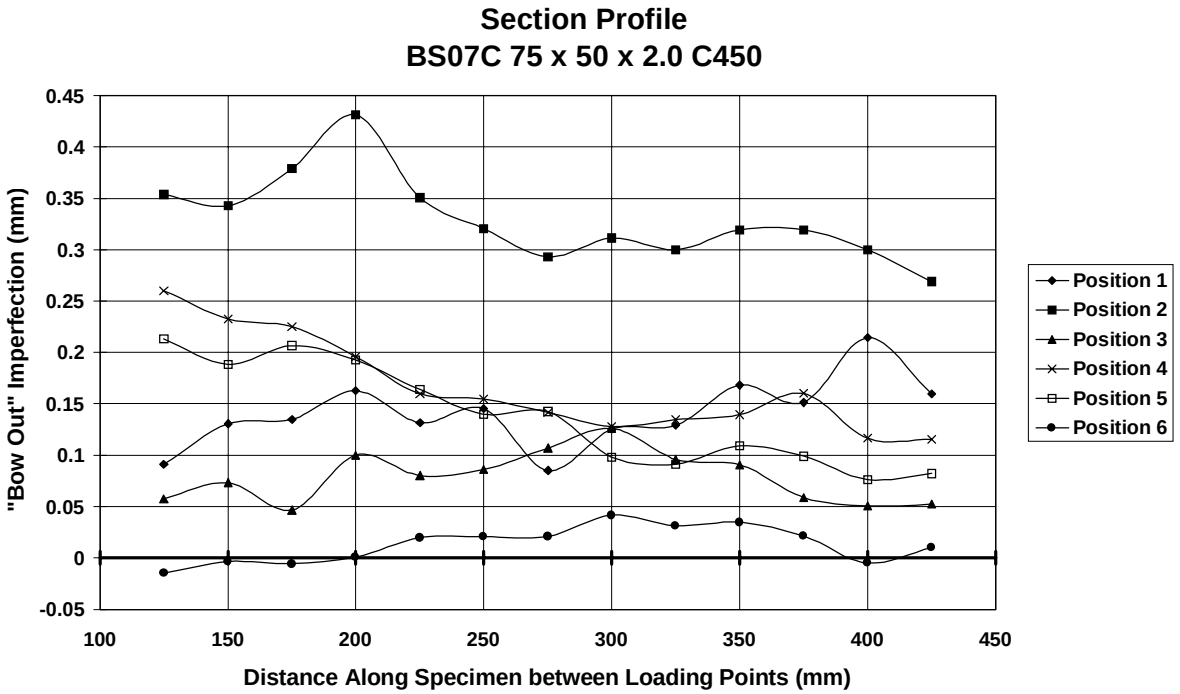
Section Profile
BS07C 75 x 50 x 2.0 C450
"Bow Out" Imperfection (mm)
0.45
0.4
0.35
0.3
0.25
0.2
0.15
0.1
0.05
0
-0.05
100
150
200
250
300
350
400
450
Distance Along Specimen between Loading Points (mm)
Position 1
Position 2
Position 3
Position 4
Position 5
Position 6

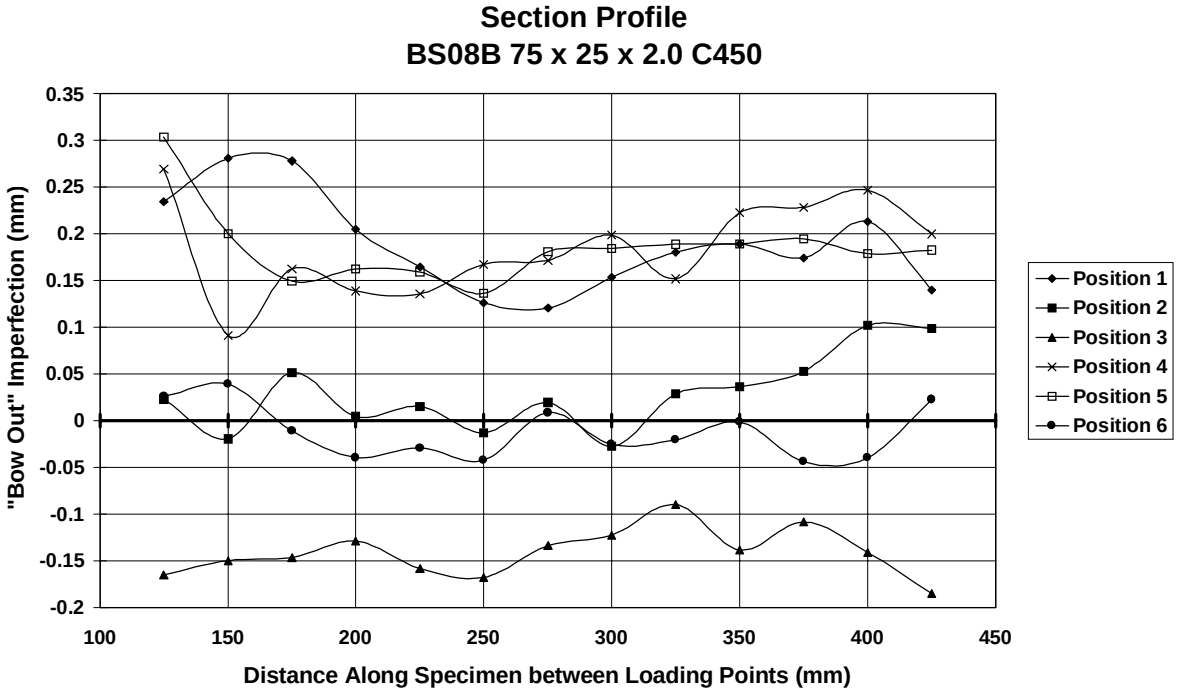
Section Profile
BS08B 75 x 25 x 2.0 C450
"Bow Out" Imperfection (mm)
0.35
0.3
0.25
0.2
0.15
0.1
0.05
0
-0.05
-0.1
-0.15
-0.2
100
150
200
250
300
350
400
450
Distance Along Specimen between Loading Points (mm)
Position 1
Position 2
Position 3
Position 4
Position 5
Position 6

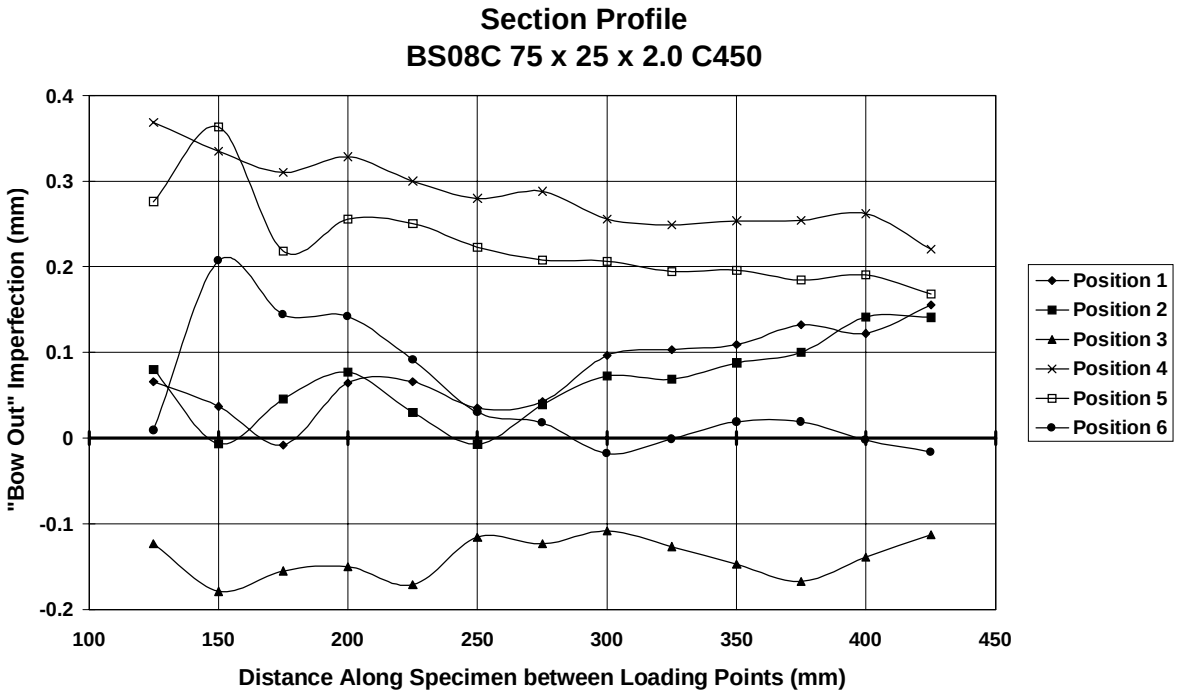
Section Profile
BS08C 75 x 25 x 2.0 C450
"Bow Out" Imperfection (mm)
0.4
0.3
0.2
0.1
0
-0.1
-0.2
100
150
200
250
300
350
400
450
Distance Along Specimen between Loading Points (mm)
Position 1
Position 2
Position 3
Position 4
Position 5
Position 6

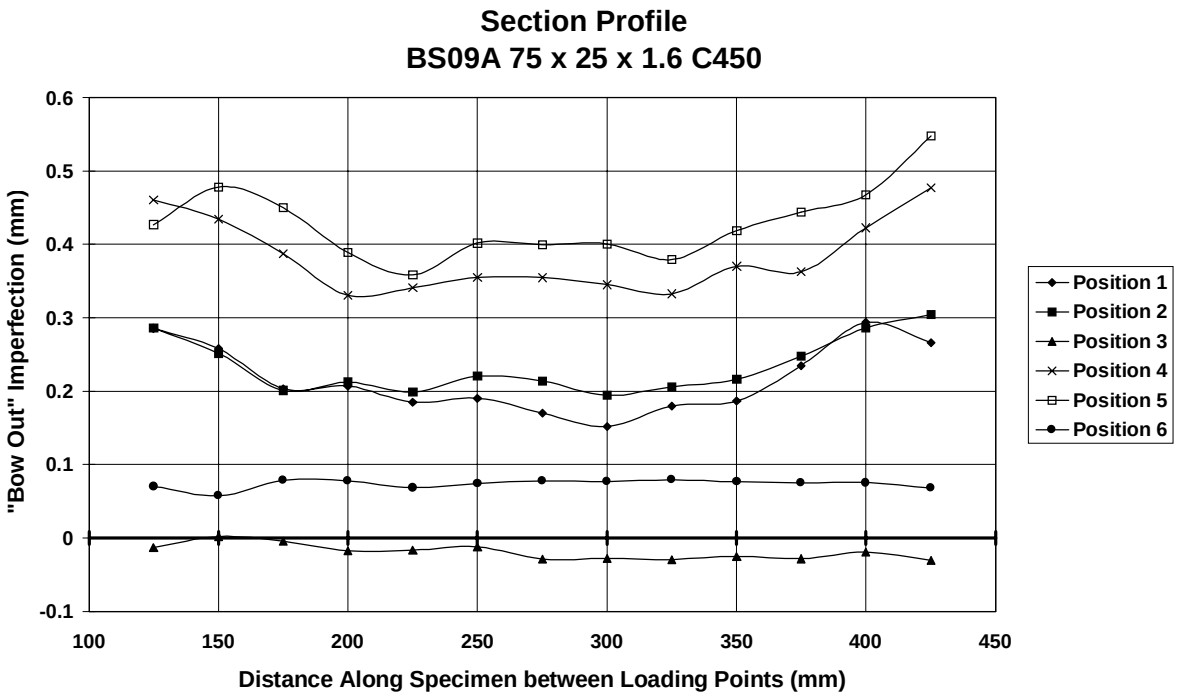
Section Profile
BS09A 75 x 25 x 1.6 C450
"Bow Out" Imperfection (mm)
0.6
0.5
0.4
0.3
0.2
0.1
0
-0.1
100
150
200
250
300
350
400
450
Distance Along Specimen between Loading Points (mm)
Position 1
Position 2
Position 3
Position 4
Position 5
Position 6

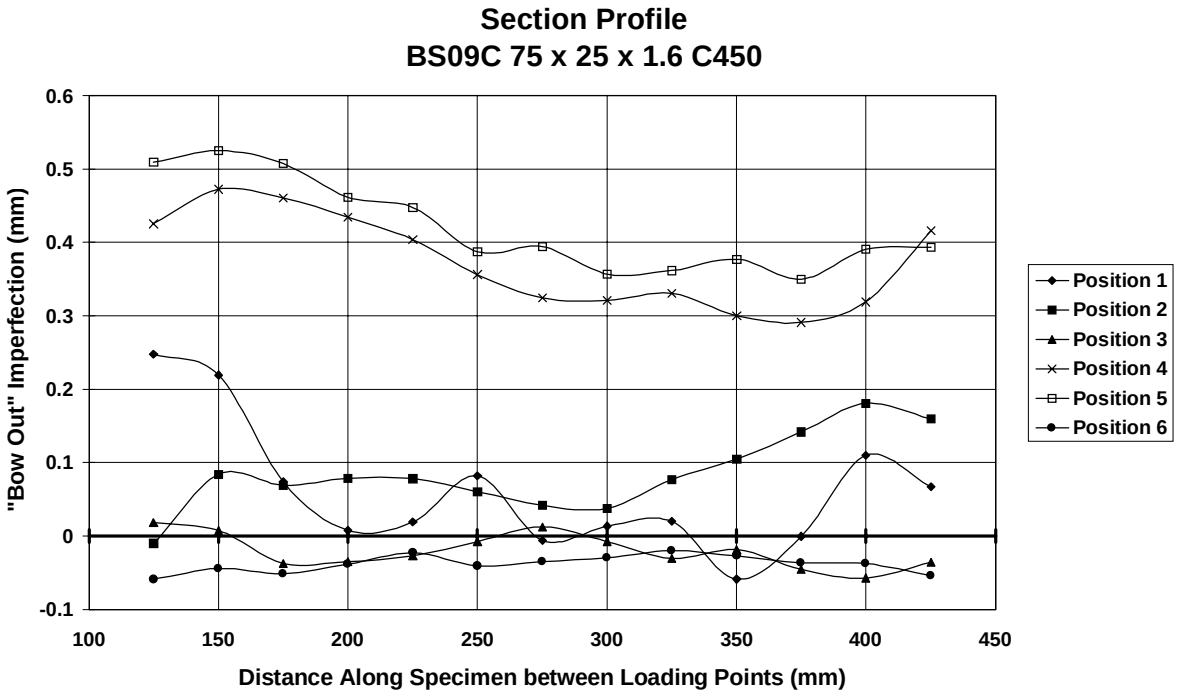
Section Profile
BS09C 75 x 25 x 1.6 C450
"Bow Out" Imperfection (mm)
0.6
0.5
0.4
0.3
0.2
0.1
0
-0.1
100
150
200
250
300
350
400
450
Distance Along Specimen between Loading Points (mm)
Position 1
Position 2
Position 3
Position 4
Position 5
Position 6

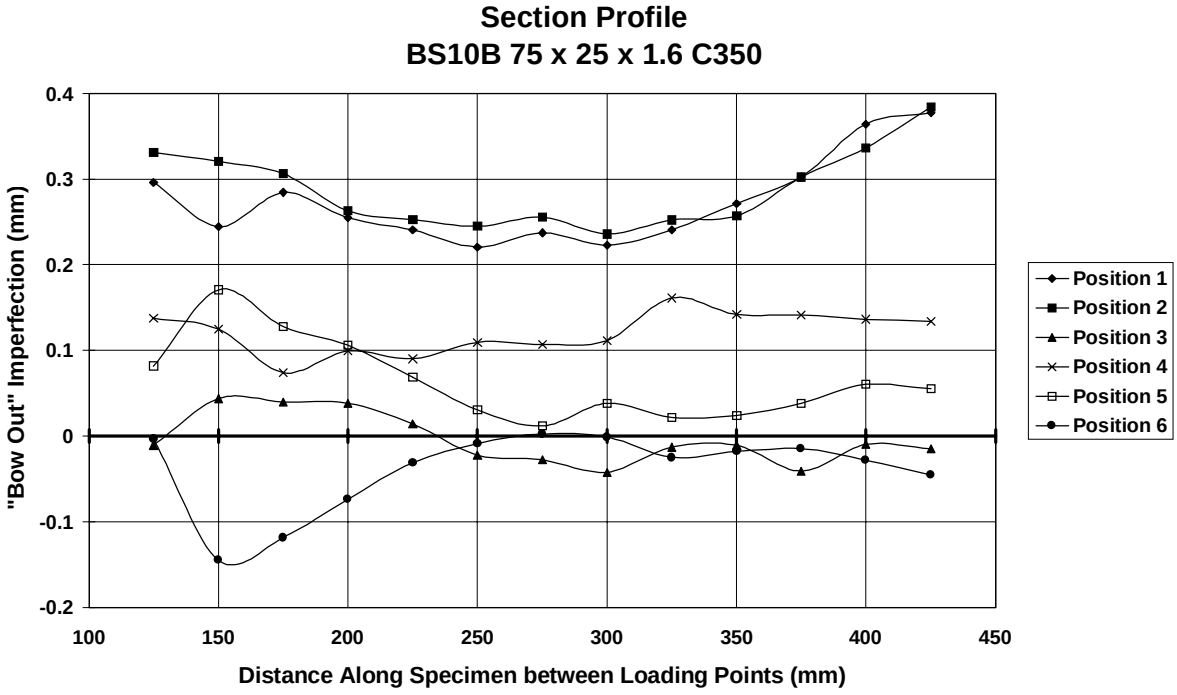
Section Profile
BS10B 75 x 25 x 1.6 C350
"Bow Out" Imperfection (mm)
0.4
0.3
0.2
0.1
0
-0.1
-0.2
100
150
200
250
300
350
400
450
Distance Along Specimen between Loading Points (mm)
Position 1
Position 2
Position 3
Position 4
Position 5
Position 6

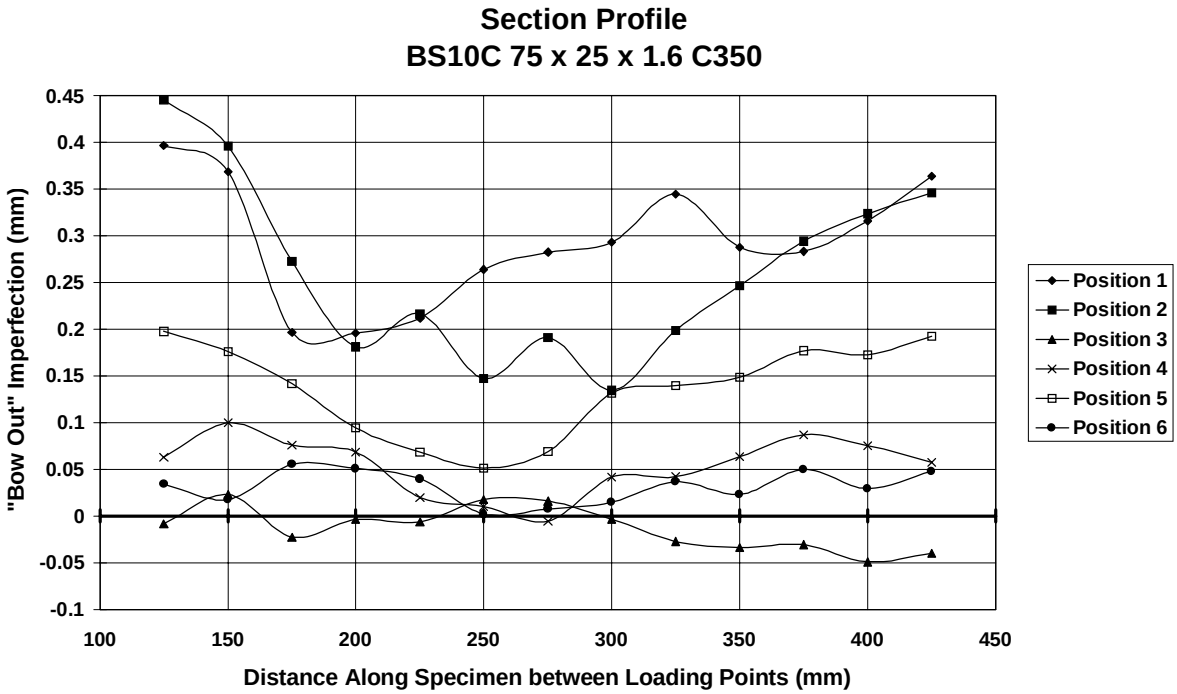
Section Profile
BS10C 75 x 25 x 1.6 C350
"Bow Out" Imperfection (mm)
0.45
0.4
0.35
0.3
0.25
0.2
0.15
0.1
0.05
0
-0.05
-0.1
100
150
200
250
300
350
400
450
Distance Along Specimen between Loading Points (mm)
Position 1
Position 2
Position 3
Position 4
Position 5
Position 6

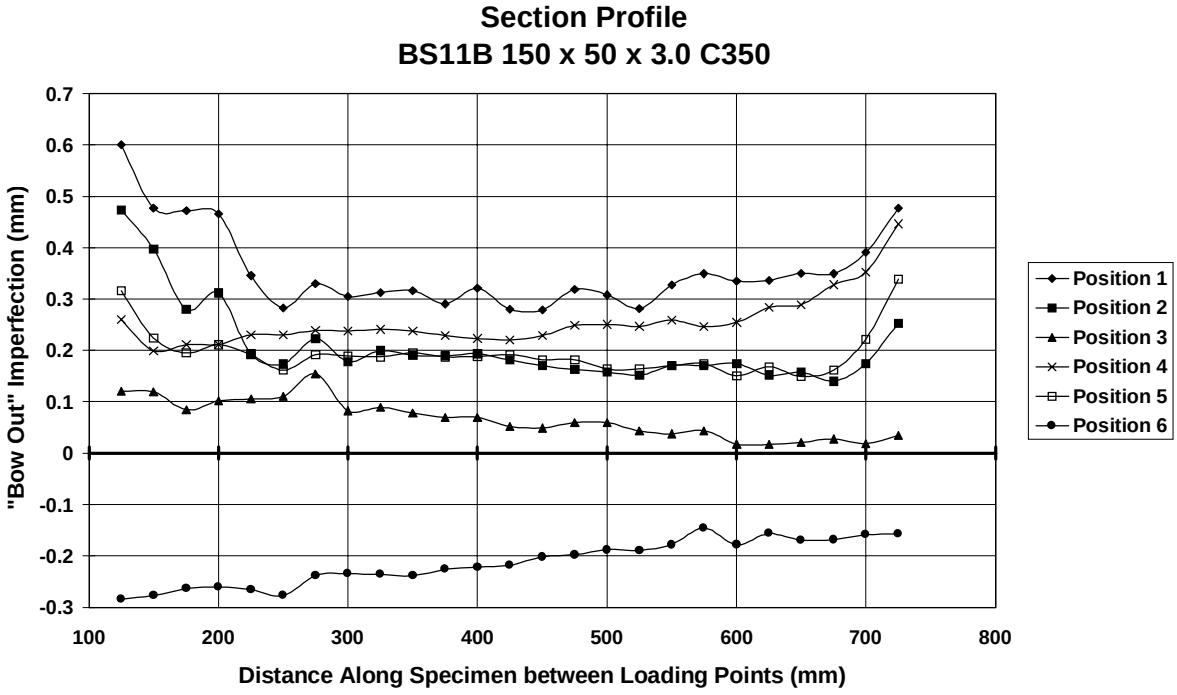
Section Profile
BS11B 150 x 50 x 3.0 C350
"Bow Out" Imperfection (mm)
0.7
0.6
0.5
0.4
0.3
0.2
0.1
0
-0.1
-0.2
-0.3
100
200
300
400
500
600
700
800
Distance Along Specimen between Loading Points (mm)
Position 1
Position 2
Position 3
Position 4
Position 5
Position 6

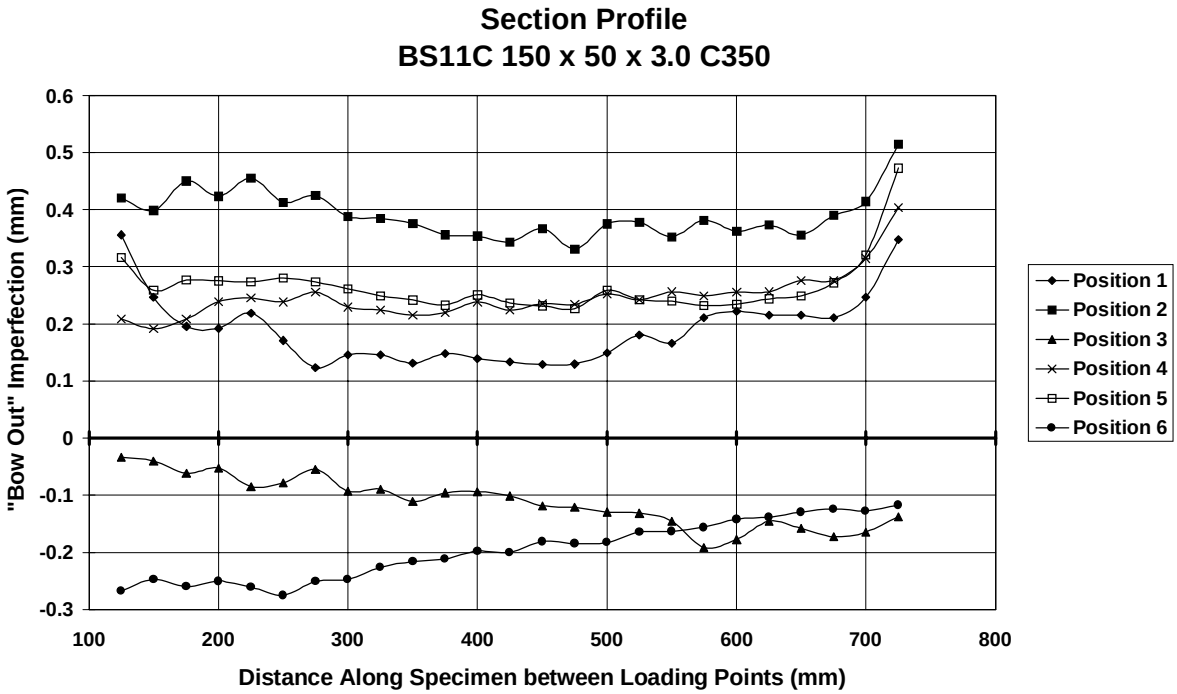
Section Profile
BS11C 150 x 50 x 3.0 C350
"Bow Out" Imperfection (mm)
0.6
0.5
0.4
0.3
0.2
0.1
0
-0.1
-0.2
-0.3
100
200
300
400
500
600
700
800
Distance Along Specimen between Loading Points (mm)
Position 1
Position 2
Position 3
Position 4
Position 5
Position 6

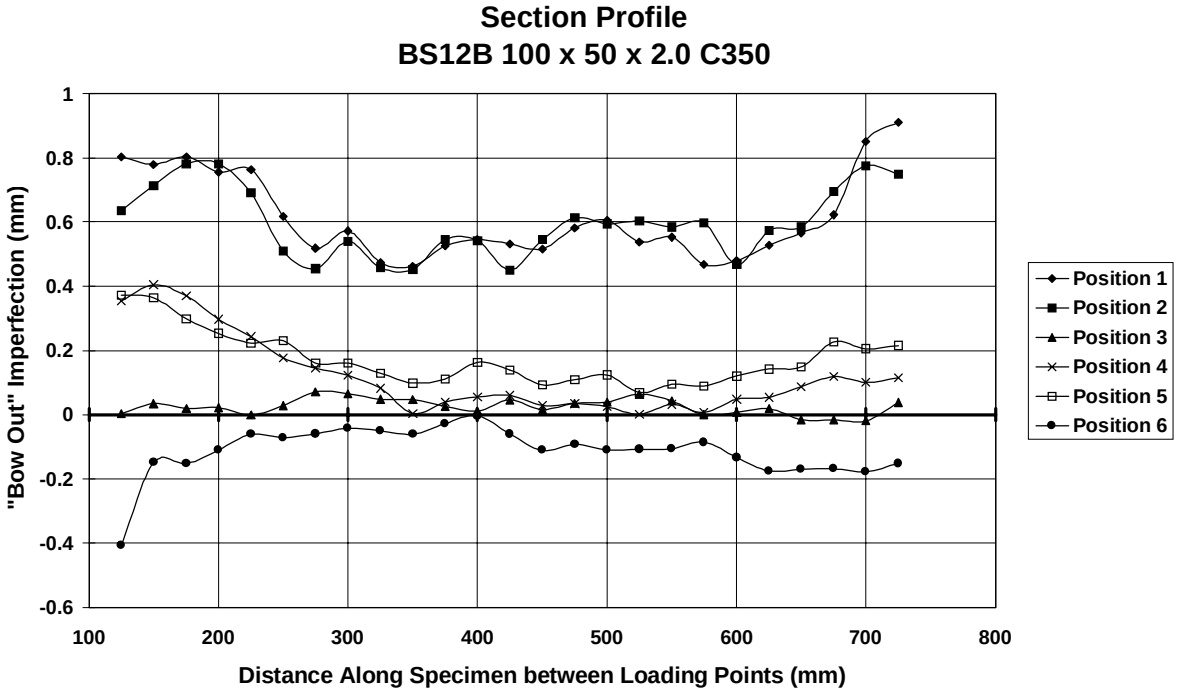
Section Profile
BS12B 100 x 50 x 2.0 C350
"Bow Out" Imperfection (mm)
1
0.8
0.6
0.4
0.2
0
-0.2
-0.4
-0.6
100
200
300
400
500
600
700
800
Distance Along Specimen between Loading Points (mm)
Position 1
Position 2
Position 3
Position 4
Position 5
Position 6

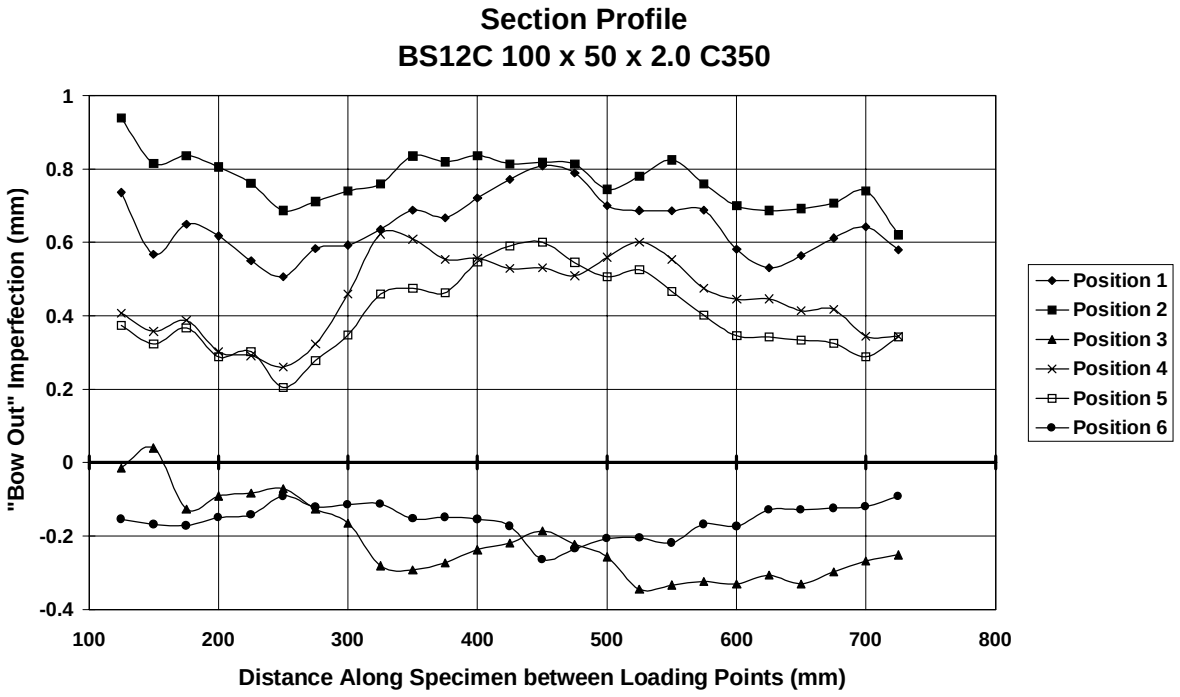
Section Profile
BS12C 100 x 50 x 2.0 C350
"Bow Out" Imperfection (mm)
1
0.8
0.6
0.4
0.2
0
-0.2
-0.4
100
200
300
400
500
600
700
800
Distance Along Specimen between Loading Points (mm)
Position 1
Position 2
Position 3
Position 4
Position 5
Position 6

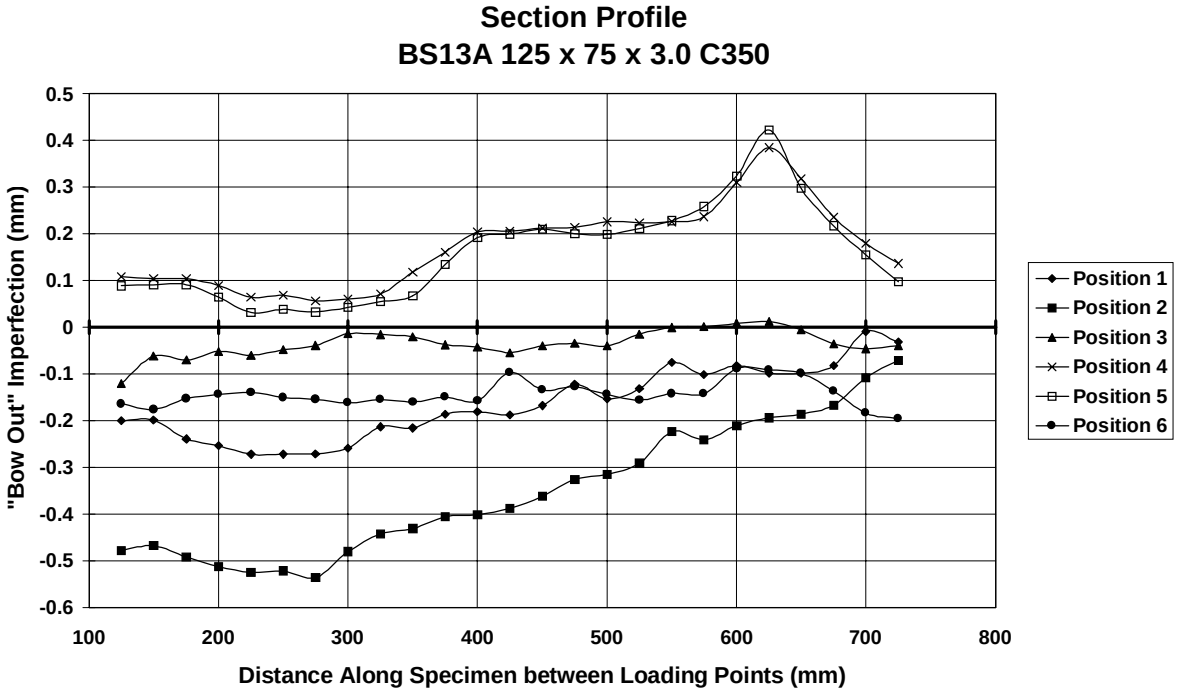
Section Profile
BS13A 125 x 75 x 3.0 C350
"Bow Out" Imperfection (mm)
0.5
0.4
0.3
0.2
0.1
0
-0.1
-0.2
-0.3
-0.4
-0.5
-0.6
100
200
300
400
500
600
700
800
Distance Along Specimen between Loading Points (mm)
Position 1
Position 2
Position 3
Position 4
Position 5
Position 6

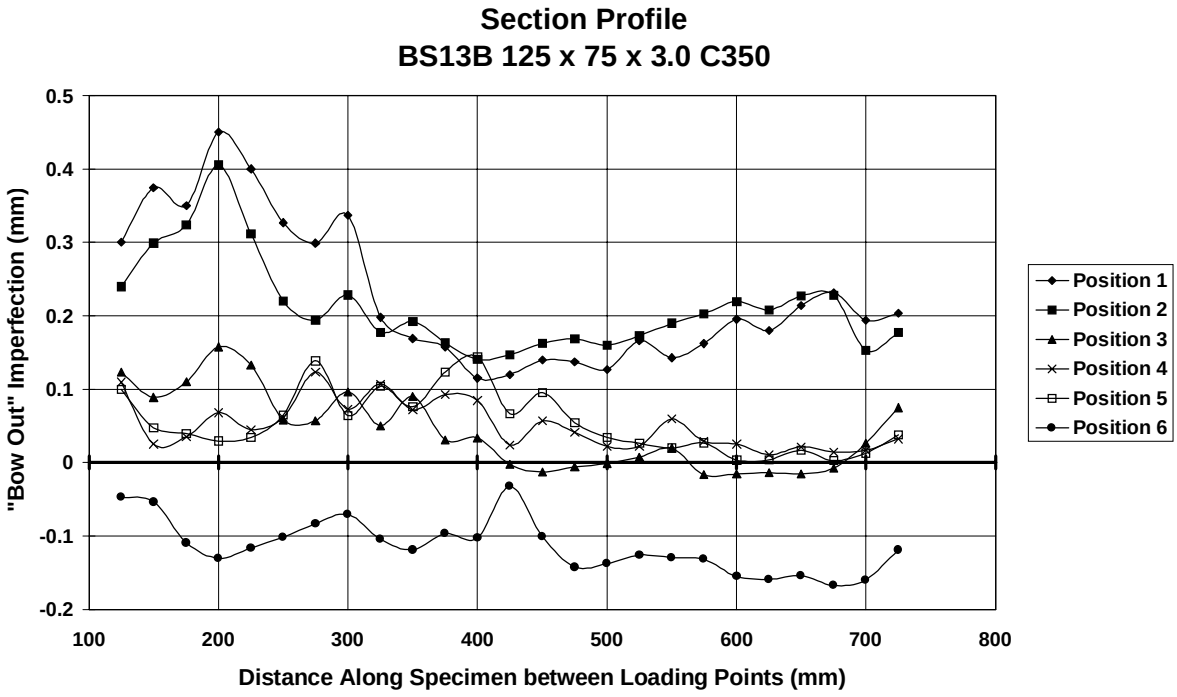
Section Profile
BS13B 125 x 75 x 3.0 C350
"Bow Out" Imperfection (mm)
0.5
0.4
0.3
0.2
0.1
0
-0.1
-0.2
100
200
300
400
500
600
700
800
Distance Along Specimen between Loading Points (mm)
Position 1
Position 2
Position 3
Position 4
Position 5
Position 6

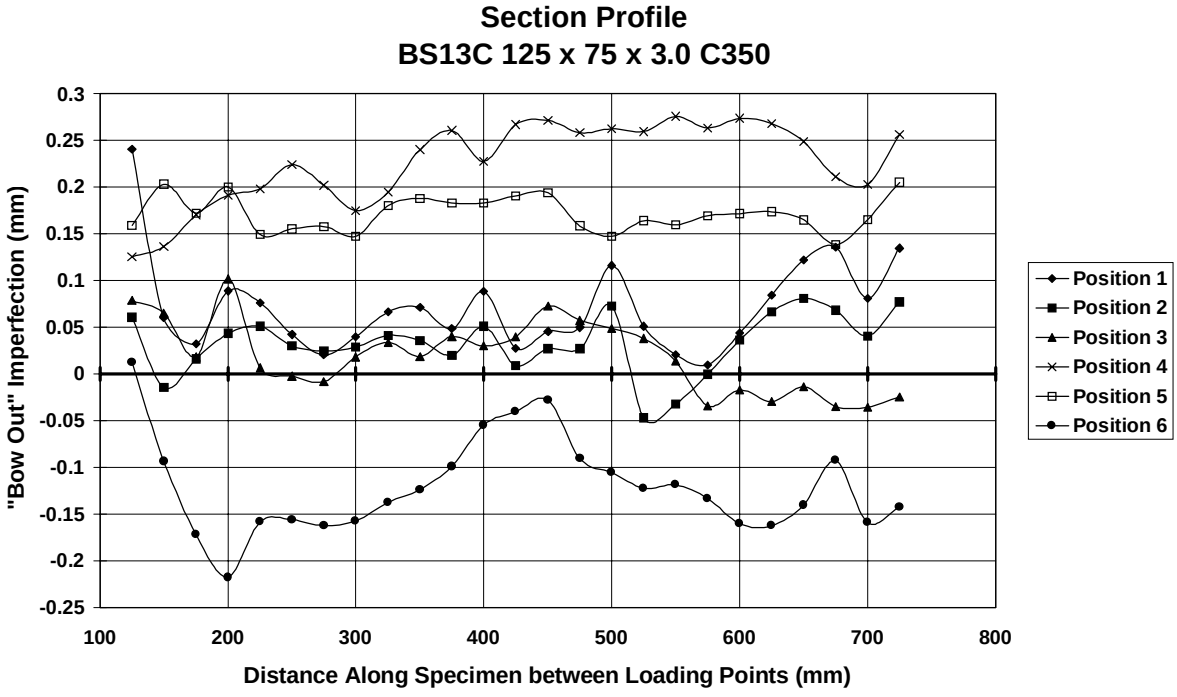
Section Profile
BS13C 125 x 75 x 3.0 C350
"Bow Out" Imperfection (mm)
0.3
0.25
0.2
0.15
0.1
0.05
0
-0.05
-0.1
-0.15
-0.2
-0.25
100
200
300
400
500
600
700
800
Distance Along Specimen between Loading Points (mm)
Position 1
Position 2
Position 3
Position 4
Position 5
Position 6

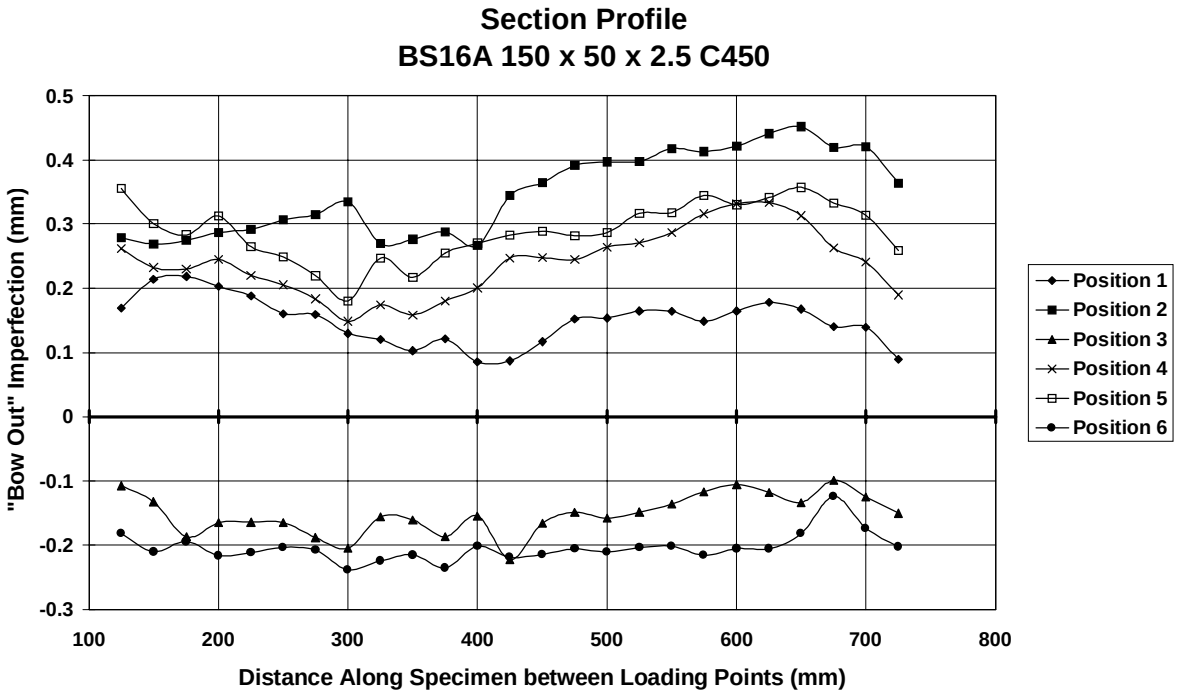
Section Profile
BS16A 150 x 50 x 2.5 C450
"Bow Out" Imperfection (mm)
0.5
0.4
0.3
0.2
0.1
0
-0.1
-0.2
-0.3
100
200
300
400
500
600
700
800
Distance Along Specimen between Loading Points (mm)
Position 1
Position 2
Position 3
Position 4
Position 5
Position 6

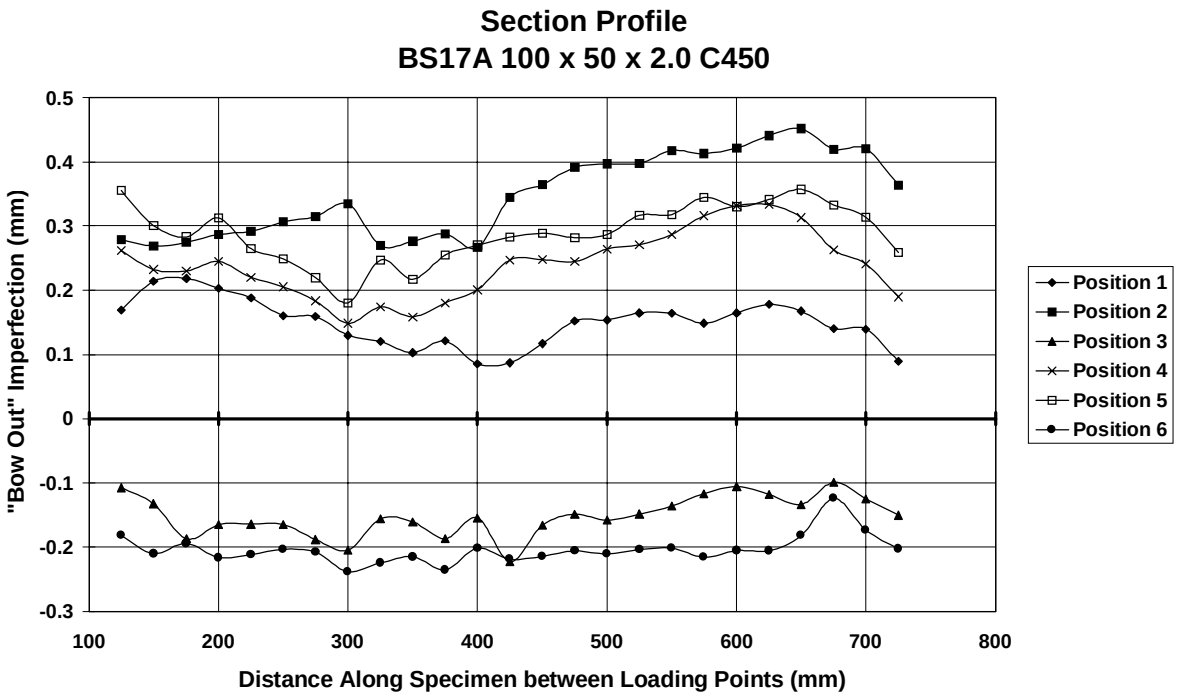
Section Profile
BS17A 100 x 50 x 2.0 C450
"Bow Out" Imperfection (mm)
0.5
0.4
0.3
0.2
0.1
0
-0.1
-0.2
-0.3
100
200
300
400
500
600
700
800
Distance Along Specimen between Loading Points (mm)
Position 1
Position 2
Position 3
Position 4
Position 5
Position 6

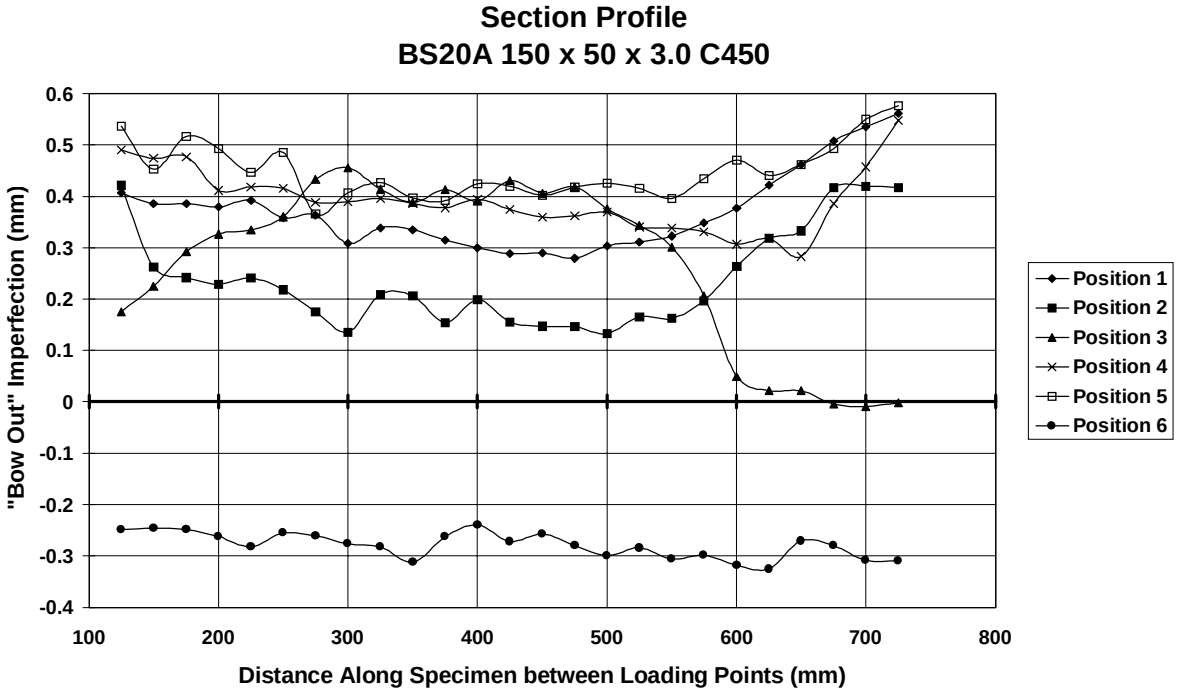
Section Profile
BS20A 150 x 50 x 3.0 C450
"Bow Out" Imperfection (mm)
0.6
0.5
0.4
0.3
0.2
0.1
0
-0.1
-0.2
-0.3
-0.4
100
200
300
400
500
600
700
800
Distance Along Specimen between Loading Points (mm)
Position 1
Position 2
Position 3
Position 4
Position 5
Position 6

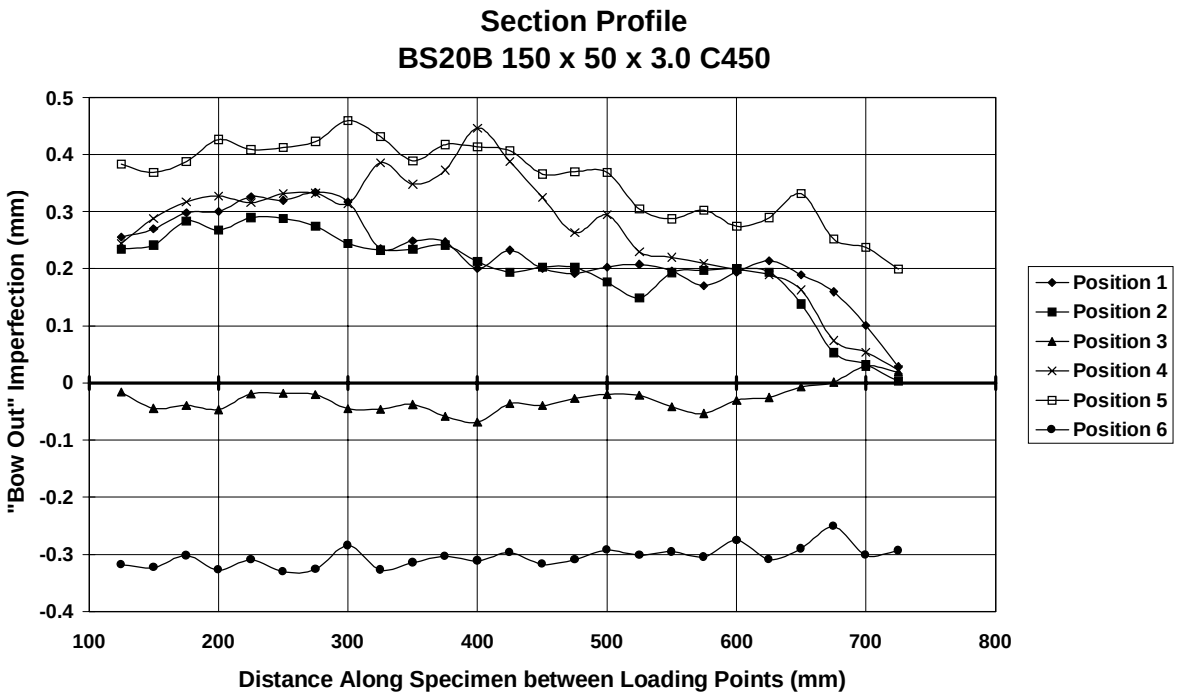
Section Profile
BS20B 150 x 50 x 3.0 C450
"Bow Out" Imperfection (mm)
0.5
0.4
0.3
0.2
0.1
0
-0.1
-0.2
-0.3
-0.4
100
200
300
400
500
600
700
800
Distance Along Specimen between Loading Points (mm)
Position 1
Position 2
Position 3
Position 4
Position 5
Position 6

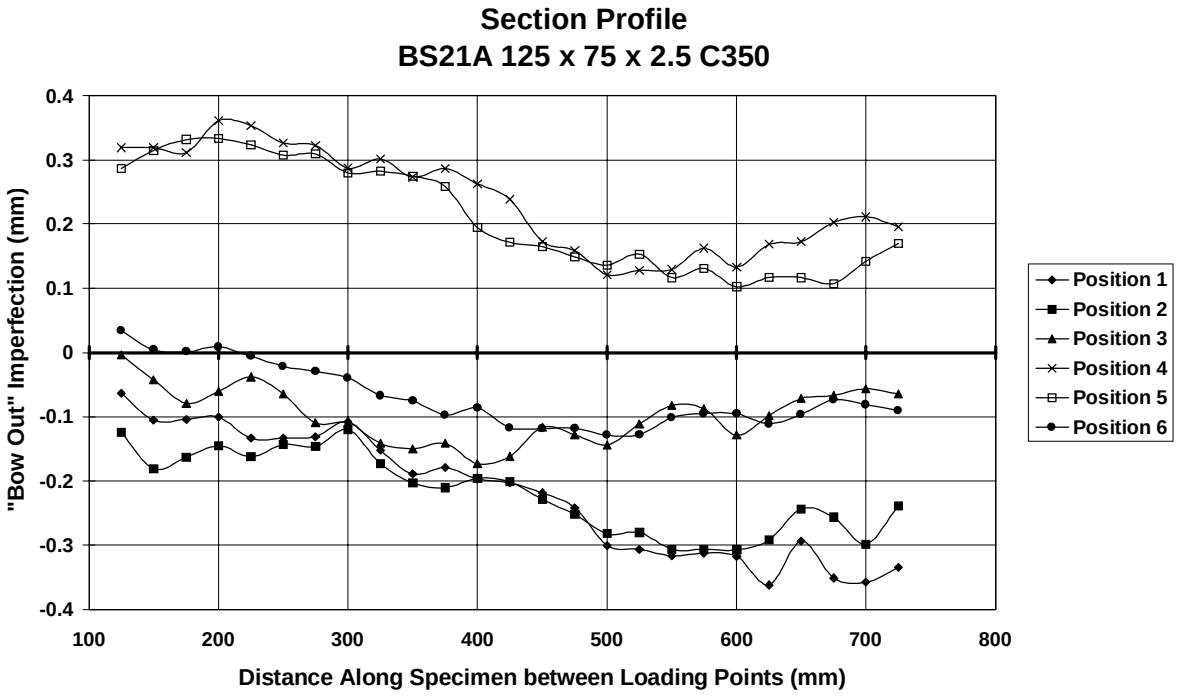
Section Profile
BS21A 125 x 75 x 2.5 C350
"Bow Out" Imperfection (mm)
0.4
0.3
0.2
0.1
0
-0.1
-0.2
-0.3
-0.4
100
200
300
400
500
600
700
800
Distance Along Specimen between Loading Points (mm)
Position 1
Position 2
Position 3
Position 4
Position 5
Position 6